

Development of a Robot-based Magnetic Flux Leakage Inspection System



Dissertation

zur Erlangung des Grades
des Doktors der Ingenieurwissenschaften
der Naturwissenschaftlich-Technischen Fakultät III
Chemie, Pharmazie, Bio- und Werkstoffwissenschaften
der Universität des Saarlandes

von

M.Sc. Yunlai Li

Saarbrücken 2011

Tag des Kolloquiums: 26. Oktober 2011
Dekan: Prof. Dr. Wilhelm F. Maier
Berichterstatte: Prof. Dr. M. Kröning
Prof. Dr. W. Arnold
Vorsitz: Prof. Dr. D. Bähre
Akad. Mitarbeiter: Dr.-Ing. F. Aubertin

Preface

First of all, I would like to express my deep gratitude to my adviser Prof. Michael Kröning who gave me the opportunity to start my PhD work at Fraunhofer Institute IZFP. I am also very grateful for his endless support and guidance. It is his unselfish support and help that encouraged me to overcome the difficulties encountered during my PhD study. I thank Prof. Boller for his support as executive director of IZFP.

I would also like to express my thanks to Prof. Arnold for his work as the second valuator.

I thank Dr. Altpeter and Dr. Valeske for the good working conditions and support they have provided to me.

I am really grateful to Dr. Szielasko for his insightful advice and support on both technical and non-technical issues during my work at IZFP. Many fruitful discussions and guidance are gratefully acknowledged.

I would also like to thank colleagues of the department, especially Dr. Kloster, for their help and support on my work.

Finally, I would like to thank all my family, particularly my wife and my son, for their endless support, encouragement and love.

Abstract

Surface cracking is one of the primary factors leading to failure of mechanical components. One of the most sensitive methods for surface or near surface crack detection is MFL inspection.

Magnetic sensor based MFL inspection, MSI, has shown many advantageous over MPI and gives the opportunity for automated MFL inspection after its equivalent detectability to MPI is validated.

A standard industrial robot is introduced and applied in this work as an automated solution for precise sensor guidance and a more accurate, flexible and efficient automatic MSI system is developed as an extension of the already existing automatic MFL inspection scheme at IZFP. Performance of the system is demonstrated by applying the system on different inspection situations of concern. The measurement results obtained validate the application of the system on the inspection.

Kurzfassung

Oberflächenrisse sind eine der wichtigsten Faktoren, die zum Versagen von mechanischen Komponenten führen können. Eine der empfindlichsten Methoden für Überprüfung von Oberflächen auf Risse im Bereich der Werkstückoberfläche ist die magnetische Streuflussprüfung.

Die auf dem Magnetsensor basierte magnetische Streuflussprüfung, MSI, hat viele Vorteile bei der praktischen Anwendung gegenüber MPI gezeigt und bietet die Möglichkeit zur automatisierten MFL mit dem Gegenwert der Validierung des MPI Verfahrens.

In dieser Arbeit wird ein Standard-Industrieroboter vorgestellt, welcher für eine automatisierte Lösung zur Prüfungsdurchführung verwendet wird. So kann die präzise Sensorführung für ein genaues, flexibles und effizientes automatisches MSI-System gewährleistet werden. Das System dient auch als Erweiterung zu den bereits bestehenden automatischen MFL Prüfsystem besteht. Schließlich wird die Leistungsfähigkeit des Gesamtsystems durch die Anwendungen in unterschiedlichen Prüfsituationen demonstriert. Die erhaltenen Prüfergebnisse bestätigen die Anwendung des Systems als Grundlage für unterschiedliche Prüfaufgaben im mechanisierten Prüfbetrieb auch im Produktionsprozeß.

Symbols and abbreviations

B	magnetic flux density [T]
D	electric flux density [$\text{C}\cdot\text{m}^{-2}$]
E	electric field intensity [$\text{V}\cdot\text{m}^{-1}$]
H	magnetic field strength [$\text{A}\cdot\text{m}^{-1}$]
I	current [A]
J	current density [$\text{A}\cdot\text{m}^{-2}$]
L	inductance [H]
m, M	magnetic moment [$\text{A}\cdot\text{m}^{-1}$]
V	voltage [V]
q	electric charge [C]
μ_0	permeability of free space, $\mu_0 = 4\pi \cdot 10^{-7} \text{N} \cdot \text{A}^{-2}$
μ_r	relative permeability, $\mu_r = \frac{\mu}{\mu_0}$
μ	permeability, $\mu = \mu_0 \mu_r$ [$\text{H}\cdot\text{m}^{-1}$]
σ	conductivity [$\text{S}\cdot\text{m}^{-1}$]
χ	magnetic susceptibility
DAQ	data acquisition
FEM	Finite element method
MFL	magnetic flux leakage
MMS	modular measurement system
MPI	magnetic particle inspection
MSI	magnetic sensor inspection
NDT	non-destructive testing
PP-Amplitude	Peak-to-Peak-Amplitude
GMR	giant magneto-resistance

Table of Contents

1	Introduction	1
2	Theory	9
2.1	Ferromagnetism.....	10
2.2	Magnetic flux leakage testing	11
2.2.1	Principle of MFL testing	11
2.2.2	Description of flaw induced magnetic flux leakage.....	11
2.2.3	Magnetic particle inspection	17
2.2.4	Sensor based MFL test.....	18
2.3	Micro-magnetic testing technique	24
3	State of the art	25
3.1	Magnetic particle testing.....	25
3.2	Sensor based MFL.....	26
3.3	Automatic schemes for sensor based MFL	28
3.4	Standard industry robots and its application in NDT.....	30
3.4.1	Most widely used robot in industry.....	31
3.4.2	Application of industrial robot for NDT Automation.....	34
3.5	Robot based automatic scanning.....	39
3.5.1	Robot programming	39
3.5.2	Robot kinematics	42
3.6	Modular measuring system (MMS)	45
3.6.1	Modular software concept.....	45
3.6.2	Graphical programming language LabVIEW™	45

3.6.3	Modular Measuring System (MMS) of IZFP	46
3.6.4	Existing MMS modules for MFL scanning	47
4	Design and implementation of a modular robotic scanning platform	49
4.1	Selection and implementation of Robot.....	49
4.1.1	Requirements analysis	49
4.1.2	Specific consideration for robot selection	50
4.1.3	Selection of robot.....	51
4.2	KUKA Robotics	53
4.2.1	KUKA Robot.....	53
4.2.2	Controller	54
4.2.3	Software.....	57
4.2.4	Robot installation	63
4.3	Design of the scanning platform	65
4.3.1	Passive or active role of the measuring PC.....	65
4.3.2	Modular software concept.....	68
4.3.3	KUKA-specific motion module	69
4.3.4	Robot script controller module (non KUKA-specific)	80
4.3.5	3D Result visualization module.....	90
5	Application examples	93
5.1	System detectability verification on a test block.....	93
5.2	Remanence detection on steel bar	97
5.3	Measurement of cheek dimension on crankshaft	100
6	Conclusion and outlook.....	104

7 Bibliography	107
Appendix	114

1 Introduction

Non-destructive testing (NDT) is widely applied in various industrial domains such as traffic industry (automotive, railway, aerospace), energy production (power plants, wind mills, off-shore structures), petrochemical facilities and distribution systems (pipelines), and the related producing industries (steel, mechanical engineering). Due to its nondestructive nature, NDT plays a definitely important and irreplaceable role in the quality policy of manufacturing and the safe and reliable operation of technical systems. National and international laws, regulations, and codes require the use of NDT methods and procedures that have to be validated and certified by qualified personnel or institutions for the inspection problem of concern.

Nowadays, progress in NDT, or more specifically the development of new methods and systems has become very fast because we may take advantage of common mega-trends in technical progress, in automation, computing, microelectronics, and measurement physics. Generally we may state that NDT methods are based on solutions in the field of measurement physics with the specific features that measurement results have to be correlated to quality deficiencies or flaws, or to material properties. The most important methods are visual inspections, X-ray, ultrasonic, electro-magnetic, and penetrant inspections. We also distinguish between methods that detect flaws in the volume or at the surface of the material. The inspection for surface cracks is of primary importance because of the dominant role of high quality surfaces of technical components under load. Surface cracks like hardening cracks for example can cause later failure of the technical structure under load, a fact that makes surface inspections a common part of quality procedures.

Magnetic flux leakage testing, (MFL), is a magnetic NDT method and often considered the oldest of the modern methods of nondestructive material testing. MFL is one of the most sensitive methods for detecting surface and subsurface cracks or similar discontinuities in ferroelectric structural materials such as iron, nickel, cobalt, and some of their alloys. Therefore MFL has become the commonly used method to detect surface breaking or subsurface cracks in ferromagnetic materials. In many industries the use of MFL is part of the product specification especially when safety and quality is of concern. The common method for stray flux visualization is the magnetic particle or Magnaflux inspection technique, MPI [Ivan2006]. The specimen is magnetized by direct or indirect magnetization and the presence of surface or subsurface discontinuities causes the magnetic flux to leak. Ferrous iron particles are applied to the part either dry or in a wet

suspension. The particles will be attracted to the area of flux leakage and will build up and form what is known as an indication.

Usually MPI is a manual inspection. However, there are two reasons for its automation: Safety and quality requirements call for reducing human error as part of the inspection procedure. Secondly, with the rising level of industrial automation, automated tools and processes have become common, and automation technology is available both in respect to given practical and to economic constraints. For advanced automated industrial production, the manual MPI can no longer meet the general production standards but very often a station for manual MPI is still part of fully automated production lines.

The reason is the complexity of MPI [Vett2006] although it looks like a simple measurement problem. The reliability of inspection depends on a workflow of very different nature [DIN2001, Schm1989]: the surface must be prepared and cleaned for the inspection without the risk of closing possibly existing surface cracks. The quality of magnetic particles and/or the suspension has to be controlled and documented, the appropriate magnetization has to be verified, and last but not least the formation of indications has to be detected and assessed by visual inspection. For that reason, automated MPI systems are very complex and expensive.

Nevertheless, commercial automated MPI systems can be found on the market due to their relevance as an important tool of quality inspections. However, they are designed for very specific inspection problems. Usually, the system cannot easily be adjusted to different component geometries.

For example, the MFL systems from the institute DR. Förster, CIRCOFLUX®, ROTOMAT® and TRANSOMAT® are designed for hot-rolled black steel bars and oil field/boiler tubes respectively [Förs2007]; the DEUTROFLUX Magnetic Particle Crack Detection Bench UWE is used for the surface inspection of cast and forged components [Karl2011]. Furthermore, especially small enterprises have to organize a flexible production of different parts. The low number of components in the workflow and the need for high flexibility in respect to their produced parts cause problems with the return of investment. Therefore, we may assume a handicap for small enterprises that will become more serious when the automated inspection is part of the order specification.

Very often, the visual inspection for MFL indications is not part of the automation and done by inspectors. The reason for this is the difficult assessment of some indications, for example at component edges or in the ground of grooves that need the experience of experts. Therefore, very often the full automation by camera based visual control with

subsequent image processing for flaw evaluation cannot be achieved reasonably [Vett2006].

We may state that economic reasons, limitations or at least severe problems with automated flaw evaluation, and the system complexity pose problems for the automation of MPI. Different solutions for the automation of the various processes of MPI have to be developed, e.g. for the surface cleaning before and after the inspection, the mixing and control of the fluid suspension, the removal and recycling of the particles, the drying of the surface and its protection after inspection increase the complexity of automation greatly. Last but not least, the use of powder is considered to be harmful to the environment.

The value of an automated MPI system is beyond dispute. Several years ago, new magnetic sensors, for example the Giant Magnetic Resistor (GMR) sensor [Grün2001], were developed and conventional magnetic sensors like the Hall sensor [Rams2006] could be improved in respect to accuracy, usability and costs. Therefore different groups started the development and validation of sensor-based MFL inspection methods [Hart1999]. Kloster [Klos2008] discussed the usability of available sensor techniques for different inspection problems and could validate the substitution of MPI by sensor-based MFL. We will call this technique magnetic sensor inspection MSI corresponding to MPI. The magnetic sensor or sensor arrays when scanned above the magnetic stray flux field measure signals that can be composed to form magnetic field images.

The verified equivalent detectability of surface and subsurface material deficiencies of MPI and MSI gives reason for further improvements of MFL testing:

- Processing of sensor signals for identification of false calls
- Defect detection in edges, grooves, toothed wheels, and other complex shaped surface geometries
- Detection of subsurface cracks in deeper positions
- Control of inspection performance
- Inspection documentation and reports
- Automation of MFL inspection

MSI simplifies the inspection procedure compared with MPI. There is no harsh requirement on the surface condition and surface working is greatly reduced. MSI is a scanning NDT technique comparable to other scanning techniques like ultrasonic or Eddy Current automated inspection systems. It is flexible in respect to the design and dimensioning of the sensor system. Therefore the access to surfaces with complex

geometries is less difficult. Furthermore, this method is free of contamination and doesn't demand any post-processing beside demagnetization if it is required.

However, until now MSI can be applied only after a successful performance demonstration that validates its use for the inspection problem of concern. There are no general technical rules and procedures applicable as provided by engineering rules for standard NDT methods [DIN2001, ASTM2009, Schm1989]. Therefore we have to consider the control of all system parameters of MSI that may influence the defect detection of the system, especially the magnetization (magnetic flux) as required also for MPI and the guidance of the magnetic sensor or sensor array (lift-off, tilt). Since MSI is a scanning technique similar to automated ultrasonic inspection we have to prove the completeness of inspection for the chosen scan index, for example. Also, we have to establish rules for the best use of sensors that depend on material properties, component geometry, crack orientation, etc. Nevertheless, the criteria for quality controlled inspection procedures and performance can certainly also be met by established and recognized engineering rules since these are rather common and certainly less complex than those for MPI. MSI is already applied and common for special inspection problems of limited or difficult access conditions, especially after the successful development of stray flux pigs for the in-service inspection of gas or oil pipelines [Nest1999]. The sensor based MFL inspection has gained more and more attention not only by inspection companies but also as a matter of engineering with the objective to use MSI systems also as an inspection tool integrated into production lines.

One of the key issues for the automation of sensor based MFL inspections is scanner technology. Accurate, fast but complete scanning of the component surface is crucial because sensor lift-off and scanning index may influence the sensitivity of flaw detection and the reproducibility of inspection results.

The Fraunhofer Institute for Nondestructive Testing, (IZFP) has developed automated scanners for sensor based MFL testing. One scanner consists of a 3-axis manipulator applicable to objects of elementary shape and relative small dimensions, e.g. flat surface, cylinder geometry, etc. The second scanner, a six-arm articulated robot of extremely high accuracy was used for the inspection of components with free form geometry. However, the use and handling of the robot is time consuming because of its general purpose design and the related complex programming and controlling [Karn2009]. We are still missing an automated but flexible sensor based MFL inspection tool that can be adapted to specific inspection problems and integrated into the workflow of a production.

Nowadays, the use of industrial robot is increasingly common in various areas of industry. The motivation for robotized production (and inspection) can be explained by the high reliability and availability of robotized processes and the resulting increase of productivity and decrease of costs. Industrial robots have become a trend setter for the development of automation technologies and handling systems. They symbolize industrial automation and progress in advanced manufacturing.

As a good example, we may consider also ultrasonic inspection systems where scans must be performed very precisely or under difficult access conditions. Figure 1-1 shows the robot supported ultrasonic system used for the inspection of nozzles of nuclear reactor pressure vessels [Engl2009, Krön2010]. This application of robots demonstrates the advantage when access is difficult but precise and controlled scanning is mandatory. Figure 1-2 shows the automated inspection of light-weight structures used in the aerospace industry. The ultrasonic inspection is done using a transmission technique with water coupling in a squirting technique that asks for extremely precise positioning of the transducers.

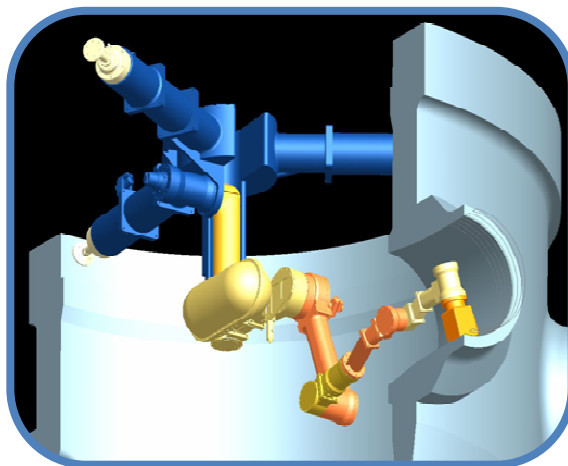


**Figure 1-1 Robot supported ultrasonic system for the inspection of nozzles
[Inte2011]**

Obviously, because of its high efficiency, high precision and the reprogrammable feature, industrial robots are the best choice to develop a robust and universal automatic scheme for sensor based MFL testing. However, both research and development and application of industrial robot for MSI are still in the first stages.

In addition to the already mentioned problem that MSI is not regulated by applicable engineering rules there are also some technical problems we have to face: The use of robots in NDT is not part of common skills and knowledge of NDT engineers and practitioners. Reasons are the complex configuration, the non-intuitive programming

and the very specific control of the robot motion. Therefore one objective of R&D includes both task definition and definition of robot control by external sensors [Bolm2005]. The flexibility in respect to the robot motion control is important in view of the various inspection problems. The flexible motion control is particularly difficult since the system user has to access the core real-time software functions that are critical for the performance and safe operation of the system. Therefore we may ask for a NDT specific scheme to be developed to extend robot applications to this demanding application area.



Figure 1-2 Ultrasonic system with twin robots for the inspection of light weight structures [Inte2011]

It is our general R&D objective to develop a robust and related to NDT applications universal engineering tool for the design and realization of automated MSI systems supported by commercially available industrial robots and modules. The robot supported automation has the following advantages:

1. The programming of inspection scan and its control should become independent of the robot specific programming language, which is not a generally used programming language. The programming of scan features must be easily to use by NDT experts.
2. The NDT expert should be able to modify and adjust the robot supported scanning to various and different inspection problems and component geometries.
3. Scanning speed, accuracy and performance control of inspection can be improved based on performance parameters of industrial robots.
4. We also recommend the numerical simulation of the inspection problem for the system optimization and validation that includes the right choice of sensors and robots. The COMSOL software Multi-physics can be used for this purpose [Nemi2010].

- The inspector may have his own choice on data recorded in real-time for his inspection control. Also, we need some flexibility in respect to the presentation of inspection results meeting the potential requirements of system operators. For example, the scanned surface may be visualized in 3D for a general and fast documentation of inspection results. These visualization techniques are available and can be integrated into robotic tools.

Finally we have to organize a standard link between the inspection computer and the Robot Local Controller. Figure 1-3 indicates a standard structure of robot supported NDT inspection systems [Krön2011].

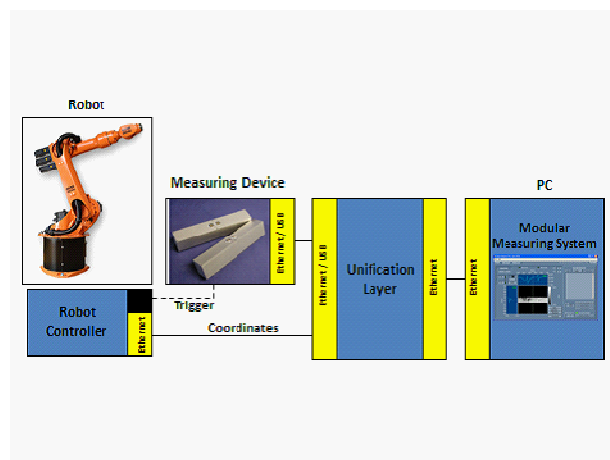


Figure 1-3 Structure of robot supported automated inspection systems

For that reason we propose the Ethernet standard for the communication between the external PC and Robot Local Controller. This link allows controlling the industrial robot by the inspection system computer with the further advantage of implementing commercial or our own software needed or helpful for the inspection. One example is the use of LabVIEW for the programming and control of scans. Third, based on the concept of modular software design, the automated inspection system is composed of several parts viewed as system modules. Each of them is controlled independently. Such a system structure allows the easy change or modification of one or more of the system modules that makes the system design very flexible for different inspection problems. Furthermore, the modular testing system can be combined with other testing platforms, for example with scanning ultrasonic inspection systems with significant cost and time benefits.

The present thesis is structured as follows: In the first introductory part, we discuss the motivation for the present research and the current state-of-the-art. We review the basic theory about MFL testing in Chapter 2 only for a general understanding of the state of this NDT method. In Chapter 3, we focus on the state-of-the-art of automation of sensor

based MFL and robot supported automated scanning. Chapter 4 and 5 form the central part of the thesis and provide insight in the development of the automated inspection system and its application. Finally, conclusion and outlook of the results are presented in Chapter 6.

2 Theory

The physics of stray flux phenomena observed on ferromagnetic materials is well known and described. According to the general common understanding the term ferromagnet is used for materials that are magnetic in the absence of an external magnetic field. The pioneering description and discoveries were made by the Russian physicist Aleksandr Stoletov from the Moscow State University who measured the magnetic permeability, known as the Stoletov curve 140 years ago [Stol1872]. Many textbooks have been written on ferromagnetism and more generally on magnetism but the classic one should be cited here as a reference [Bozo1951].

[Jile1990] gives a guideline to the literature of magnetic methods for nondestructive inspection of materials with emphasis on magnetic particle inspection, magnetic flux leakage, and leakage field calculations.

The main contrast sensitivity for flaw detection is shown by the leakage field strength around a flaw. It is linked linearly with the field strength inside the flaw [Förs1986]. Also the shape, position and size of the flaw are important parameters for their detectability by flux measurement.

Although the physics of magnetism and the related stray or leakage flux phenomena are well described in many publications we will outline some theoretical aspects that are important for MSI:

- The spontaneous magnetization allows MSI of high scanning speed with local magnetization
- We may use rotating magnetic fields for the detection of cracks of arbitrary orientation
- We may understand the nature of false calls caused by the component geometry at positions with sharp edges or also by local permeability gradients as found for example in the heat affected zone close to the weld
- We may assess the sensitivity of flaw detection for various defect types and alignments for the validation of MSI
- Further, the understanding of the principles of stray flux phenomenon helps to establish the criteria for reliable inspection performance.

2.1 Ferromagnetism

Magnetism is one of the basic physic properties of the material. The macro-magnetic property appears if the energy of the material changes with the external magnetic field. From the microscopic point of view, the movement of charged particles forms a moment unit and the magnetic property appears if all the moments align themselves.

Ferromagnetism is a type of magnetism in which the magnetic moments of atoms in a solid are aligned within domains in the absence of an applied field, below a temperature known as the Curie temperature. The susceptibility for ferromagnetism is noticeably greater than other kinds of magnetism such as diamagnetism, (order of magnitude is about -10^{-6} ~ -10^{-3}) and paramagnetism, (order of magnitude is about 10^{-6} ~ 10^{-2}).

Ferromagnetic materials include (at room temperature) iron, nickel, cobalt and some of the rare earth elements, such as gadolinium. Ferromagnetism is produced by two types of electron movement: rotation of electrons around atomic nucleus and electrons spin. Both movements of an electron can be seen as closed current, magnetic moment is produced by these two kinds of closed current. The magnetic moment produced by the rotation movement around the atomic nucleus is the so-called orbital magnetic moment, and magnetic moment produced by an electron's spin is the so-called spin magnetic moment. The internal magnetic moment which is the vector summation of all the magnetic moments is zero when there is no external magnetic field, no magnetism appears; when an external magnetic field is attached, magnetism appears after the magnetization.

The basic properties of ferromagnetism are spontaneous magnetization which is caused by electrons exchange interaction of adjacent atoms and the magnetic domain. Exchange interaction occurs when two atoms approach each other and exchange energy is produced when all the magnetic moments in one tiny region align themselves in one direction. Although magnetic moments in any tiny region of ferromagnetic material align themselves in one direction, the material has no net magnetism as a whole. The reason is the existence of magnetic domain, the so-called tiny region in which all the magnetic moments align themselves in one direction. The directions of magnetic moment in domains are different, therefore net magnetic moment which is the superposition of the all the magnetic moments of domains is zero, hence, no magnetism appears for ferromagnetic material without external magnetic field (except for permanent magnet).

When ferromagnetic material is placed in a magnetic field, strong magnetism appears when magnetic moments in every domain align themselves in the same direction as the

external magnetic field. The interlayer by which the adjacent domains are separated is called the domain wall; thickness of which is approximately equal to several hundred times that of atom distance. From a stability point of view, the domain structure possesses the lowest level of energy.

The process from the disordered state to the orderly state of the magnetic domains in ferromagnetic material is called magnetization. It is accomplished through the shift of domain wall and the rotation of the domain.

2.2 Magnetic flux leakage testing

2.2.1 Principle of MFL testing

A crack whether in the internal structure or on the surface is one of the most dangerous defects requiring detection. It is defined as discontinuous: one direction has a relatively large surface, and the other direction can be neglected.

In MFL testing on ferromagnetic material for surface crack, the ferromagnetic specimen usually has a higher magnetic permeability than the surrounding medium. This leads to an increase in the density of magnetic line of flux flowing through the specimen with respect to those flowing outside. Hence, a surface-breaking defect presents high reluctance to the flow of magnetic lines of flux, thereby causing the flux lines to leak out from the specimen surface [Dutt2009a, Dutt2009b].

This magnetic flux leakage field is postulated to contain information about the shape and size of the defect, as well as the permeability of the specimen and the strength of the applied magnetic field.

2.2.2 Description of flaw induced magnetic flux leakage

Methods used to describe the magnetic flux leakage on a defect include the analytical method, numerical method and approximation model. Due to its complexity, the analytical method is limited to use only in some of the simplest cases. [Förs1985, Shu1977]. The numerical method is frequently used in practice, but it is very time-consuming [Dobm1980, Syku1884] and the model method can be used for appraisal of the magnetic field [Muzs2003, Shur1988, Zag1998, 1994].

2.2.2.1 Analytical solution

When there is a surface-breaking, most of the flux lines are diverted around the defect, generating opposite magnetic polarities or a dipolar magnetic charge DMC on the defect walls. The DMC generates its own field and the problem becomes analogous to a uniform electric charge distribution.

The magnetic field $d\vec{H}$ generated at a distance \vec{r} by this element of charge dp is given by

$$d\vec{H} = \frac{dp}{4\pi r^3} \vec{r} \quad (2.1)$$

The magnetic dipoles distributed on the walls generate the magnetic leakage field out of the crack.

The leakage flux over a crack can be simplified as a field. The leakage field of a surface-breaking crack is a function of the applied magnetic field strength, crack dimensions and permeability [Edwa1986].

The shape of the cracks is mainly composed of rectangular and V-shaped crack [Förs1986]. Therefore, the rectangular crack as a basic but important defect form has obtained a lot of attention [Zhan2009]. A rectangular slot is used as a simplified representation of a surface-breaking crack, assuming a constant pole density on their faces [Zats1966, Shch1972].

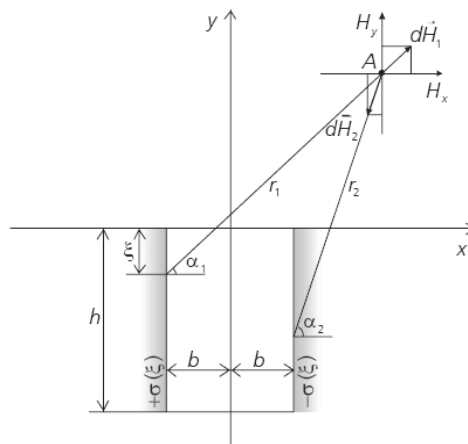


Figure 2-1 Calculation of the magnetic field over a crack with the help of the magnetic charge

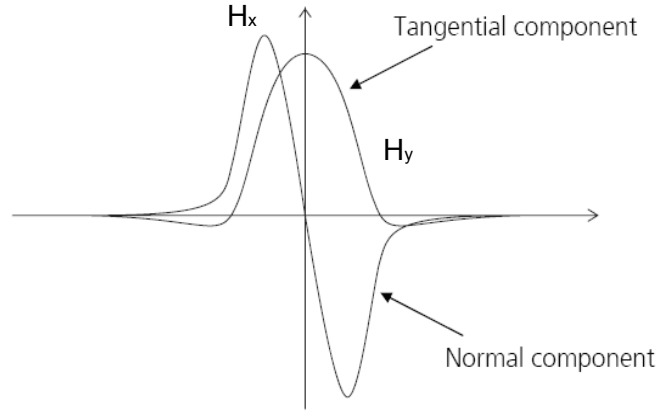


Figure 2-2 Schematic of the tangential and the normal component of the magnetic leakage field

Expressions for the leakage field of rectangular slots assuming a constant pole density on their faces:

$$H_x = \frac{\sigma}{2\pi} \left[\arctan \frac{y}{x-b} - \arctan \frac{y}{x+b} + \arctan \frac{y+h}{x+b} - \arctan \frac{y+h}{x-b} \right] \quad (2.2)$$

$$H_y = \frac{\sigma}{4\pi} \ln \frac{[(x+b)^2 + (y+h)^2][(x-b)^2 + y^2]}{[(x+b)^2 + y^2][(x-b)^2 + (y+h)^2]} \quad (2.3)$$

The model provides good qualitative agreement with experimental measurements.

If $b \ll y$ and h , then Equation 2.2 and 2.3 can be approximated by

$$H_x = \frac{\sigma b}{\pi} \left[\frac{y}{x^2 + y^2} - \frac{y+h}{x^2 + (y+h)^2} \right] \quad (2.4)$$

$$H_y = \frac{\sigma b}{\pi} \left[-\frac{x}{x^2 + y^2} + \frac{x}{x^2 + (y+h)^2} \right] \quad (2.5)$$

2.2.2.2 Numerical computation

It is difficult to model the MFL with analytical method because of the complicated and irregular boundaries associated with realistic defect shapes and the lack of generality. Those are necessary assumptions needed to obtain traceable analytical solutions [Edwa1986, Cata2003].

The finite element method (FEM) has been proven to be an effective method [Kato2003] that helps in understanding the ways in which fields and defects interact to produce

measurable indications and to investigate the detectable MFL signals under various measurement parameters. Due to the increasing computational capabilities, finite element analysis method is already comparable with analytical method since the pioneering numerical modeling of MFL phenomena by Lord and his co-workers [Mand2003]. The MFL problem is treated as magneto-static problem by the magnetic scalar potential method. It can be expressed by Maxwell equations below:

$$\vec{\nabla} \times \vec{H} = \vec{j} \quad (2.6)$$

$$\vec{\nabla} \cdot \vec{B} = 0 \quad (2.7)$$

where \vec{H} is magnetic field intensity. Vector \vec{j} is applied source current density vector and \vec{B} is magnetic flux density vector.

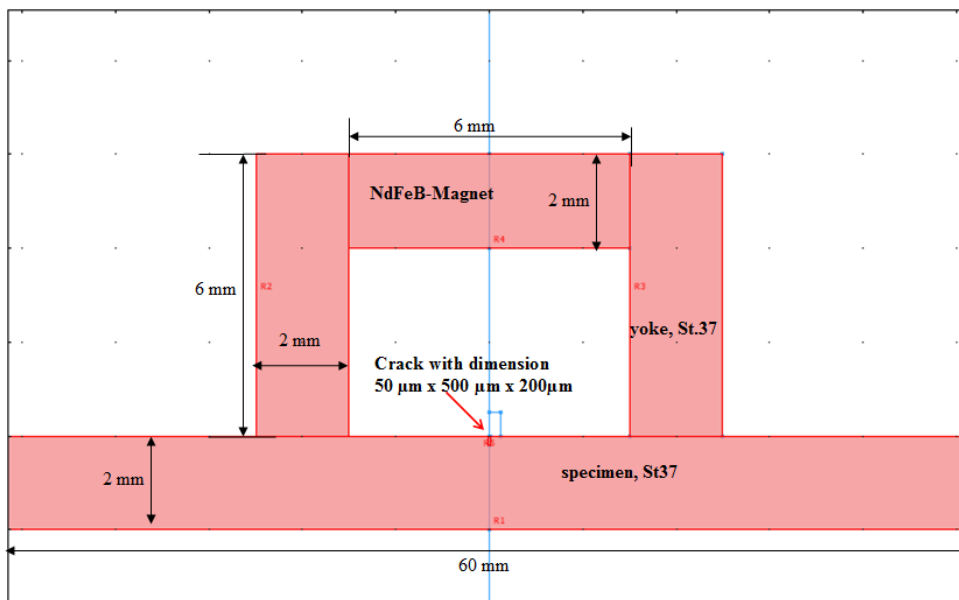


Figure 2-3 2D Model for simulation of magnetic field distribution

In industrial practice, due to welds, debris, surface processing states of work piece and etc., lift-off of magnetic sensor during the MFL testing is unavoidable. Lift-off is a highly critical parameter in the MFL technique and has the potential to affect the acquired magnetic flux leakage data. With the given parameters of a crack, the magnetic leakage field density is mainly determined by two factors. The first one is the air gap between the specimen and the sensor, i.e. the lift-off value of the sensor, the other one is the magnetic condition [Kato2003]. This is simulated by applying COMSOL (3.5a) software and enables qualitative evaluation of the sensor lift-off effect on the measured MFL signal. Using a two-dimensional model for simulation, the plate has a relative size

compared to the defect as shown in Figure 2-3. The surface crack has a dimension of $500\ \mu\text{m} \times 200\ \mu\text{m} \times 50\ \mu\text{m}$ (length \times depth \times width).

The specimen is magnetized by a permanent NdFeB-Magnet. B-H curve is shown in Figure 2-4. The material of the yoke and the specimen is the steel St.37.

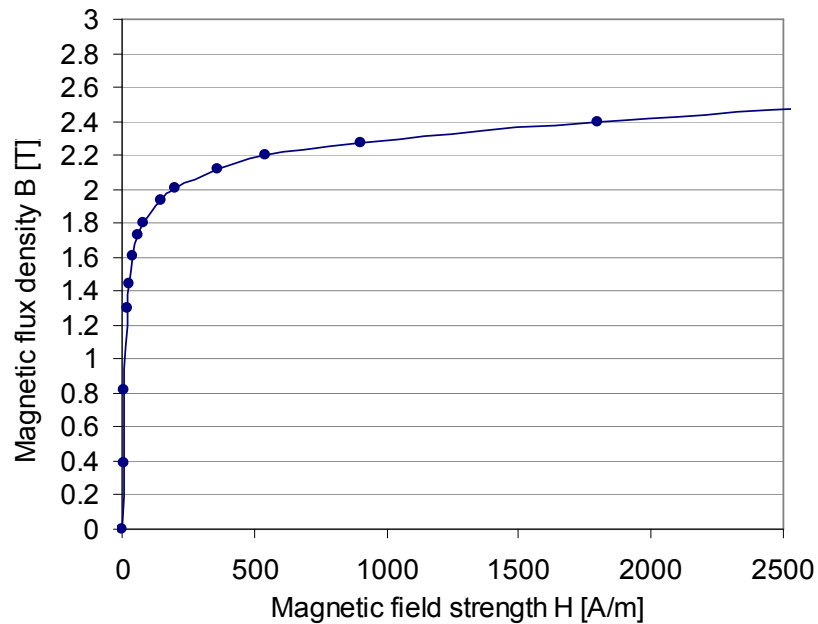


Figure 2-4 B-H curve of St. 37

Due to the symmetry of the model, a quarter model simulation result is shown in Figure 2-5.

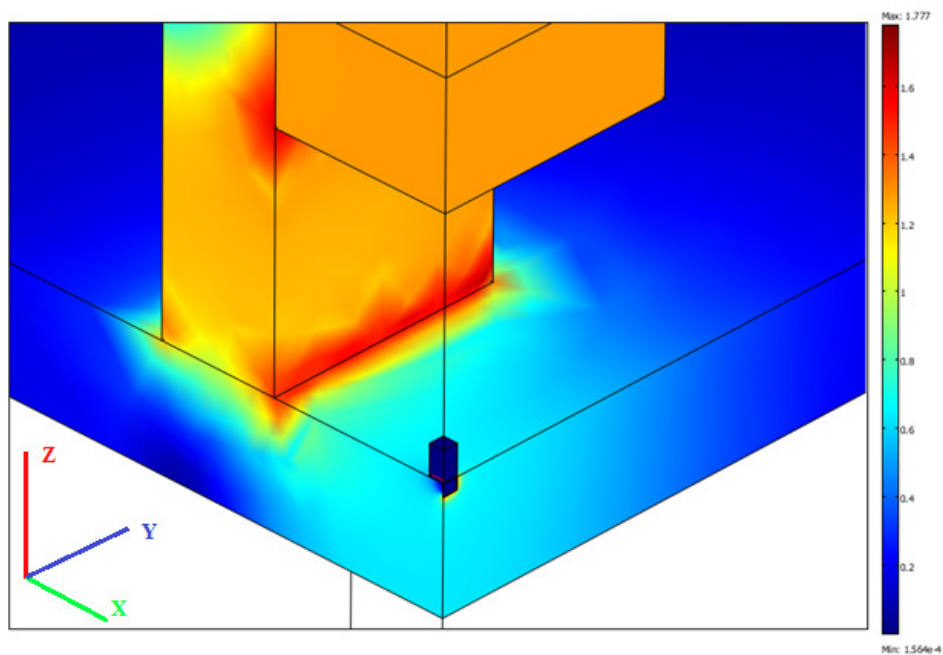


Figure 2-5 3D Simulation result

The magnetic leakage field around the crack is detected at sensor lift-off at 0 μm , 2 μm , 5 μm , 10 μm , 20 μm and 50 μm respectively.

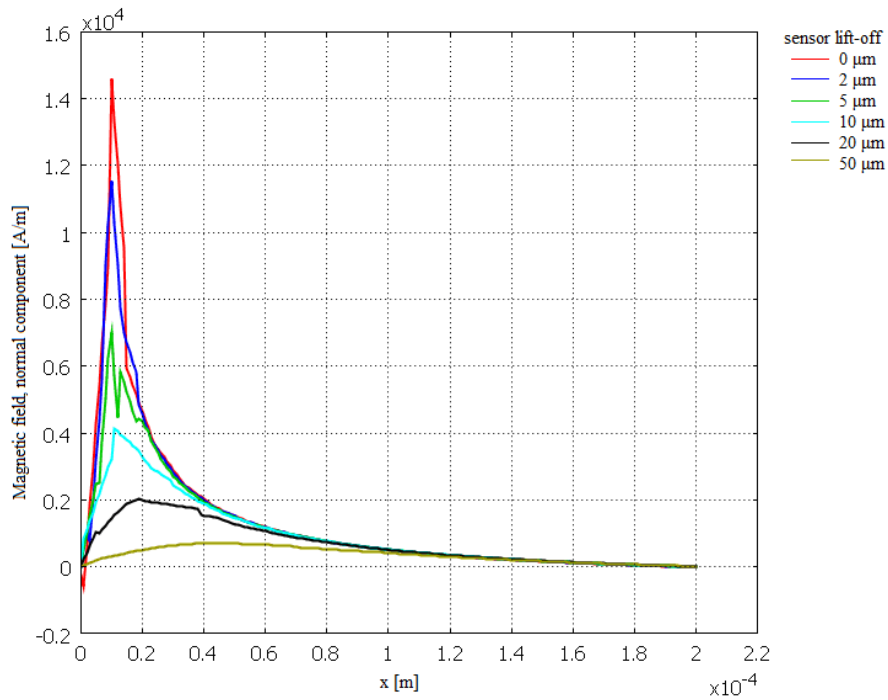


Figure 2-6 Normal component of magnetic field strength detected with different sensor lift-off

At low lift-off, the normal component of MFL signal exhibits sharp positive and negative peaks. At higher lift-off, the signals are broadened.

Influence of sensor lift-off

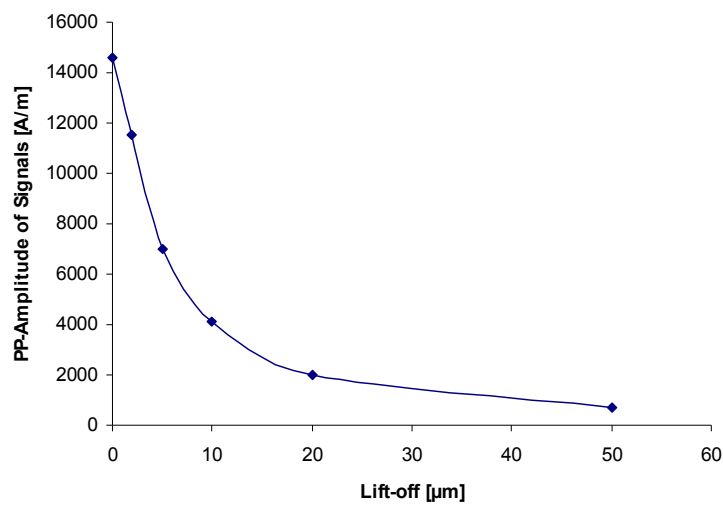


Figure 2-7 Sensor lift-off effect on measurement result

As shown in Figure 2-7, low levels of sensor lift-off have a significant effect on the measured peak flux leakage magnitude. The magnitudes of MFL components decreased drastically as lift-off increased.

In this section, magnetic leakage field around a defect is studied by the numerical method. The obtained quantitative simulation results can serve as comparative data for experimental and analytical solutions. The inverse problem process for crack characterization can be greatly simplified. Additionally, the simulation result also demonstrates how the magnetic signals are influenced by parameters configured during the scanning and referenced for design of the automated scheme of MFL testing with enforced detectability is provided.

2.2.3 Magnetic particle inspection

Magnetic particle inspection has been extensively employed for the non-destructive testing of ferromagnetic material for the past eighty years. The method is particular sensitive to fine surface-breaking cracks. [Edwa1986].

Fine ferromagnetic particles are used to make the flux leakage visible. The magnetic particles are attracted by the surface field in the area of the defect and hold on to the edges of the defect to reveal it as a build up of particles.

Particles are made of metal with high magnetic permeability and low retentivity. High magnetic permeability is important because it makes the particles attract easily to small magnetic leakage fields from surface-breaking crack. Low retentivity is important because the particles themselves never become strongly magnetized so they do not stick to each other or the surface of the part. Typically, particles are tiny milled pieces of iron or iron oxide with pigment boned to their surface which gives color to the particles. Particles are available in a dry mix or a wet solution.

The magnetic force on a particle can be described as:

$$\vec{F}_m = \mu_0 (\vec{p}_m \cdot \nabla) \vec{H} \quad (2.8)$$

Here, \vec{p}_m is the magnetic moment of the particle

The magnetic moment of one particle can be described as:

$$\vec{p}_m = V \vec{M} = V \chi_p \vec{H} \quad (2.9)$$

Where V is the volume, \vec{M} is the magnetization and χ_p is the susceptibility of the magnetic particle. Under the action of the magnet field, the particles turn into a line with the magnet pole $+m$ and $-m$ in a line with the magnet field line.

The function (2.8) can be rewritten as:

$$\vec{F}_m = \mu_0 V \chi_p (\vec{H} \cdot \vec{\nabla}) \vec{H} = \mu_0 V \chi_p \left[\vec{\nabla} \left(\frac{1}{2} H^2 \right) + \vec{H} \times (\vec{\nabla} \times \vec{H}) \right] \quad (2. 10)$$

The information included in these functions can be concluded as follows: First, magnetic force in direction along which the magnetic field changes is the maximum force. This leads to the result that magnetic particles gather along the crack where the local magnetic field change is maximal. Second, the force decreases drastically with the distance. For a concealed defect, the force acting on the particle will be very weak. Thus, the difficulty of inspection is significantly increased due to the dependency of detectability of the inspection on the field gradient. Figure 2-8 shows a result of wet MPI on test block.

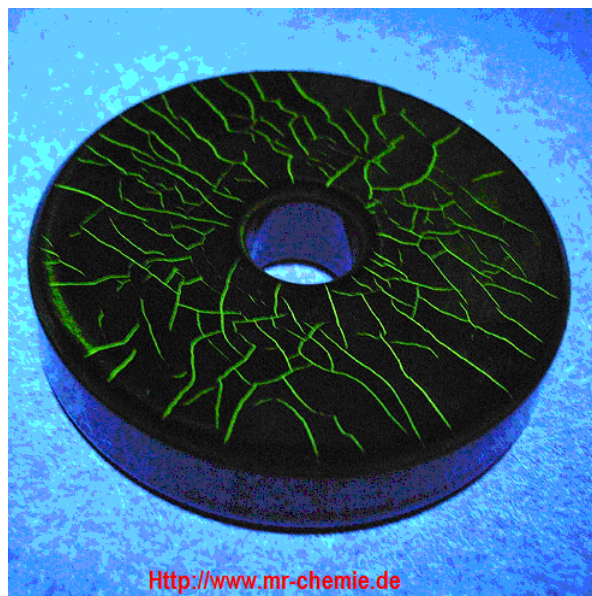


Figure 2-8 Result of Magnetic particle testing on standard test block

2.2.4 Sensor based MFL test

Due to its advantages over MPI in many aspects, a sensor based MFL testing has gained much attention by researchers and users. It has recently been more widely applied in industry with the fast developed magnetic sensor technology.

The Hall sensor and GMR sensor are the magnetic sensors that most likely to meet the requirements of a variety of tests due to their dynamics, relatively small dimensions, easy to control and economical factors [Klos2008]. They are designed based on the Hall Effect and GMR effect respectively.

Hall Effect

Hall-effect was discovered in 1879 by the American physicist Edwin Hall. It makes the measurement of magnetic field possible by utilizing the Lorentz force acting on the moving charge in a current-carrying conductor.

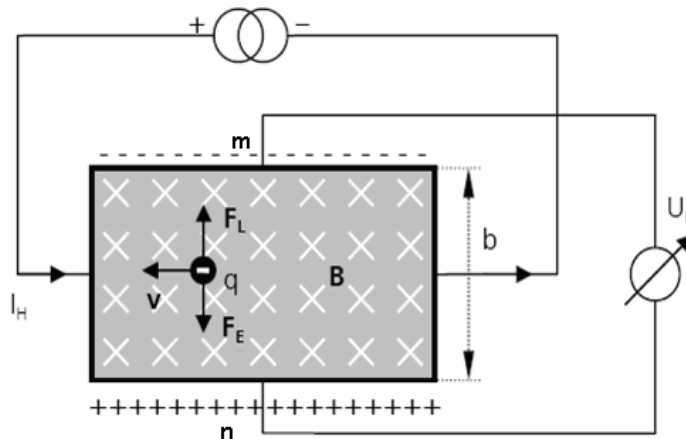


Figure 2-9 Schematic description of the Hall Effect in a plate

The magnetic forces press the charge carriers towards the upper boundary of the plate so that a Hall voltage appears between the charge edges of the plate [Tipl1994]. The Hall effect occurs in any conductor carrying a current with the presence of a transverse magnetic field. The current flowing through the conductor is formed through the movement of many small charge carriers. Charge carriers which are moving at the speed v experience the so called Lorentz force if a magnetic field with the magnetic flux density B is present and the field direction is not parallel to the motion of the charge carriers. Direction of the force is vertical to both the moving direction of charge carriers and the direction of the magnetic field. The Lorentz force can be described as:

$$F_L = qv \times B \quad (2.11)$$

Here q denotes the electrical charge of a carrier v is the velocity of a charge carrier and B is the magnetic flux density, which is perpendicular to the strip plane.

In Figure 2-9, the moving path of the charge carriers are distorted due to the Lorentz force, direction of the force is from n to m, an electric field with the intensity E develops between m and n through accumulation of the charges on the m side. At the same time, charge carriers experience a force from the electric field E . The direction of the force is

also vertical to the moving direction of the magnetic field but opposite to the direction of the Lorentz force.

$$F_E = qE \quad (2. 12)$$

The electric field intensity keeps increasing until F_E is equal to F_L . No distortion will happen for the following charges carriers.

$$F_E = F_L \quad (2. 13)$$

$$vB = E \quad (2. 14)$$

The voltage between both sides of the electric field can be described as:

$$U_H = Eb = vBb \quad (2. 15)$$

Since a constant current can be defined as the total charges flow through the cross-sectional area of the conductor at the unit time; the current run through the plate can be described as:

$$I_H = nqvA \quad (2. 16)$$

Here, I_H is the current across the plate length, n is the charge carrier density and A is the cross section area.

Equation 2.15 can be rewritten as:

$$U_H = \frac{I_H B b}{nqA} = \frac{I_H B}{nqd} \quad (2. 17)$$

The Hall voltage U_H is proportional to magnetic field intensity. The magnetic field intensity can be determined by the Hall voltage measured. The Hall sensor has the sensitivity direction vertical to the sensor surface, which makes it suitable to pick up the normal component of the magnetic field.

2.2.4.1 GMR Effect

Giant magneto-resistance (GMR) effect is a quantum mechanical magneto-resistance effect observed in ultra-thin film structures composed of alternating ferromagnetic and non-magnetic layers. The effect was first discovered in the multilayer structure of

Fe/Cr/Fe layer as a large change in resistance with a magnetic field [Baib1988]. In comparison to conventional anisotropic magneto-resistors (AMR) which exhibit a change of resistance less of than 3%, various GMR materials achieve change of resistance of 10 to 20%.

GMR films usually have two or more magnetic layers separated by a non-magnetic layer. These layers are typically just a few nano-meters thick, and the thickness of the layer is critical. Only within a certain thickness, the polarized conduction electrons cause anti-ferromagnetic coupling between the adjacent ferromagnetic layers, making it energetically preferable for the magnetizations of adjacent layers to align in a anti-parallelization [Grün1986].

A common term to describe the physical mechanism of GMR is spin dependent scattering. The GMR effect is due to differences in the conduction properties of spin-up and spin-down conduction electrons. These differences arise because certain metals have a sizable mismatch in the density of states for up and down electrons at the Fermi energy. When two magnetic thin films are separated by a nonmagnetic film thin enough to allow electrons to pass from one magnetic layer to another, those electrons probe the density of states of the other magnetic layer.

When the magnetization directions of two magnetic layers are parallel, their state densities are spatially matched and no unusual scattering occurs. But when the two magnetizations are anti-parallel, the electrons which traverse the non-magnetic layer experiences an inversion of the three-dimensional density of states upon reaching the other magnetic layer.

In other words, electrons that were spin-up become spin-down, and vice versa. The mismatched densities of states of the two anti-parallel magnetic layers result in increased scattering. The most common base systems are Co/Cu and Fe/Cr. In practice, the structures are more complicated. Due to spin-dependent scattering of the conduction electrons, the resistance is at its lowest level when the layer's magnetizations are parallel at presence of external magnetic field and at highest level when their magnetizations are anti-parallel. It is true for all GMR structures [Carb1987].

The most common structures in GMR sensors include anti-ferromagnetic multi-layers, unpinned sandwiches and anti-ferromagnetic pinned spin valves.

Figure 2-10 shows the structure of a spin valve. It consists of two ferromagnetic layers (alloy of nickel, iron and cobalt) separated by non-ferromagnetic layer (usually copper). One of the ferromagnetic layers is "pinned" by the adjacent anti-ferromagnetic layer in a fixed direction. The other magnetic layer can rotate freely. AFM stands for

anti-ferromagnetic, FM for ferromagnetic, and NM for non-ferromagnetic. Red point stands for spin up electrons while blue point for spin down electrons. The corresponding arrows across the spin valve show the electron path. A bend in the path shows that an electron was scattered. If the external magnetic field is applied in a direction parallel to the magnetization of the pinned layer, magnetization directions of both ferromagnetic layers are the same.

As shown in Figure 2-11 a, in the presence of an external magnetic field, the magnetization directions of both ferromagnetic layers are the same. Spin up electrons that have the same direction as the magnetization direction of the ferromagnetic layers can easily go through both of the magnetic layers and present a low level of resistance. On the contrary, it is difficult for spin down electrons to go through the ferromagnetic layer whose magnetization direction is opposite to electron spin direction. Thus, the number of the electrons that go through the layers is reduced and a high level of resistance is presented. Lower equivalent resistance is shown, and in Figure 2-11 b, the magnetization directions of both ferromagnetic layers are opposite. Electrons go through the ferromagnetic layers easily when magnetization direction is the same with the electron spin direction and scattering happens if the two directions are not parallel. Higher equivalent resistance is shown.

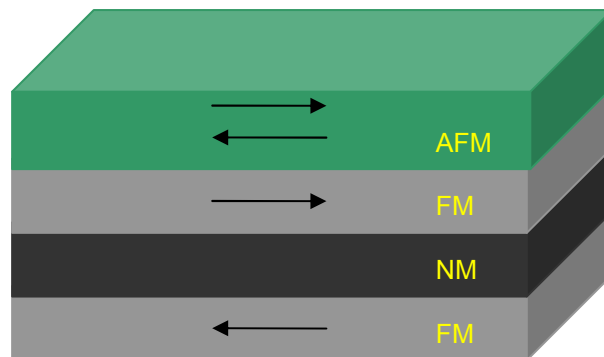
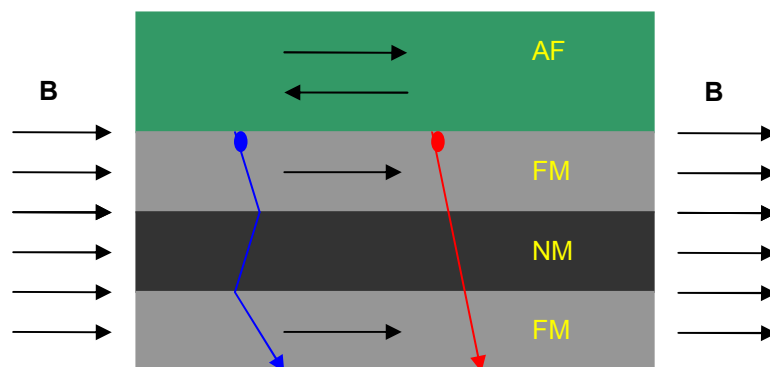
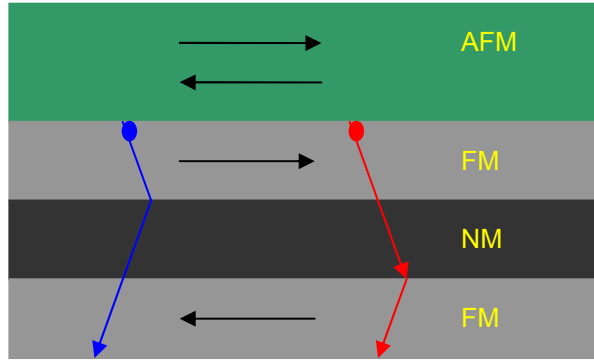


Figure 2-10 Spin-valve Structure



a. With magnetic field



b. Without external magnetic field

Figure 2-11 Schematic diagram of GMR effect

$$\Delta R = R_{anti} - R_{par} = R_{max} - R_{min} \quad (2.18)$$

$$GMR = \Delta R / R_{min} = (R_{anti} - R_{par}) / R_{par} \quad (2.19)$$

Here, ΔR is the magnitude of the maximum change of resistance as angle between two ferromagnetic layers changes from parallel to anti-parallel, R_{par} is the resistance when the layers are parallel, and R_{anti} is the resistance when the layers are anti-parallel.

The MFL testing with a magneto-resistive sensor (MR sensor) can not only deal with a changing field but also with a stable field. GMR was first made possible for magnetic field measurement in 1991 after the GMR effect was found at room temperature [Park1991]. The sensitive direction of GMR sensor is parallel with the sensor surface, which make it suitable for recording the tangential component of the magnetic field. A GMR-gradiometer has a direction dependent sensitivity, and allows us to detect the crack with a tendency which is vertical to the sensitivity direction.

GMR-gradiometer based MFL testing is very similar to the magnetic particle inspection, by which only the local field fluctuation is recorded in the magnetic sensor signal. The low frequency field variation has no influence on the test value. Thus, external factors which are recorded by both sensor elements are cancelled out and have no influence on the testing result.

The expression of the tangential field in equation 2.4 can be rewritten as follows if GMR-gradiometers are used:

$$H_x = \frac{sb}{p} \left[\left| \frac{y}{x^2 + y^2} - \frac{y+h}{x^2 + (y+h)^2} \right| - \left| \frac{y}{(x-a)^2 + y^2} - \frac{y+h}{(x-a)^2 + (y+h)^2} \right| \right] \quad (2.20)$$

Here, a is the distance between the sensor elements of the gradiometer.

In order to get the maximal H_x , sensor distance of the sensor element can be at least

$$a = \sqrt{\frac{2yh + h^2}{1 - \frac{y}{y+h}} - (y+h)^2} \quad (2.21)$$

In the equation (2.21), a also determines the highest resolution the inspection can reach by applying GMR-gradiometers. It also indicates the influences of lift-off on the testing result.

2.3 Micro-magnetic testing technique

3MA is a non-destructive testing technology developed by IZFP for characterization and defect detection on ferromagnetic material. The name 3MA stands for micro-magnetic, multi-parameter, micro-structure and stress analysis [Dobm2007]. This technology combines four different electromagnetic testing methods: Magnetic Barkhausen noise analysis, upper harmonic analysis of tangential magnetic field strength, incremental permeability analysis and multi-frequency eddy current testing in one portable equipment (3MA – II), analyzing up to 41 micro-magnetic parameters, simultaneously. Mechanical properties, hardness, hardness depth, yield stress and tensile strength etc. can be measured using this methodology after the device is properly calibrated.

Why are these micro-magnetic properties of ferromagnetic materials suitable for microstructure characterization in terms of mechanical properties? The reason is that the lattice defects such as vacancies, interstitials, dislocations, precipitates, grain boundaries and phase boundary etc. are responsible for strengthening by impeding dislocation movement under mechanical loads. The same lattice defects impede the Bloch wall movements which are the essential micro-magnetic events under magnetic loads, i.e. when the material is magnetized in a hysteresis loop.

3 State of the art

Surface crack may lead to serious accidents in aviation, train transportation and so on. Due to the fact that a surface with a crack is much weaker than the internal part, but has to bear a larger load, the stress concentrations increase the crack and lead to disruption. Serious accidents caused by such disruption happen each year in the world. Therefore, surface crack detection plays a pivotal role in product quality inspection and operation process monitoring. Alone in Germany, there are more than one billion parts per year tested for surface cracks non-destructively in the automotive industry [Vett2006].

The magnetic flux leakage testing is one of the most sensitive methods for crack or discontinuity detection on ferromagnetic material. MPI has already been applied for crack or discontinuity detection on ferromagnetic material for more than 80 years. Due to its high sensitivity and simplicity of the test equipment, it is applied widely in various industrial fields. With the high productivity and low-cost oriented modern industrial production, automation of NDT is to be enhanced to adapt to modern industrial production. However, the development of automation of MPI is restricted due to the complexity of the whole process. Another MFL testing method, the sensor based MFL which shows its potential for automation of MFL becomes a focus and a new research topic.

3.1 Magnetic particle testing

The magnetic particle inspection technology is one of the most sensitive and simple NDT methods for crack detection on ferromagnetic materials. The use of iron particles to locate defects in magnetized articles stems from the observations by Hoke in 1917 in the United States and others in the United Kingdom [Love1993]. Due to the high sensitivity and the simplicity of the experimental equipment, the method spread wildly in the industrial area after the successful application for weld seam inspection. Up to now it is commonly used to inspect the surface crack in the important industrial field, e.g. railway wheels, railway track and railway axis for rail way traffic field, gas or oil pipeline for petrochemical industry as well as weld joints inspection for the automobile industry [Vett2006].

Nowadays, since NDT is an inevitable step in the production process, a fully automated and production line integrated NDT system is in great demand to adapt to the quality reliability, high productivity and low-cost oriented modern industrial production. A lot of

researchers have dedicated their effort to develop the automation of MPI in the recent years. In the railway traffic field, with the high safety standards required in the management of railroad lines, railway wheels are inspected directly after production in order to detect the presence of surface cracks that may seriously affect the integrity of the railway. An automated system designed for non-destructive testing of railway wheels based on MPI is introduced by Starman [Star2007]. Instead of searching defects manually with ultraviolet lights in the traditional way, a high speed and a high resolution digital camera is applied in the automated system to scan the whole surface of wheel with diameter from 500 mm to 1300 mm. Warning is given if any surface flaw is detected.

However, there is a common weak feature of these automatic schemes: they are specifically designed to detect specific work pieces and are not able to adapt to test of specimen with different forms. Such an automatic scheme is seldom affordable for small and medium sized enterprises due to the high cost to update the automatic system frequently for different objects. Therefore, an object of the existing automatic schemes to improve the level of automation of general MFL is restricted.

Furthermore, it is complicated and difficult to automate the whole process of MPI due to its own nature. There are a large number of parameters related to MPI and the interaction of these parameters is strong. The appropriate choice with the purpose of getting accurate measurement is heavily dependent on the experience. Additionally, too many alternatives and interaction of the parameters leads to uncertainty in the sensitivity and detectability, therefore it is very difficult for the process operator to keep all these variables consistent [Love1993, Ched2003].

For result evaluation, visual test is automated by using a digital camera to mechanically scan the surface of component and the image algorithm is applied in image processing, but the influence of human factors on the measurement result still can not be eliminated [Star2007].

As a conclusion, the process of MPI is dependent on operator experience, thus making the measurement very easily affected by human factors and the repeatability of the measurements cannot be guaranteed. A less human-dependent experience and more flexible method are urgently needed to automate MFL.

3.2 Sensor based MFL

The sensor based MFL is another magnetic flux leakage testing method. It uses a magnetic sensor rather than magnetic particle to capture the magnetic leakage field

signal. Sensor based MFL is characterized with low cost, high checking speed, robustness and high sensitivity to large classes of defects. It has gained much attention not only from researchers but also from users of MFL.

Dobmann et al. investigated the influence of various affecting factors of the magnetic flux leakage testing with sensors [Dobm1987]. The equivalence of detectability of the sensor based MFL to the MPI for surface crack detection of ferromagnetic components has been proven by Kloster in his PhD thesis with analytical, numerical and experimental investigation, respectively. It is concluded that the sensor based MFL has advantages not only in the detection of near-surface defects but also in the detection of surface cracks [Klos2008].

GMR line sensor is used by Kataoka to visualize the magnetic field distribution near a defect, the result shows that a magnetic leakage field distributed near the defect can be detected and the shape of defect is identified [Kata2002].

A sensor based MFL for the inspection of a welded seam in steel production is introduced by Ewald. Enhanced sensitivity and detectability of the MFL testing was obtained with improvement made in sensor system [Ewal2003]. Hwang et al. introduces a new and unique method for small crack detection on express train wheels with the Hall sensor. High speed and high spatial resolution are achieved with the linearly integrated Hall sensor array [Hwan2007, Hwan2009].

An initial testing is described by Atzlesberger to test the potential and effectiveness of a sensor based MFL testing method for material testing by applying rather inexpensive but highly sensitive GMR sensors. The encouraging results show the great potential and effectiveness of GMR sensor based MFL in material testing [Atzl2010].

In order to obtain the distribution of the magnetic flux leakage, the surface of the test specimen is to be mechanically scanned by using a sensor based MFL testing. The detectability of a flaw by using this method largely depends on the magnetic flux density passing through a specimen to be examined or on the intensity of magnetic field acting in/on the specimen [Kato2000]. However, scanning speed and sensor lift-off which are greatly influenced by the surface condition of a specimen are two of the most important factors that influence magnetic flux leakage density which is caused by a flaw on specimen during the magnetic flux leakage testing [Klos2008, Dutt2009a]. Furthermore, sensitivities of magnetic sensors which can be applied for magnetic flux leakage field detection are usually direction dependent, various scan modes are in demand during the automatic scanning, and these factors are automatic scanning system dependent [Muka1988, Klos2008]. Thus, besides the optimization of sensor solution to which much

effort has been given, improvement of automatic scanning of specimen surface for high accuracy, high efficiency and high flexibility by which sensor lift-off and scanning speed are accurately controlled is also crucial and prerequisite to high detectability and sensitivity of the sensor based MFL method.

3.3 Automatic schemes for sensor based MFL

The current automated MFL measuring system applied at IZFP is a 3-axis manipulator based automatic measuring system. The system hardware consists of a manipulator, a controller and an external control PC. The drives used in the linear axes are three step motors with step of 12.4 μm which ensures high accuracy, high repeatability of the sensor based MFL testing. Reach of each axis are X= 500 mm, Y= 530 mm, Z= 260 mm respectively, by which the component to be inspected is restricted in its size. With a CNC controller, C142-4, three stepping motors are controlled to be able to make 3-dimensional linear interpolation and 2-dimensional circular interpolation. Manipulator controller is connected to external PC the serial interface RS232. The software system running at external PC is responsible for the scanning task management and measurement result demonstration.



Figure 3-1 ISEL scanning system

The capable scanning path of the 3-axis manipulator is demonstrated in Figure 3-2.



Figure 3-2 Realized scanning path with 3-axis manipulator

There is also a specifically designed scanning system for special areas of inspection. Figure 3-3 shows a mobile measurement system for diagnosis of prestressed tendons. A rotor with integrated Hall sensors scans the surface of bridge deck. The rotor has a diameter of 3.3 m and rotates with a rotating speed of 2 Hz. Linear speed can reach 720 m/h. Rotating probe and scanning path is demonstrated in Figure 3-4. The system is

especially suitable for automated inspection of prestressed steel rupture in concrete plates that have large flat surface.



Figure 3-3 Mobile measurement system for prestressed tendons rupture detection on bridge decks (TU Berlin)

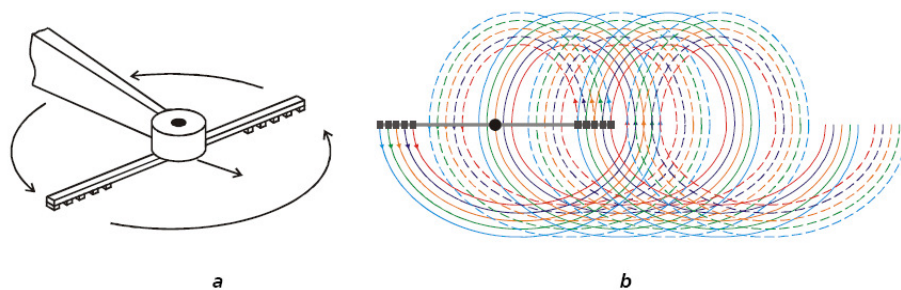


Figure 3-4 Schematic descriptions of the rotating head and the sensor traces

Figure 3-5 shows another specifically designed automated scanning system for steel rod in production area. The system is capable of scanning rod specimens with diameter ranging from 30 cm to 100 cm and a length of up to 10 m with a scanning speed of 40 cm/s in circumferential direction.

Although the existing automated measurement systems mentioned above have been considerably improved in the efficiency and accuracy of the sensor based MFL testing, they are either designed for the inspection of a component with flat surface or designed for the inspection of component in a specific industrial area, and they are unable to deal with a wide variety of work pieces of varying size, shape and surface conditions. An automated sensor based MFL testing system with high accuracy, high efficiency, high flexibility and handling ease is still missing.



Figure 3-5 Sensor based MFL measurement system for surface defect inspection on steel rod

3.4 Standard industry robots and its application in NDT

In modern industry, standard industrial robots are commonly used in various areas due to their most significant capability to reduce cost and improve productivity. The level of automation of modern production lines are symbolized by the most advantageous robot technology applied in industry. An industrial robot is defined by ISO 8373 as an automatically controlled, reprogrammable, multipurpose manipulator programmable in three or more axes, which may be either fixed in place or mobile to be used in industrial automation applications [ISO1994].

Industrial robots have the capability to perform efficiently, reliably, with low cost and they can be used in hazardous environments. In order to meet the requirements of the modern industry: improving productivity and product quality but as well as reducing labour cost, industrial robots are applied across a wide range.

Industrial robots are the key component of industrial automation. Japan, by far the most automated country in the world, has the highest robot density with 310 operating robots per 10,000 employees in the manufacturing industry. It is followed by Germany, with an operating density of 234 robots per 10,000 employees in the manufacturing industries.

The application of industrial robots is becoming more and more popular. In 2007 alone, 114,365 new industrial robots were installed worldwide and in this year the world market grew by 3%. At the end of 2008, more than 1 million industrial robots were operating worldwide in factories and in dangerous or tedious environments. By the end of 2011 more than 1.2 million industrial robots will populate the world, which is reported by the IFR Statistical Department in the new study "World Robotics 2009".

Industrial robots were originally used in automotive industry. One robot per 5 production workers were operating in the automotive industry in Japan. Tailored robotic solutions are offered increasingly by robot suppliers for various areas including welding, painting, assembly, handling, packaging and palletizing, product inspection and testing. With the further development of techniques, applications will become more versatile. Improvements in sensor technology like robot vision, force sensing and environment recognition applications will enhance quality control and inspection. Improvements in system technology, such as off-line programming, safety and multi-robot cooperation will guarantee sophisticated solutions for automating processes.

According to the report from International Federation of Robotics in 2010, the four most widely used types of industrial robots are articulated robots with a market share of 60%, gantry robots with a market share of 22%, SCARA (Selective Compliant Articulated Robot Arm) robots with a market share of 13% and cylindrical robots with a market share of 4% [IFR2010].

3.4.1 Most widely used robot in industry

3.4.1.1 Articulated Robot

Articulated robots are the most versatile robots being used in industry. The word articulated means jointed. Articulated robots are robots with rotary joints which are arranged in a chain. Number of joints can range from two to ten. Typical articulated robots have five or six free programmable arms or axes. The more joints an articulated robot has, the greater the range of motion. It can generally achieve any position and orientation within the working envelope.

Figure 3-6 shows an articulate robot with 6 degrees of freedom. The three basic rotary joints are able to perform arm swing, shoulder swivel and elbow rotations that allows the positioning in 3D space (X, Y, Z). The additional 3 revolute joints make them capable of the movements roll, yaw, and pitch, which is for orientation of the end effector. Pitch is up and down movement, yaw is right and left movement, and roll is rotation. Articulate robots are compact and provide the largest work envelope relative to their size. They also have some advantages over other types of robots in payload capacity and flexibility. This makes them suitable for a wide variety of industrial applications. Nowadays, they appear more frequently in manufacturing lines, mainly used for welding, painting, gluing, grinding, packaging, material handling, and assembly.

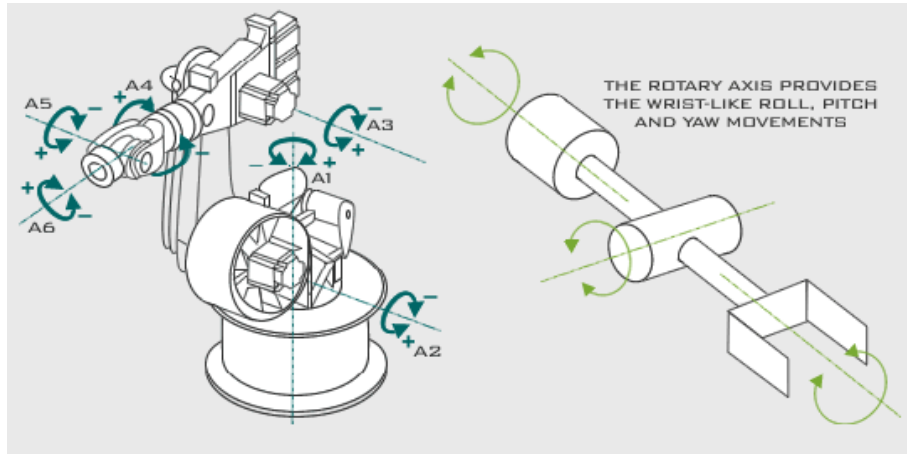


Figure 3-6 Articulated robot

3.4.1.2 Cartesian coordinates Robot

A Cartesian coordinate robot (also called a linear robot) is an industrial robot that has three principal prismatic axes which are at right angles to each other. The three axes are coincident with a Cartesian coordinator. Cartesian coordinate robots with the horizontal member supported at both ends are sometimes called Gantry robots. They are often quite large.

Cartesian robots have a rectangular work space. Due to the mechanical arrangement of this kind of industrial robots, robot control and programming is relatively easier than other kinds of industrial robots such as articulated robots.

Because of the linear nature of their movements, Cartesian robots are inherently more accurate than rotary motion style robots such as the SCARA (in 3.4.1.3). However, typical Cartesian robots have offered a trade-off of lower speed for this greater repeatability. They usually require large volumes to operate and their linear joints are difficult to seal which makes them unsuitable for use in damp and dusty environments.

The Cartesian Coordinate Robot's relatively simple design and straightforward operation make it highly desirable in manufacturing. A popular application for this type of robot is a computer numerical control machine assembly and material-handling applications, additionally they are also widely used for automatic assembly, laboratory measurements, and testing.

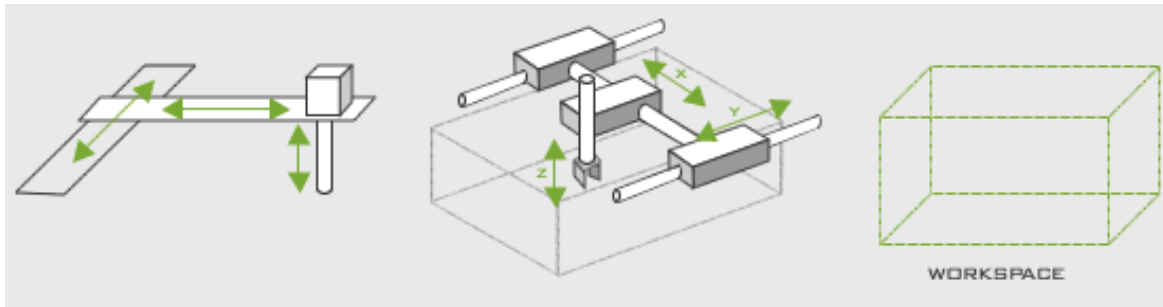


Figure 3-7 Cartesian coordinate robot

3.4.1.3 SCARA robots

The SCARA acronym stands for Selective Compliant Assembly Robot Arm, sometimes also referred to as Selective Compliant Articulated Robot Arm. It was developed based on the concept presented by Sankyo Seiki, Pentel and NEC in 1981. Due to the parallel-axis layout, the arm of the robot can be compliant in the X-Y direction but rigid in the “Z” direction.

The selective compliant feature of the SCARA robot which provides substantial rigidity for the robot in the vertical direction but flexibility in the horizontal plane makes it suitable for many types of assembly operations. Because of their relative high speed, compactness, installation flexibility etc, they are also advantageous for a variety of general-purpose applications requiring fast, repeatable and articulate point to point movements such as palletizing, de-palletizing, machine loading/unloading, pick-and-place and packaging applications in addition to assembly. The electronic printed circuit board industry, in particular, uses large numbers of SCARA robots for placing semiconductor IC. Disadvantages are relatively high cost compared to other types of industrial robots because of the requirement for specialized controlling software with inverse kinematics for linear interpolated moves.

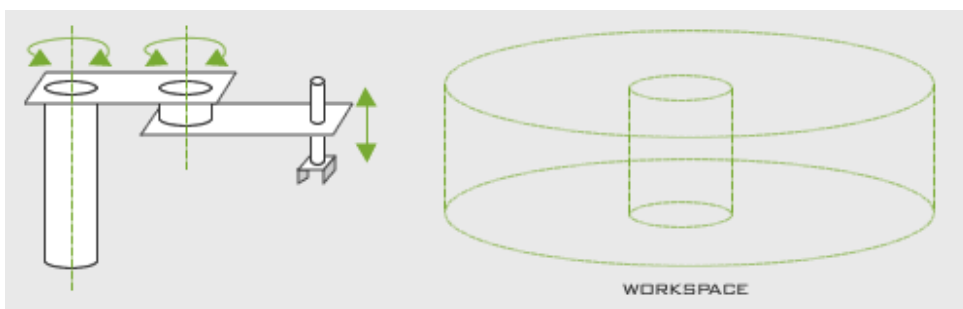


Figure 3-8 SCARA robot

3.4.1.4 Cylindrical Robot

The classical Cylindrical Robot has two linear axes and one rotary axis around its origin by which a cylindrical coordinate system can be formed. The workspace is a cylinder.

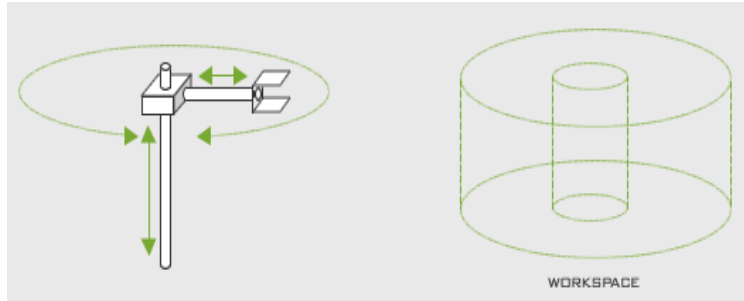


Figure 3-9 Classical cylindrical coordinate robot

3.4.2 Application of industrial robot for NDT Automation

With the reprogrammable capability and prominent features such as high efficiency, stable repeatability and high endurance, the application of industrial robots in the NDT field becomes more popular.

One trend of NDT is the automation of the inspection process with the objective to meet the increasing requirement of high accuracy, low cost as well as the ability to meet the requirement of scanning more complex specimen forms. Robotic technologies are more and more frequently applied in inspections in order to meet the needs of NDT development. Robotics will be the main challenge in the future for non-destructive testing automation.

Sackenreuther et al. used two synchronized palletizing Robots to replace the linear controlled scanner-mechanical application which till now widely used in ultrasonic testing with phased array technology [Sack2009].



Figure 3-10 Synchronized Robot used for Ultrasonic NDT

Robot supported measurement of surface structure in complex freeform using air ultrasonic technology has been introduced by Dillhöfer et al. [Dill2009]. An articulated robot was used as the manipulator of the sensor for discrete scan of the specimen surface. The surface form is recorded for reconstruction of the defect's structure, position, size and orientation. As a result of the mechanized scan, reproducibility and efficiency has been greatly improved.



Figure 3-11 Robot based surface structure detection with UT method

Haase et al. has introduced a Charon XRD X-ray robot diffractometer for the non-destructive characterization of near-surface material states concerning residual stresses and work hardening on large components with complex geometries in a paper: "Charon XRD- a New Twin Robot X-ray Diffractometer for Surface Analysis of Complex Aircraft Components", see Figure 3-12.

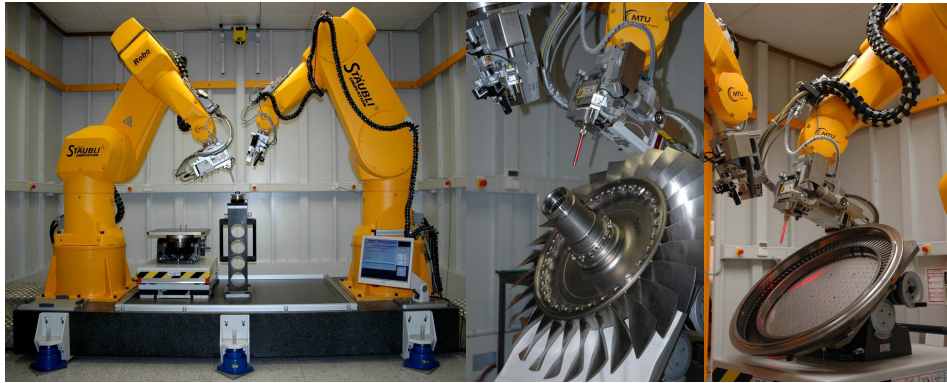


Figure 3-12 Application of Robot team for X-Ray NDT testing

Two six-axis RX170B-HP industrial robots from Stäubli™ have been used to guide an X-ray tube and the detector respectively. The robot has a range of 1835 mm and a maximum load capacity of 60 kg with the best presently available spatial positioning accuracy of ± 0.5 mm and angular accuracy of $\pm 0.03^\circ$. Repeatability of this type of robot is about ± 0.04 mm under constant temperature [Haas2006]. Standard software SEIFERT RAYFLEX software is used to control the diffractometer. The use of the industrial robot in NDT permitted the improvement of test productivity.

The precision is already proven by the successful application of robots in several types of non-destructive testing and also in some traditional human-dependent fields. Synoptically, because of its high efficiency, high precision and the reprogrammable feature, a standard industrial robot is our best choice to develop a robust and universal automated scheme of sensor based MFL testing by which sensor motion and sensor lift-off is accurately controlled during the scanning even on components with complex forms. However, the research and development for the application of a standard industrial robot in sensor based MFL testing is still in its first stage. There are two main problems hindering such research and development, one is related to the complexity of robot path planning and robot controlling for ordinary users of the measurement system, the other is about the low efficiency universal property of robot reprogramming for inspection. These can be concluded from the applications of robots for NDT automation at IZFP.

Complete testing of the volume range is necessary for NDT of specimens with uneven surfaces for the quality and safety. For the ultrasonic testing of the specimen, position of the UT probe must be vertical or at an angle relative to the surface to ensure that the component is acoustically irradiated with maximum energy. The test for complex

geometry with a free form surface is usually carried out manually in a time-consuming manner using ultrasonic test methods in immersion baths.

Effort has been made to automate the testing process but still an automatic reproducible test is only possible where the surface permits a precise, well-defined acoustic irradiation and ultrasonic probe-to-specimen contact, for instance on sufficiently planar surfaces. In which case, the probe scans across the surface at a predefined distance using scan systems, usually an X-Y-Z scanner.

For automatic testing of complex geometries with free-form surfaces, test equipment was designed and set up by Herzer et al. by using a precise 6-arm articulated robot. The robot used is μ -KRoS316 from BGT GmbH. Unlike the standard test and assembly robots, its individual axes do not have a mechanical gear. Each of its three rotation and bending axes has three directly driven DC motors and high accuracy optical angle sensors which ensure its precision. It possesses a static repeatability of 5 μm compared to a repeatability of 0.1 to 0.5 mm that can be achieved by an ordinary articulated robot. The repeatability during movement is 10-50 μm , depending on the current motion and the speed of the robot [Herz1995].

The space coordinates of any point of the tested specimen can be obtained during testing with a coordinate frame linked to the piece. For robot programming, after the coordinate frame is linked to the specimen, characteristic surface points are roughly predefined manually with a mechanical sample after the gridding of the specimen surface. At each point of the grid, first the robot is placed manually about 2 mm above the point, then it moves along the positive direction of the principal axis of the sample. The space coordinates can be recorded as soon as the surface is reached and then the robot moves up again to the next grid point. The grid point is limited within 16 \times 16 points for speed reasons [Karn2009]. With the points recorded and a bicubic splines interpolation, grid points are interpolated and normal parts are calculated. The rough approximation is then refined automatically by a non-contracting technique where the distance between the ultrasonic probe and the work piece surface is measured using the time-of-flight of the ultrasonic signals. Data collected in this way is used to reconstruct the surface geometry. In the second step, the robot automatically performs the high-frequency ultrasonic test.

Path calculation of the robot, control of the UT probe, mathematical reconstruction of the specimen surface, data acquisition, storage and evaluation of the measurement values are carried out in a computer. The inverse transformations of the coordinates in the Cartesian coordinate system into the axis specific coordinate (axis angles) system are

achieved by using the software developed by the company Bodenseewerk, in cooperation with IZFP. With menu driven software, components with almost any free-form surface can be rapidly acquired, modeled and tested with a freely selectable path of very high resolution [Herz1995].

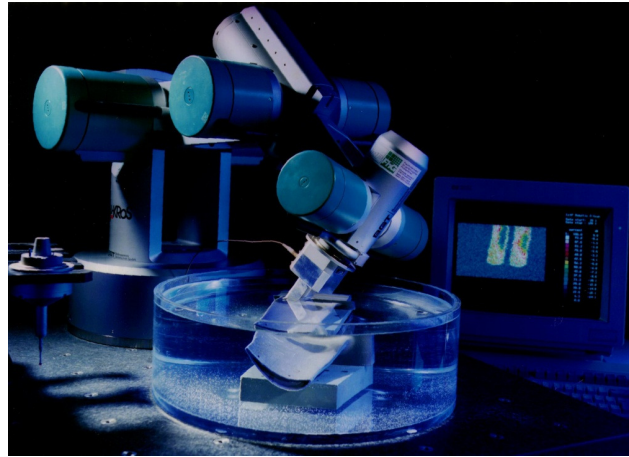


Figure 3-13 Robot guided high frequency test center inspecting a Turbine blade

Another application is the residual stress state investigation on thin ferromagnetic films. Barkhausen noise technique which can be used to sense variations of micro-structural and to display the stress state are applied to evaluate the maps of the residual stress distribution for the given objects, the shower head “GROHE Tempesta Mono” with complex geometry and ferromagnetic multi-layer coating. The coating is vulnerable to physical contact. To perform the inspection, the electromagnetic sensor should be separated from the specimen surface by applying a controlled sensor lift-off. However, as the magnetic field induced by the sensor yoke fades exponentially with the growth of the distance, the distance should be kept as small as possible.

Precise positioning of the sensor is ensured by applying the extremely precise robot; μ -KRoS 316 articulated robot from BGT with algorithms computing scan trajectories and including sensor position and orientation. Software implementation of the robot coordinate interface which involves forwards and backwards robot kinematics computation problems has been developed to enable the tasks of the scan trajectories planning.

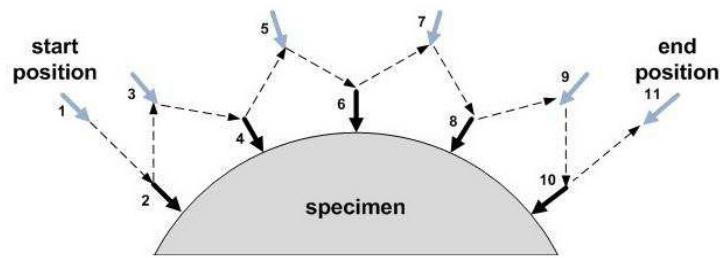


Figure 3-14 Point-to-point manner of robot movement path, Solid arrows represent the sensor positions and orientation in 2D-plane; dashed lines shows the robot movement path

The robot is operated in point-to-point manner. A number of intermediate positions of the trajectory are required in order to avoid physical damage of the specimen and the sensor.

The experimental result shows that, crude errors which may be introduced by human factors into the data acquisition process can be eliminated. The time used to compute the robot coordinates is negligible in comparison with the sensor positioning time and the Barkhausen noise acquisition time. The BGT μ -KROS316 Robot can also be equipped with variety of sensors for non-destructive testing applications. However the complexity of the inverse kinematic computation of this kind of articulated robot has prevented their wide use for NDT at IZFP [Karn2009].

3.5 Robot based automatic scanning

In order to utilize an industrial robot for NDT automation, robot scan path planning and movement control are two essential issues to be considered.

3.5.1 Robot programming

In a review of robot programming systems written by Lozano-Perez [Loza1982], the programming system was divided into three categories, (a) guiding system, (b) robot-level programming system and (c) task-level programming system. For guiding systems the robot was manually moved to the desired position and the joint position recorded. For robot-level systems a programming language was provided with the robot. Task-level systems specified the goals to be achieved for example, the position of objects. Programming of an industrial robot can be defined as two types, one is off-line programming and the other is a learning based system (robot teach) [Neto2008]. In the

off-line programming method, the programs are created separately and subsequently integrated with the robot. On the contrary, for the learning based method the robot has to be involved during the programming process.

3.5.1.1 Off-line programming

Text based robot programming

An original method of controlling industrial robot is the off-line programming with the text based robot specific language. Most industrial robots have their own specific language for programming. A good example is the robot programming language KRL specific for KUKA robot. Despite the simplicity and efficiency of the robot specific programming language, their application is limited due to some drawbacks such as the lack of a universal standard of the robot languages from different robot manufacturers. Thus a program written for one robot cannot be used for robot from other manufacturers. This creates many challenges for systems comprised of multiple robots from different manufacturers.

In order to avoid collision or damage caused either to the robot or the tools mounted on the robot, the robot program written off-line can be tested with the simulation software which is usually supplied by the robot manufacturer with the robot specific programming language.

Robot program generation based on CAD data

In traditional off-line programming, the robot path is generated from a CAD model of the work piece. Robot motion information is then extracted from DXF file which is generated from a CAD application such as AUTOCAD. The prerequisite of the method is having the 3D drawing of the specimen and the surroundings such as a base that supporting the specimen [Boop1995, Freu1998, Rubi1998, Chan2003, Norb2004, Kim2004, Neto2010]. Modelling of the specimen and the environment could be achieved with CAD if they are not available depending on the knowledge of the operator.

Pires et al. introduced a CAD interface for automated robot welding programming [Norb2004]. The solution starts by having a 3D drawing of the specimen and the environment. The 3D models are supposed to supply useful information such as work piece size and position in space precisely. Scan path should then be defined and organized in the desired sequence by drawing all the trajectories required to scan the specimen, using available layers. That is to say, use one layer for each trajectory. A trajectory is composed of a start-point and an end-point, both with orientation and the type of motion (scan trajectory or help trajectory). Parameters such as velocity are

introduced in the selected layer just by adding labels with the corresponding values. Thus the DXF (Drawing Exchange Format) data generated from CAD application includes all the information added to specify the scanning process. It is converted into robot commands that can be immediately tested for detailed performance. The whole process can take several hours.

For a KUKA robot, programming with the help of KUKA Robot specific software technology package KUKA.CAMRob is an example of using the CAD data for the robot path programming. Scan path programming of the specimen with DXF geometry models provided are carried out by converting the model into the program file which is the executable for a KUKA robot. The software technology package KUKA.CAMRob works as a data interface which enables programming the paths, area sizes and shape of scanning directly from the manufacturer's CAD data.

However, the prerequisite for this solution is that the DXF geometry models must be available. This is not the case for most of the specimens waiting to be tested. Additional specific software must be installed on the external control PC and robot controller respectively before the technology package can be utilized. Extensibility and flexibility of the method are restricted by the specificity of the software technology applied.

3.5.1.2 Robot teaching

Manual training system with teach pendant

Robots can also be taught via a teach pendant. It works as a handheld control and programming unit. The common features of such units are the ability to manually control the robot and move the robot to desired positions. Robot motion parameters such as speed can be adjusted to be suitable for measurement tasks that require precise positioning and scanning processes. Scanning path of the robot can be taught by moving the robot along the surface of the specimen in the initial run during which the target points are stored. The stored target points can be used to program the robot scanning path and control the robot to carry out the scanning during the subsequent runs.

For complex robot movement programming, the teaching process by using a teach pendant is very time-consuming and complex and cumbersome. Once the path has been planned using a teach pendant, modification to the robot scanning path or motion parameter is very troublesome as the same steps have to be repeated.

Lead-by-the-nose

Lead-by-the-nose is a technique offered by most robot manufacturers to teach the robot. In this method, one user holds the robot's manipulator, while the other users enter a command which de-energizes the robot causing it to go limp. The first user then moves the robot by hand to the required positions and along a required path on the probe surface while the software logs these positions into memory. The program can later relocate the robot to these positions or along the taught path. This technique is popular for tasks such as paint spraying.

Touch sensing

The physical geometrical characteristic of an object can be measured and defined by a touch sensing probe attached to the robot. Renishaw is a kind of touch probe which can be applied in touch sensing. Robot scan can be carried out with the geometry obtained by touch sensing method. Furthermore, with applications that require a much higher degree of precision, a touch sensing probe can be used to compensate for deviations in the shape or position of object.

3.5.2 Robot kinematics

The movement path of the robot has been decided after the robot programming process. That means the desired coordinates of end effectors during the movement is already stored in the robot controller, the next step is to control the robot to fulfill the movement. The most important issue is the transformation of the coordinates of the end effectors from one coordinate system to another coordinate system. For example, to move the robot to a desired position with coordinates in Cartesian coordinate system, the task will be accomplished by moving the joints and links which forms a kinematic chain. But how much should the joints values be set if a desired position in the space is to be reached and where are the end-effectors located when joints of the kinematic chain has moved by a certain angle? Both questions are associated with the robot kinematics solving the transformation of the coordinates among different coordinates system. These two issues are essential for the robot control.

Robot kinematics consists of forward kinematics and inverse kinematics. Forward kinematics can be used to calculate the corresponding end-effectors position for the given joint positions while the inverse kinematics can calculate the values of the corresponding joint variables for the given actual end-effectors pose. Both kinematics processes are very complex. Inverse kinematics is usually much more complex than the forwards kinematics. This can be concluded from the application of BGT μ -KRoS316

robot at the IZFP by Karnauhov [Karn2009] for the investigation of residual stresses in thin ferromagnetic film.

For the robot application by Karnauhov, a mathematical formulation given by John Craig [Crai2004, Karn2009] is applied for the transformations taking place in the kinematic chains of the manipulator for the forward kinematics of the μ -KRoS316 Robot.

Actions of each joint of the BGT μ -KRoS316 robot are described by a single real number (here the angle of rotation since the robot has only one kind of joint, the revolutionary joint. This means that each joint has only one degree-of-freedom.

A Coordinate frame is attached rigidly to each link in order to perform the kinematic analysis. The matrix which expresses the position and orientation of each coordinate frame is obtained from the basic translation and rotation transformations based on the fact that both translation and orientation transformation of the robot movement can be represented by a 4x4 homogeneous coordinate transformation matrix. The resulting matrix representing the position and orientation of the end-effectors is obtained by multiplication of the homogeneous transformation matrix obtained from the basic translation and rotation transformation.

$$T_0^6 = A_1 \times A_2 \times A_3 \times A_4 \times A_5 \times A_6 \quad (3. 1)$$

T_0^6 is the resulting matrix representing the end effectors position and orientation. A_i , $i=1\dots 6$ are the homogeneous transformation matrix that expresses the position and orientation of the coordinate frame $O_i X_i Y_i Z_i$ with respect to the frame $O_{i-1} X_{i-1} Y_{i-1} Z_{i-1}$. The resulting matrix is very complex. 196 instances of addition/ subtraction operations and 256 instances of multiplication operations are required for a single coordinate calculation using the matrix equations approach according to the result stated in the thesis.

For the inverse kinematics of the μ -KRoS316 Robot, solution obtained from the forward kinematics.

$$H = T_0^6(\theta_1, \theta_2, \theta_3, \theta_4, \theta_5, \theta_6) \quad (3. 2)$$

H represents the desired position and orientation of the end-effectors.

The inverse kinematics aims for the solution of $T_0^6(\theta_1, \theta_2, \theta_3, \theta_4, \theta_5, \theta_6) = H$. According to the forward kinematics, there are 6 equations with 6 unknown elements after simplifying of the equation set because of the simplicity of the link parameter of the BGT

μ -KRoS316 robot. The equations are nonlinear and transcendental, they are quite difficult to solve. Furthermore, for the general mechanism with 6 degrees of freedom the kinematics equations would be much more complex than the equations obtained by application of BGT μ -KRoS316 robot. The inverse kinematics can be simplified by restricting the workspace based on the following facts:

- The specimen dimensions are rather small in comparison with the robot dimensions
- The sensor is directed towards the specimen
- Elbow-up configuration
- The first three joint coordinates are supposed to be positive

The problems of computing the inverse kinematics are preceded by dividing the inverse kinematics problem into the kinematics of position (the coordinates of the wrist) and the kinematics of orientation (orientation of the wrist with respect to the base frame taken in angles). Geometric approach and algebraic approach are applied respectively after the decoupling procedure. The results obtained from the inverse position kinematics have been used in the inverse orientation kinematics in order to solve the matrix equations. A coordinate interface is developed based on the both forward and inverse computation. From the computation process of the forward and inverse kinematics for the BGT μ -KRoS316 robot, we can conclude that it is very complex and time-consuming to proceed both forward and inverse robot kinematics computation in order to control the robot.

As far as KUKA robot is concerned, the forward and backward kinematic has been calculated automatically by the robot controller.

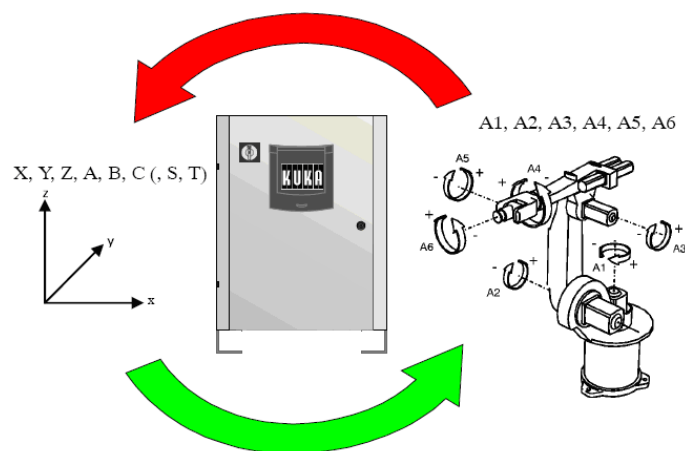


Figure 3-15 Forwards and backwards transformation

Resolvers are used as position sensing systems in KUKA robots. The resolvers are rigidly connected to the motors. The positions of the main and wrist axes (A 1 to A 3 and A 4 to A 6) are sensed by means of a cyclically absolute position sensing system featuring a resolver for each axis. Real-time coordinate can be obtained by accessing system variable of KUKA System software KRL (in section 4.1.4). A singularity problem may arise during the backwards transformation due to the difficulty of setting the axis angles unambiguously. Take the KUKA robot as example: it possesses they have 3 singularity positions: over-head singularity, hand axes singularity, streak location. Behavior of the robot can be settled unambiguously by setting system variable \$SINGUL_POS [1-3] for these three positions, respectively.

3.6 Modular measuring system (MMS)

3.6.1 Modular software concept

Modular software programming is a software design technique that breaks down program functions into modules, each of which accomplishes one function and contains all the source code and variables needed to accomplish that function [Nguy2004]. The need to develop a modular, flexible test software framework has become more evident as the ratio of development costs versus capital costs increases. Application of the approach to test system development which is shifting from using application-specific, turnkey test system to focusing on building a modular test framework ensures not only the acceleration of system development cycle but also the reduction of development cost. The modular test framework is able to accommodate the test requirements of multifunction, module reuse and facilitate the addition of new test technologies for additional test coverage in the future [Ni2011].

Development of a modular software system starts with choosing a software development environment that is designed for efficient programming and quickly performance of any type of measurement and analysis required for the test.

3.6.2 Graphical programming language LabVIEW™

LabVIEW (short for Laboratory Virtual Instrumentation Engineering Workbench) is a kind of G programming language provided by the American company National Instruments. G indicates that the programming language is graphically oriented. The G-program in the LabVIEW program is also called Virtual instruments (VIs). LabVIEW is designed to program efficiently and perform quickly any type of measurement and

analysis required for the test. It is becoming increasingly popular among engineers and scientists for its powerful functions to develop sophisticated measurement, test and control systems using intuitive graphical icons and wires that resemble a flowchart since its first introduction in 1986 [LabV2010]. The most significant characteristic of the programming environment is the graphically oriented and data flow programming manner which ensure that is easy to get started.

3.6.3 Modular Measuring System (MMS) of IZFP

MMS is a measurement platform developed at IZFP using the LabVIEW programming environment [Szie2001]. The concept of MMS is derived from the requirement to combine dynamically the entire function unit on one platform of a system.

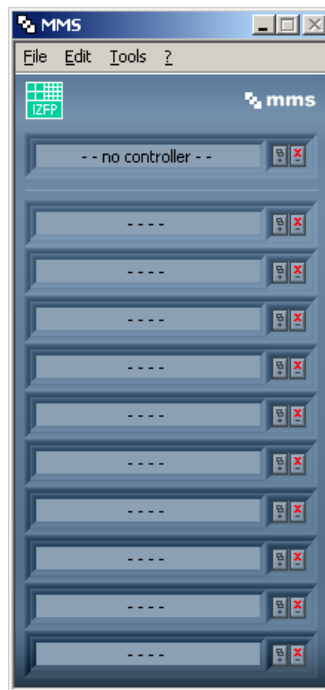


Figure 3-16 MMS operational panel

It is similar to device cabinets with several drawers. Modules will be placed in these cabinets according to the desired implementation order. The MMS main program is responsible for the management of the module integrated on it. It leads information from module to module in cyclical manner. The main program MMS does not necessarily need to know exactly the task of each module. Its task is only to establish storage space which is essentially a data array initialized by a cycle controller in every cycle and a handshake signal which is responsible for the control of the program running cycle.

The modules in the cabinet can be activated from the top to the bottom cyclically after a MMS cycle is started. The modules become activated one after another and handle the

data from the previous module in addition to generating data of their own. The flowing data can be read from each module at any time but can only be written by the module which is activated. Modules are allowed to have a time limit to react but no time limit for data handling, thus every module may block up the system without time limit if an error exists. Also the current selected modules including the position on the screen as shown in figure 3-16 can be stored as a configuration file in order to re-call the used modules as well as the configuration again.

The current module selection, configuration of the module including the position on the screen can be stored as a configuration file for easy use the next time. All the modules will be opened, configured and placed as the last time stored.

3.6.4 Existing MMS modules for MFL scanning

According to the design concept of MMS, software modules already exist at the IZFP for a scanning system based on the ISEL manipulator are subdivided into following types:

4D Scan Controller

The 4D Scan Controller is a universal scanner controller for manipulator with up to 4 axes. It is responsible for measurement sequence control, calculation of the motion path and regulation of the measurement and manipulator movement coordinates.



Figure 3-17 4D Scan Controller

ISEL Positioning System

The ISEL Positioning System is responsible for control of ISEL-step motor controller. With the ISEL Positioning System, manual operation of the manipulator is possible. It is designed for implementation of each movement command.

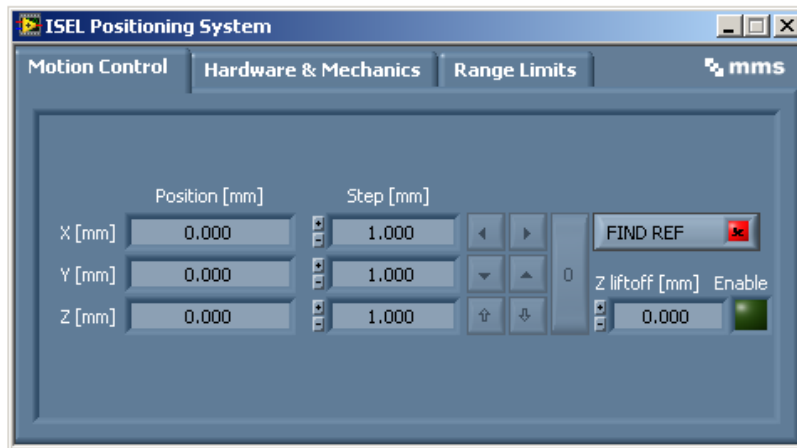


Figure 3-18 ISEL Positioning System

Scan Inspector Pro

The Scan Inspector pro is designed to record the sensor measurement value and coordinates, graphically represent and document the two dimensional scanning results. It also provides the possibility for image processing such as signal filtering, data and calibrated series export in ASCII-Format, polynomial expressions and scripted presentation for the batch processing of measurement series.

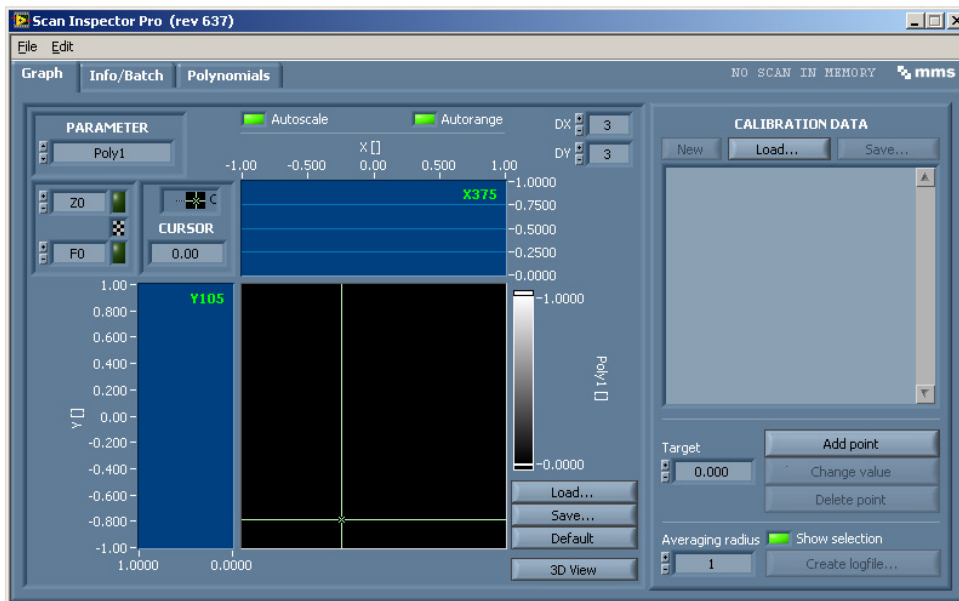


Figure 3-19 Scan Inspector Pro

4 Design and implementation of a modular robotic scanning platform

4.1 Selection and implementation of Robot

Due to the recent developments in information technology and engineering sciences, robots are used in a variety of advanced manufacturing facilities. Robots with vastly different capabilities and specifications are available for a wide range of applications. The selection of robots from a large number of available robots in the market specially for a particular application environment has become a difficult task. Various aspects need to be considered before a suitable robot can be selected. For the application of a standard industrial robot in specific area of automatic material inspection, robot specification and performance desired to be achieved must be considered in detail.

4.1.1 Requirements analysis

The objective of the work is to develop an advanced robot based automated magnetic flux leakage testing system which is characterized by high speed, high resolution and a high level of flexibility. The robot based scanning platform is the most important part of the realization of the automated measuring system. With the geometry features of the components to be inspected becoming more complex, the capability of the robot system for versatile robot motions is required to ensure the automatic and the flexible scanning of the components. Meanwhile, efficient robot motion control and programming has to be developed. In order to meet the various demands on the measurement efficiency and measurement resolution, motion parameters e.g. scanning speed is required to be adjustable. Integration of external sensor technology has to be accommodated in order to ensure more intelligent scanning during the measurement. Furthermore, the most important factors which influence the sensitivity and the detectability of sensor based MFL measurement system should to be taken into account for design of the measurement system, e.g. sensor lift-off, sensor movement speed and direction dependency of the sensor sensitivity etc. The requirements from the end user of the system are mostly concentrated on the efficiency of robot programming and handling of the automated measurement system. The analysis and the management of measurement tasks, the development of robot program, the measurement data

evaluation, the presentation of results and the documentation are desired to be performed with ease.

4.1.2 Specific consideration for robot selection

The requirements resulting from the above analysis can be concluded as demands on performance, controlling/ programming and safety system, respectively.

Performance characteristics

As for the performance characteristic, an articulated industrial robot with 6 arms is selected to ensure the ability of the system to inspect components with complex geometry. The load capacity is desired to be at least 12 kg in order to accommodate the possibility for integration of other sensor system for NDT testing e.g. the sensor system for thermograph (about 12 kg) without impairing the repeatability and the accuracy of the sensor movement [Offo1991].

The spatial resolution reached during the robotic scanning can greatly influence the detectability and sensitivity of the measurement system. It is required that the spatial resolution should be equal or less than the applied sensor resolution itself. Based on the empirical value obtained in the practical MFL measurement and the requirement of other NDT measurements which the robot is to be involved with, the accuracy of the robot positioning is desired to be less than 0.2 mm [Klos2008].

The demand on the workspace is considered to be medium and can be determined to have at least 600 mm extension. The value is concluded from dimensions of the components to be inspected with the robot based automatic measuring system. Constant speed of the robot is considered to be important for scanning during some NDT measurements. Other characters such as acceleration and weight are not crucial with respect to our application.

Control/ Programming characteristics

The possibility of the integration of the robot with a standard PC should be accommodated in order to facilitate the control and programming of the robot either by robot specific high-level structured object-oriented programming language or with the more commonly used standard programming environment on the standard external PC. Thus, high-speed communication between robot local controller and external PC is to be established with support of standard communication interface e.g. Ethernet-, fieldbus-, serial-, digital-interface from both hardware and software aspects. The available standard communication interfaces also ensure the integration of external sensor

technology to the measurement system, e.g. force/ torque sensor, machine etc., with which more intelligent control of the robot can be realized.

As for robot programming, the capability of online and offline programming and teach programming is essential for a flexible and powerful scanning solution of the measurement. Robot specific simulation software or compatibility with commercially available simulation software such as RobCAD®, ICGRIP®, RobSim®, etc. enables the offline programming. Moreover, the ability to import and to convert of CAD data into robot programs reinforces the offline programming function further and the robot programming is simplified by this method if the CAD data of the component to be inspected is available. Rectification of the robot path during the running of the robot is also crucial for online programming when a precise standard of accuracy is in demand.

Since sensor position information is a key issue to demonstrate the result of material testing, the real-time coordinates of the robot end effector should be available. Further, the information should be able to be transferred in real time to a standard external PC by the high speed communication established between the robot's local controller and the standard external PC. The motor current should be accessed in real-time, enabling contact force calculations and feedback given to the measuring system, based on which a regulation process can be carried out. The low-level access to resolver signals which are used for measuring degrees of rotation should be possible. The signals can be used to synchronize the robot movement and the sensor measurement. The absolute position is retained after the robot has been restarted, as no extra time is necessary to calibrate during the next application.

Safety systems

Since the sensor based MFL test technique requires the sensor to be kept as close as possible to the surface of the specimen, collision of the sensor with the specimen should be detected very precisely. Any damage to the sensor and surface of specimen should be avoided. Thus, a contact force limit feature should exist. The axis of the robot turns to "soft" when the moment limit is surpassed, thus no damage can be caused either to the surface of the specimen or to the surface of the sensor.

4.1.3 Selection of robot

The existing robot system μ -KRoS316 robot from BGT (Bodenseewerk Gerätetechnik) at IZFP is a flexible articulated 6-arm robot. It has the capability to achieve a complex scanning task with extremely high accuracy of 5 μ m. However, application of the robot has been limited by the complexity of the control of the robot. A robot based measure

platform can serve as a platform not only for the magnetic flux leakage scanning but also for other non-destructive testing techniques used at IZFP such as 3MA and computer tomography, provided the maximal payload conditions are not violated.

Table 4- 1 Detail performance comparison of robots

	KUKA	ABB	FANUC	Motoman
Robot 16kg/2m- class	KR16	IRB 2400	M-16iB	HP20
Accuracy 16kg/2m- class	100 µm	60 µm	70 µm	60 µm
Accuracy during robot movement	●	●	●	●
Move with constant velocity	●	●	●	●
Uniform hardware concept	●	●	●	○
Uniform software concept	●	●	●	●
Read in CAD-data	●	●	○	○
Real-time coordinate of the robot available?	●	○	●	
Ethernet-, Fieldbus-, Serial-, Digital interface	●	●	●	
Interactivity achievable	●	●	●	
Moment limitation (“soft” axis)	●	●	●	
Absolute position retained after restart	●	●	●	
Access to Motor current in %	●	●	●	
Low level access to resolver signal	●	○	○	
Sensitive collision detection	●	●	●	
Maintenance interval(oil change, lubrication)	Every 20 000 h	Every 5 years	Regular	
Note: ● Yes ○ No				

The requirement of the robot system for future NDT automation can be summarized as follows. Considering the robot type, number of axis, maximal reach, accuracy, payload, etc. options have been limited to specific robot models from KUKA, ABB, FANUC and

MOTOMAN which are the well-known manufacturers in the field of industrial robot. The robots are compared in detail as shown in Table 4-1.

It is obvious that after comprehensive consideration the above factors and the performance price ratio, the KUKA robot is the most suitable option for automated NDT.

4.2 KUKA Robotics

The KUKA robot system mainly consists of robot, robot controller, KCP teach pendant and software [KUKA2009].

4.2.1 KUKA Robot

The KUKA robot KR 16 (see Figure 4-1) is six-axis industrial robot with jointed-arm kinematics for all point-to-point and continuous-path controlled tasks. Application areas of KR 16 include handling, loading & unloading, welding & soldering, machining, etc.



Figure 4-1 KUKA Robot KR 16

The robot is characterized by good dynamic performance with high resistance to vibration due to the optimized design concept by means of CAD and FEM with regard to cost-effective lightweight construction and high torsional and flexural rigidity. All the axes are powered by brushless AC servomotors of plug-in design, which require no maintenance and offer reliable protection against overload. The main axes are lifetime-lubricated, i.e. an oil change is only necessary after 20,000 operating hours at the minimum. The robot consists of a fixed based frame, on which the rotating column turns about a vertical axis together with the link arm, arm and wrist. The wrist is provided with a mounting flange for attachment of end effectors (e.g. sensors, tools). The positions of the main and wrist axes are sensed by means of a cyclically absolute position sensing system featuring a resolver for each axis. Each axis is driven by a transistor-controlled, low-inertia AC servomotor. The working range of the robot is

limited by means of software limit switches on all axes. The working ranges of axes 1, 2, 3 and 5 are mechanically limited by end stops with a buffer function.

4.2.2 Controller

The KUKA robot is controlled by the KUKA Robot Controller KRC, its control and power electronics are integrated in a common cabinet (See Figure 4-2). The KUKA robot controller KRC is used to control the KUKA robots, KMC and external kinematic system. It features a modular hardware structure and open, PC-based software architecture, which make it possible to be tailored to the specific requirement of the system. Furthermore, accessibility to a wide range of expansion options is ensured to make it easy to adapt the robot controller to changing application requirements. The KUKA robot controller KR C2ed05 possesses a uniform control concept for all KUKA robots by which reliable planning and interchangeable use is ensured. It is well suited to control the robot from low to heavy-duty payloads.

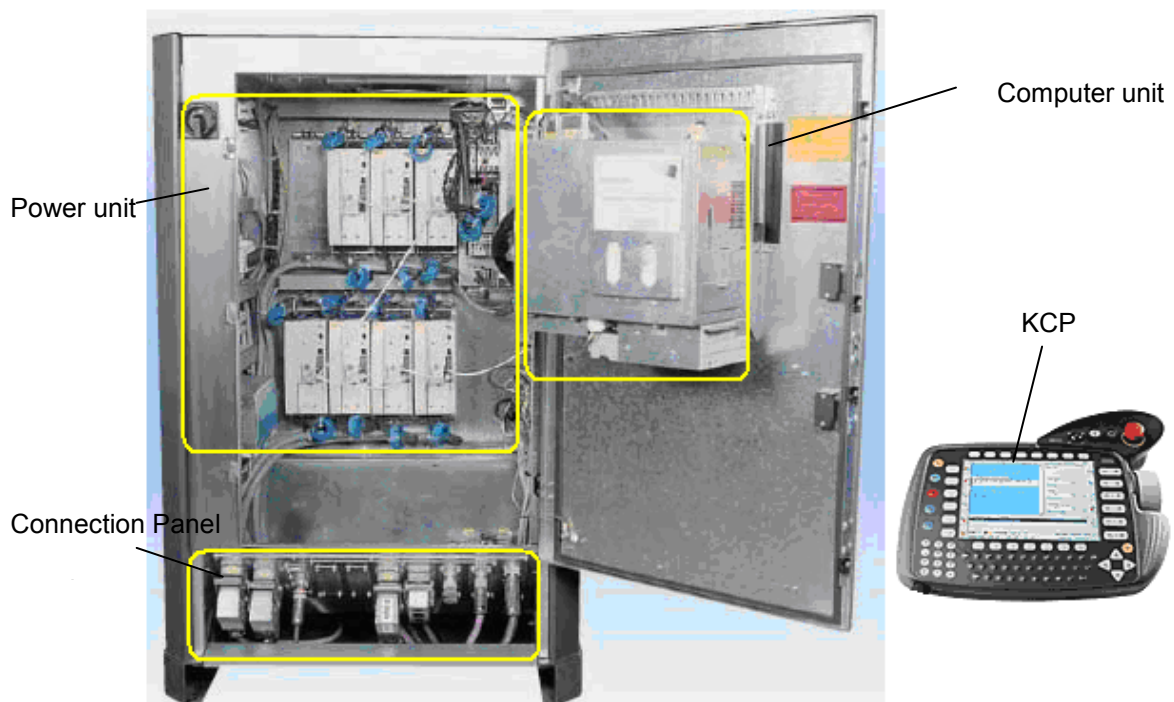


Figure 4-2 Control cabinet overview

Figure 4-2 shows the components of KR C2ed05. The main components of the robot controller include computer unit, power unit, KCP teach pendant and connection panel.

The KUKA KR C2 edition 2005 (ed05) features a plug-and-play functionality that enables rapid start-up. It can be assembled in accordance with the requirements from customer. Standard PC components and service-proven technology are applied to

ensure maximum availability with minimum maintenance and further continuous access to the benefits of cutting-edge technology are guaranteed.

The controller stands out on account of its simple maintenance, good accessibility, modular structure and service-friendly design, which allows for a range of customized hardware and software expansions with efficiency. Efficient interfaces and high compatibility due to PC-based technology enable the communication between robot system and the external system and the integration of robot system for the more complicated customer's automation scheme.

The Robot controller is installed outside the safety fence and the cable length is kept less than 25 m otherwise a ground conductor of 16 mm² is required to ensure a low resistance connection in accordance with DIN EN 60204.

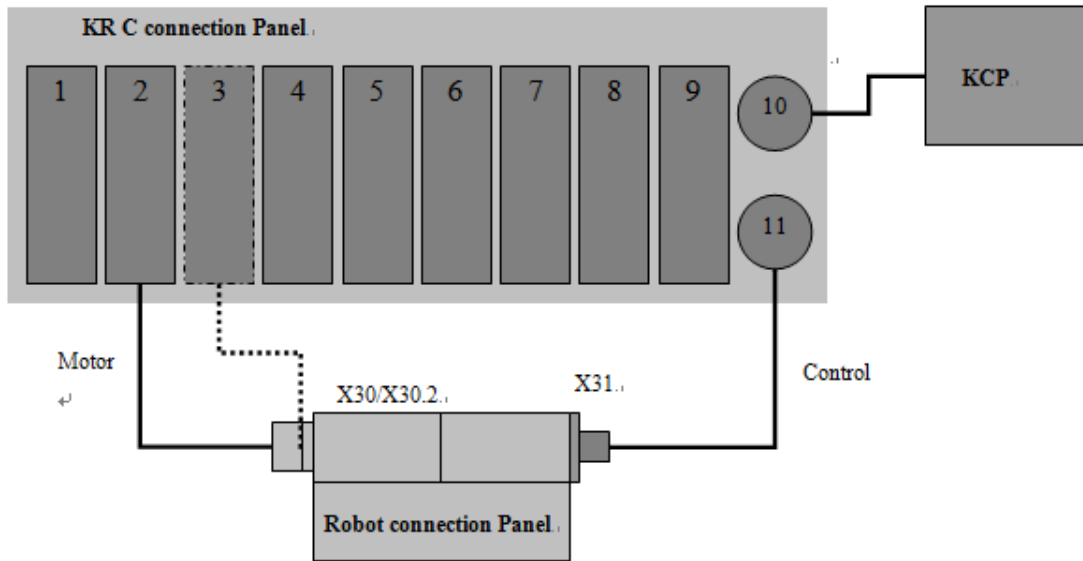
KCP

KUKA Robot is equipped with a kind of pendant named KCP (KUKA Control Panel) which has been connected to KR C2 via KVGA (KUKA VGA card) interface by a CAN-bus (see Figure 4-3). The KCP serves as a hand-held robot control terminal. It is used to teach and operate the corresponding KUKA robot controller and thus constitutes the human-machine interface. All the necessary control tasks can be performed directly on the robot, from commissioning the robot controller to creating and controlling programs, right up to diagnosis. The windows interface running on the KCP guides the user through all procedures and allows fast and efficient programming.

Three-position enabling switches and an additional emergency stop button ensure safe operation of the robot. Simple operation of the 6D input device allows fast navigation and efficient programming. Freely assignable function keys and customizable displays enable the user interface to be tailored to the customer's needs.



Figure 4-3 KUKA control panel



- | | |
|------------------------------|--------------------------|
| 1 Power supply connection X1 | 7 Customer interface X11 |
| 2 Motor connector X20 | 8 Option |
| 3 Motor connector X7* | 9 Option |
| 4 Option | 10 KCP connections X19 |
| 5 Option | 11 Data cable X21 |
| 6 Options | |
- * X7 = optional cross-sectional reinforcement for robots with high payloads

Figure 4-5 Cable connection

4.2.3 Software

For efficient programming of the KUKA robot and tailored system solutions, various powerful softwares are supplied, for e.g. from expandable system software and ready-made robotic application, through wide-ranging simulation tools right up to intelligent robot networking.

KUKA system software

The KUKA system software is an operating system. It is the heart of the controller. It contains all the basic functions that are required for operating the robot system, such as path planning or I/O management. In addition, further advanced functions are integrated into the system software, which offer the robot user a wide range of options for robot programming. The software can be simply operated using the KUKA control panel. The user-friendly, windows-based structure of the KUKA system software ensures intuitive

operation. Furthermore, the range of functions can be expanded anytime using the compatible interfaces. Most of the important features of the KUKA system software include simple programming, path planning, I/O management, inline forms for programming etc.

KRL (KUKA Robot Language) is a kind of specific programming language designed only for the KUKA robot. With KRL, robot movement can be controlled with special movement instructions. It is different from the conventional computer language such as C or Pascal language. Figure 4-6 shows the programming interface.

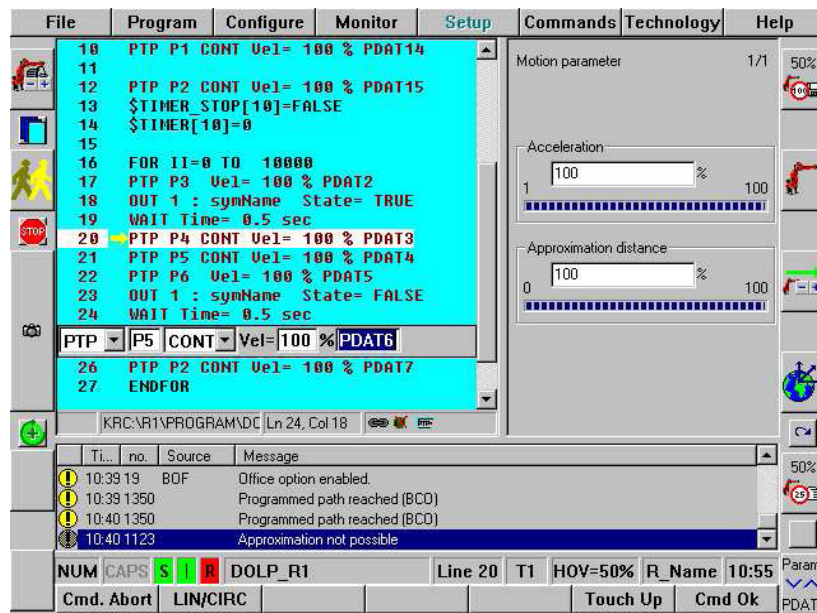


Figure 4-6 Programming interface

The movement instructions can be divided into two categories: PTP movement (point to point movement) and CP movement (continuous path movement). By PTP movement, the robot moves from the start point to the target point using the fastest way which depends on the kinematics of the robot. The robot controller calculates the required angle difference for every axis. By CP movement, the robot moves exactly on the defined path from the start point to the target point. The path can be linear or nonlinear. Simple movements of the robot can be carried out by using basic commands and setting the target. Complex movement programming of the robot can be realized by using these basic movement commands together with program running control, interaction with I/O, subroutine, interrupt function, trigger function etc. For details please see the manual book of KUKA 16F. But it is not flexible and not easy to handle if the motion path is complex or nonlinear.

Application software for communication

CREAD/CWRITE

CREAD/CWRITE is a powerful and flexible command with which the communication between KR C controller and intelligent external system e.g. camera system, other KR C controller, intelligent sensor technology can be established. Data will be transferred in real-time. The communication can be established through serial interface, external module and command channel respectively with CREAD/CWRITE for specific application. The communication through serial interface is most commonly used for data transfer between the robot controller and the external system (see Figure 4-7).

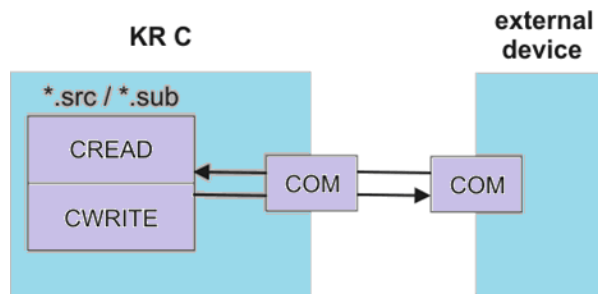


Figure 4-7 Communication through serial interface

After the interface is configured for the serial communication, the KUKA robot controller KR C can write the current coordinates of the robot to the external system for demonstration to the serial interface with CWRITE and also read from the serial interface with CREAD of the motion commands and aim positions which are sent back by external system e.g. external control PC or sensor system.

Figure 4-8 illustrates how the communication can be established through integrated external module with CREAD/CWRITE.

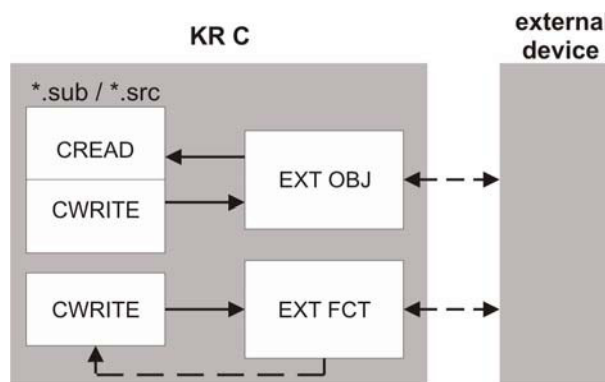


Figure 4-8 Communication through external module

The external modules are drivers for random interface, e.g. TCP/IP for Ethernet interface or serial interface. Both serial communication and Ethernet communication can be realized by establishing the communication through an external module. For this application, an external module should be realized outside the KR C as object file and then integrated in the KR C. The KR C can communicate with up to 4 modules at the

same time. The external module can not only be used to communicate within the KR C but also to communicate with other controllers. Figure 4-9 illustrates how the communication can be established through the command channel with CREAD/CWRITE. CWRITE can transfer a command to the program interpreter through the command channel. Thus, a program can be started and stopped by command through the command channel.

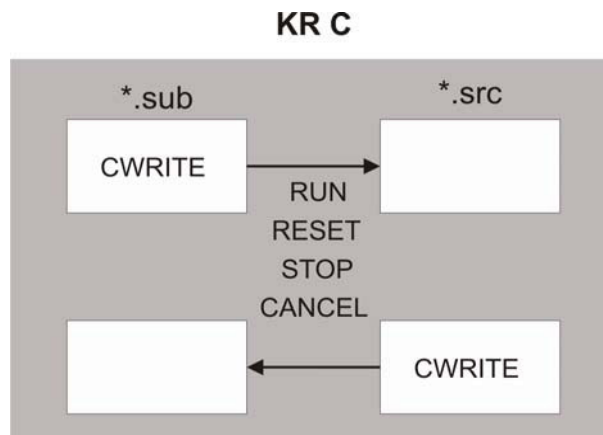


Figure 4-9 Communication through command channel

KUKA.Ethernet RSI XML

KUKA.RobotSensorInterface and KUKA.Ethernet RSI XML are software designed for intelligent networking of robots. The software KUKA.RobotSensorInterface makes it possible to influence the robot motion or program execution via sensor data. Then the sensor data and signals can be read by a field bus, processed in the RSI context and forwarded to the robot controller. Optionally, the data can also be exchanged via Ethernet as XML strings.

KUKA.Ethernet RSI XML is an add-on technology package which is developed in conformity with KUKA.Robotsensorinterface (RSI). It provides a real-time interface through which the cyclic data transformation between robot controller and external sensor system or other real-time systems can be realized. A real-time point-to-point network connection is established and the data are transmitted via the Ethernet TCP/IP or UDP/ IP protocol as XML strings.

Cyclical data transmission between the robot controller and the external system can be executed every 12 ms which means that robot controller sends real-time robot information (position data, axis angles, operating mode) to external system every 12 ms and receives data information (robot controlling commands, motion parameters) from external system within 12 ms. Robot path planning and programming can be influenced in interpolation cycle of 12 ms.

The communication established with KUKA.Ethernet RSI XML is characterized by notable features such as freely definable inputs and outputs of communication object. Data exchange timeout monitoring and expandable data frame are sent to the external system. The data frame consists of a fixed section which is always sent and a user definable section.

Based on these features, KUKA.Ethernet RSI XML can be engaged for versatile areas e.g. position checking and path planning of the robot with an external system; implementation of extensive diagnosis and analysis functions on an external system; implementation of external application (e.g. transferring computing processes to an external system)

The communication between the robot controller and the external system is established once the signal processing is activated with the communication object ST_COROB or ST_ETHERNET. The robot connects to the external system as a client. The functional principle of data exchange is illustrated in Figure 4-10. The robot controller initiates the cyclical data exchange with a KRC data packet and transfers further KRC data packets to the external system in the interpolation cycle of 12 ms. The external system must respond to the KRC data packets received with a data packet response of its own.

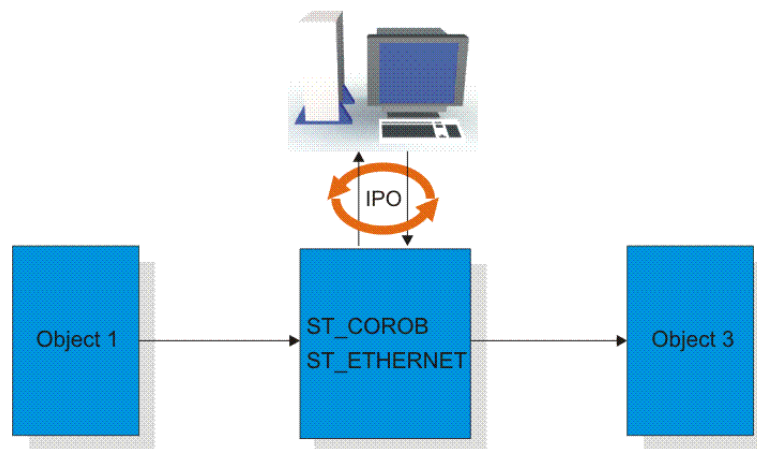


Figure 4-10 Functional principle of data exchange

Data exchange sequence is illustrated in Figure 4-11. A data packet received by the external system must be answered within approximate 10 ms. If the data packet is not received by the robot controller within this period, the response is classified as too late. When the limitation on the maximum number of external data packets that have been classified as too late is exceeded, the robot interprets this problem as an error and stops. If signal processing is deactivated, data exchange is also stopped. If the communication object ST_COROB or ST_ETHERNET is deleted, the connection between the robot

controller and the external system is interrupted. Both sides exchange data in the form of XML strings.

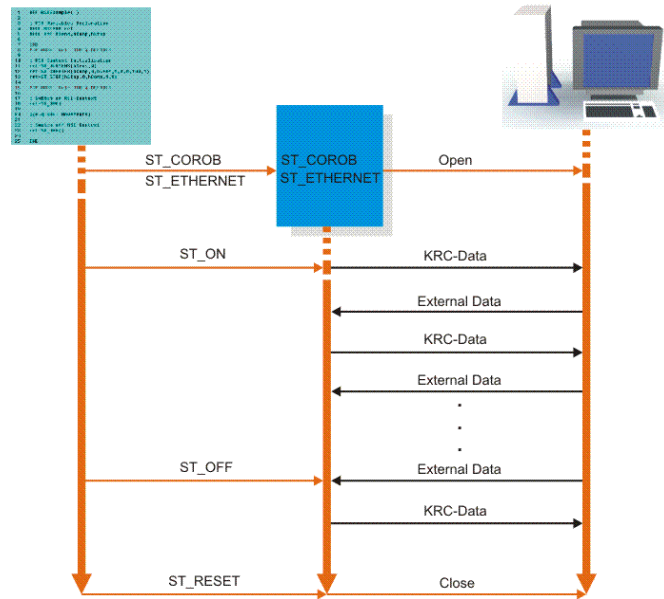


Figure 4-11 Data exchange sequence

The simulation and offline programming of the robots and systems are important for preparation of the system in advance for new or changed tasks without interrupting production. With respect to simulation of the system and 3D visualization to offline programming of the robots, KUKA robot technology offers the customer a range of program modules to reliably plan the processes in the production.

KUKA.CAMRob

KUKA.CAMRob is an add-on technology software package which enables a KUKA robot to be implemented quickly and easily for machining work pieces, on the basis of path and process data from a CAM system. KUKA.CAMRob automatically transforms the CNC data generated with a CAM (Computer-Aided Manufacturing) system into binary files or KRL programs by a PC module. The file is then copied via Ethernet, or manually, to the robot controller and executed with the KR C module. The method can process up to 30000 points (see Figure 4-12).

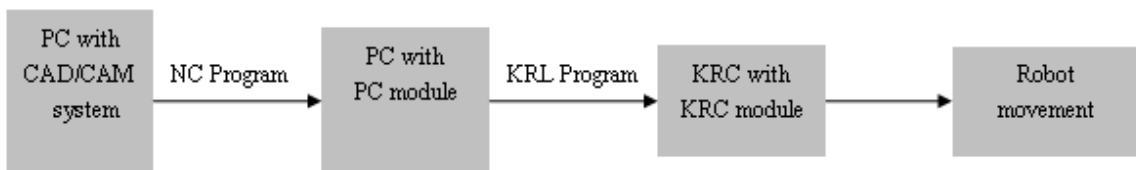


Figure 4-12 Application of KUKA.CAMRob software package

In order to generate the KRL program automatically with the help of this software package, additional software packages KUKA.SIM Pro 2.0, KUKA.SIM components Library 2.0 and KUKA.UserTech V2.1 are necessary to be installed on PC and robot controller KR C2 respectively.

Simulation /planning /optimization

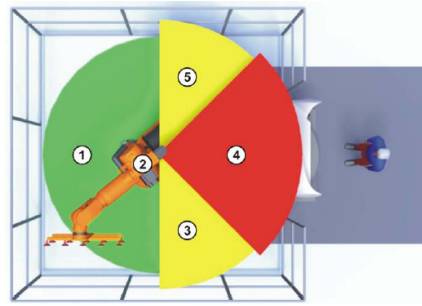
KUKA.Sim

The program KUKA.Sim allows the simulation of the planned application. The data are available in real time, which means that they are more realistic and can be coupled with other simulation programs (IGRIP, ROBCAD). The KUKA.Sim Pro in the KUKA.Sim family was developed for the offline programming and simulation of KUKA robots. Robot simulations can be created and presented to professional standards by KUKA.Sim. The product is connected in real time to KUKA.OfficeLite, the virtual KUKA controller, thus providing cycle time analyses and the generation of robot programs. CAD model can be loaded from the external system into KUKA.Sim by using the build-in tool or be built directly with the CAD tools in the system.

Together with KUKA.Sim Pro, KUKA.OfficeLite is also used for simulation. The KUKA.OfficeLite programming system has the same characteristics as the KUKA system software that runs on the robot controller. It can be used to create and optimize programs for KUKA robots offline on external PC. The finished programs can be transferred one-to-one from the KUKA.OfficeLite programming system to the robot. New robot programs are thus productive from the start. Operator control and programming can be performed using the original KUKA user interface and KRL syntax with the full range of KRL commands.

4.2.4 Robot installation

The KUKA Robot KR16F (weight: 245 kg) has been installed on a mounting base which is built out of the appropriate grade of concrete and has sufficient load-bearing capacity. The workspace and the dangerous zone of the Robot are defined as shown in Figure 4-13. The dangerous zone consists of the workspace and the braking distances of the robot. Safety fences and a gate have been installed to prevent danger to persons or the risk of material damage, as shown in Figure 4-14.



1 workspace 2 Robot 4 Safety zone 3, 5 Braking distance

Figure 4-13 Working space and dangerous zone of robot



Figure 4-14 Safety fence (left) and safety gate (right)

Safety gate has been mechanically locked by safety gate locking mechanism (AZ 16-02ZVRK from Schmersal®). The switch signal from the locking mechanism is connected to the input of a dual-channel connection to X11. Thus, the input of the safety equipment will always be monitored by ESC (Electronic Safety Circuit, which is a dual-channel computer-aided safety system). Once the safety gate is opened during the scanning, an emergency stop is triggered. The drives are deactivated after 1 second and the robot stops with a STOP 1.

The equipotential connection of all the devices existing in the testing system is crucial for data acquisition of sensor supported MFL testing. The introduction of interference power into the control cabinet via incorrectly installed or unsuitable cables can lead to a variety of disturbing influences on the controller and the magnetic flux leakage testing signals. Troubleshooting proves difficult and time-consuming because the sources of interference are often difficult to locate and the disturbances occur sporadically. Every system must be structured to ensure that all components have no potential difference between HF and LF, so that no equalizing currents can flow. The appropriate EMC measures are intended to ensure that the interference power picked up by a cable cannot enter the control cabinet via the cable shield to guarantee that no disturbance of the robot controller occurs.

4.3 Design of the scanning platform

The robot based scanning platform includes a manipulator (KR 16F), a robot controller (KR C2ed05), a KCP teach pendant and an external PC (see Figure 4-15). The manipulator KUKA Robot KR16F is used to direct the magnetic sensor to scan the object according to the command sent to it.

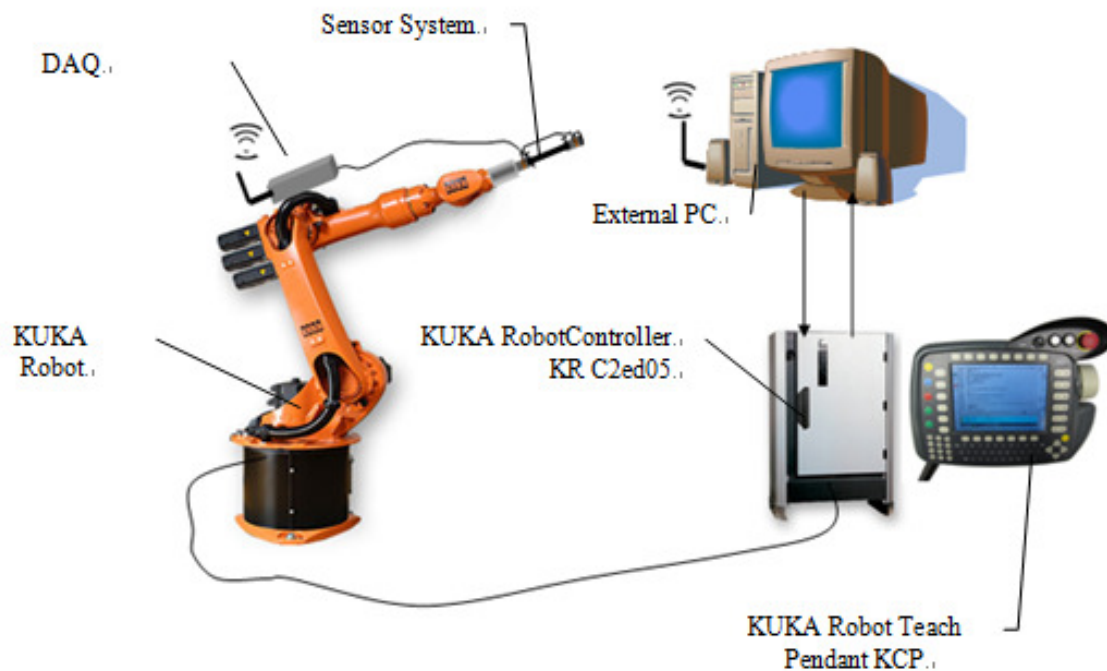


Figure 4-15 Robot based automatic measuring system

4.3.1 Passive or active role of the measuring PC

An external PC can be integrated into the robot based measuring system to provide the system with more powerful and more flexible functions. The role the PC plays can be either passive or active.

4.3.1.1 PC is passive

Passive means that the external PC only receives external data and evaluates the received data and then demonstrates the results. The PC has no role in path planning or on the motion control of the robot (see Figure 4-16). In order to scan an area of a specimen completely and accurately, the data of the position of the specimen in space and size of the test area should be first given to the scan platform. This can be done by support point's definition of the specimen which will be discussed later (in section

4.3.4.1). Then, scan route will be planned in order to control the scanning procedure and motion path of the robot. Generally this can be implemented by programming with KRL (KUKA Robot Language) in KCP, which is called the Robot Teach process. After the robot is taught, it can start to scan the testing area of the specimen with the sensor mounted on the robot flange. The sensor values and the coordinates of the motion path of robot will be recorded and will return to PC to demonstrate the results. In this scheme, the external PC only passively receives the measuring data and motion coordinates of the sensor from the robot controller and DAQ card.

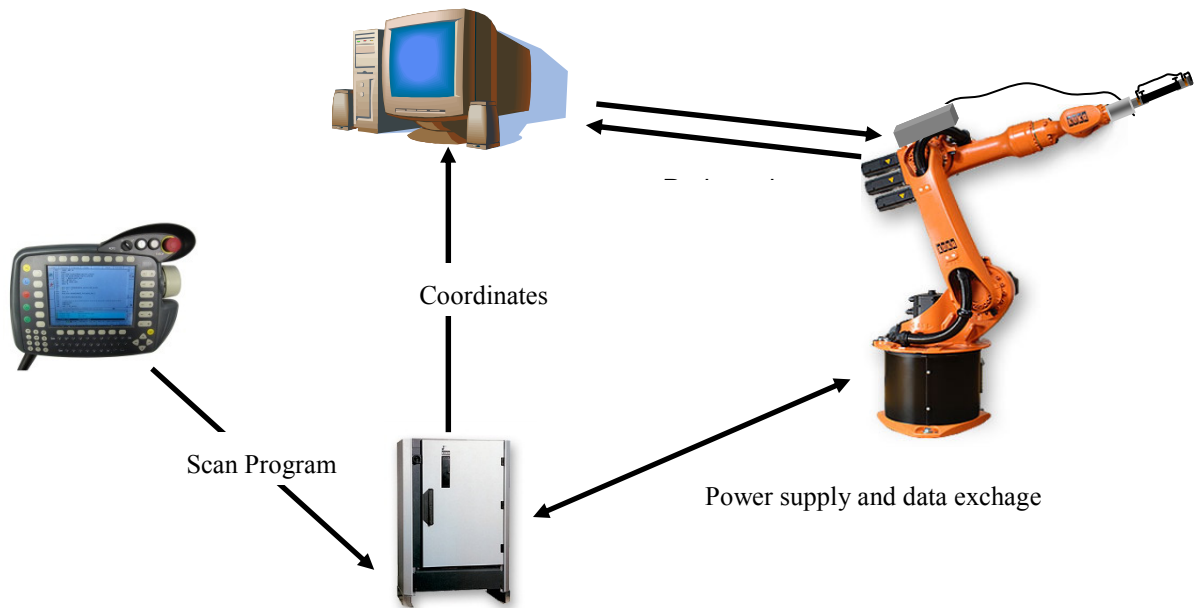


Figure 4-16 Scan system with PC serving passively as indicator

To scan a very simple specimen with a few support points, it is convenient and efficient to program directly in KCP with KRL. However, if the specimen is complex, a large number of support points are needed to get precise scanning supporting information. It is not enough to program using KRL, which can only be applied to the KUKA robot teach process. A more powerful and flexible scheme controlling the robot with standard software that can run on external PC is required. The measuring system users who care more about the precise testing data of material than the controlling of the manipulator are forced to deal with the special technology of controlling of the robot. Furthermore, if there are many specimens with various forms and sizes waiting to be tested, it is easy to understand the inefficiency of developing individual programs for each specimen. If only the KRL language is used to write the program, a specific KRL program needs to be written for each specimen due to the various geometry forms of the specimen. It is also impossible to integrate the robot scan platform into MMS, a kind of measuring system

developed at IZFP. The final aim of this project at IZFP is to integrate the robot solution into the MMS to compose a more powerful and flexible measuring system.

4.3.1.2 PC is active

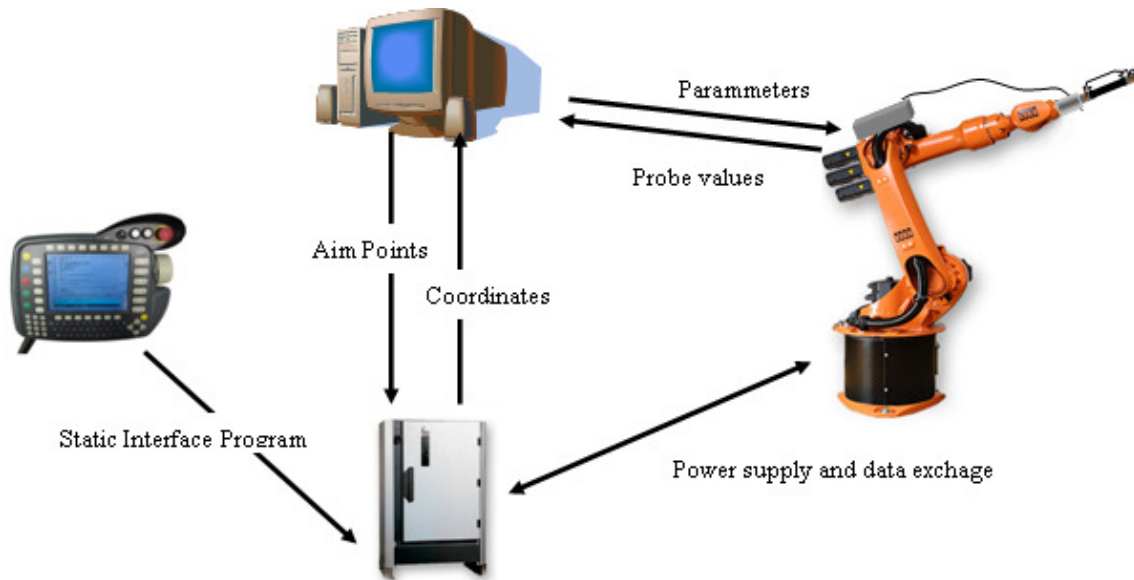


Figure 4-17 Scan system with PC serving actively as external controller

If the PC plays an active role, as shown in Figure 4-17, the external PC not only receives information passively, but also sends commands and coordinates data to control the movement of the robot. Hence, software and hardware with greater capability and flexibility can be introduced into the measuring system. It is a system with the capability of storing much more information and processing larger amounts of data swiftly.

As a conclusion, the scanning system with PC serving actively as an external controller is more powerful and flexible. The nonlinear motion path of the robot is controlled with a signal from the external sensor which has been discussed in the state of art and will be explained in detail in the later section of the sensor integration.

4.3.1.3 Robot Control Concept

While programming with robot specific language has drawbacks such as inflexibility and difficult handling for operators, it is our goal to find a way to simplify or to avoid the programming effort with robot specific programming language and leave the complex motion planning task to the external controller PC.

As we know that every nonlinear scanning path can be approximately decomposed into small linear segments, no matter how complex, it is possible that these small linear

segments can be scanned continuously by robot. What has to be done by robot programming is receiving and executing tasks received from the external controller.

Thus, a novel control concept is introduced based on the ideas mentioned above. The hidden idea is the combination of the online programming with the offline programming. As shown in Figure 4-18, robot programming on the local robot controller side can be simplified to the line movement programming. The robot controller executes the command received in real-time. That is to say the robot local controller has no information about the motion of the next step before the next motion command is received. The motion planning will be finished by the external controller off-line, which means a complex nonlinear scanning path will be decomposed according to the requirement of the scanning. The moving velocity, the coordinate data and the aim points will be generated for every linear segment and then will be sent to robot one by one according to the status of the robot. It is also possible to transform the geometry data such as CAD data into position array.

Additionally, programming with KRL at the robot's local controller is done once for all needs. That means the KRL program is independent of the geometry of the scan path. The KRL program running on the local robot controller is universally useful. The robot is kept alert for new motion command once the program is started. Furthermore, it is also compatible with the MMS testing platform. A remaining problem involves the high speed communication between the robot local controller and the external controller, which will be discussed in the next section.

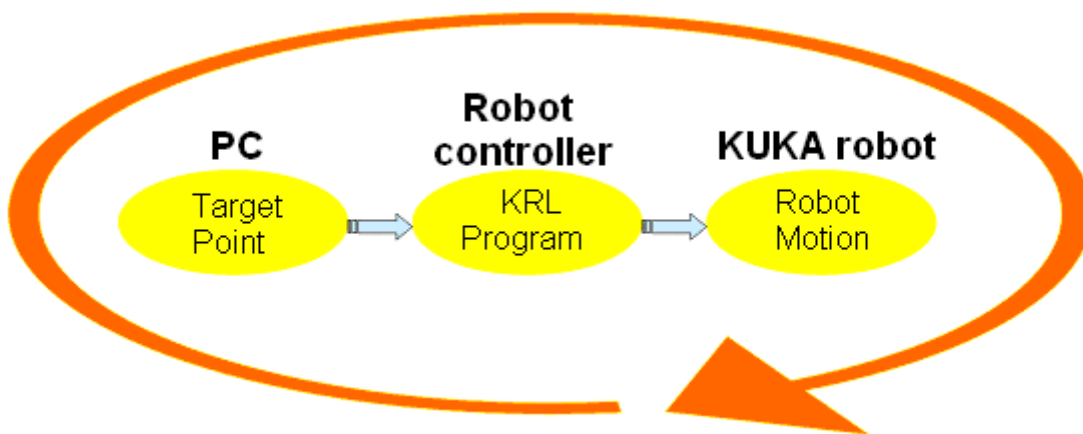


Figure 4-18 Robot control concept

4.3.2 Modular software concept

Based on the concept of robot control discussed above, at least two main functions have to be realized by the external controller: First, the high speed communication between

the robot local controller and the external controller; Second, motion planning and task management and other functions necessary for the measurement system. These functions can be realized in one program which uses a traditional monolithic software structure design. But issues such as the following should be taken into account.

- The program is designed for KUKA, but this cannot be used with robots from other producers due to the different robot technologies applied. This implies that there have to be different programs for each specific robot type which is expensive and inefficient.
- How can the functional maintenance and extension of the program be easily done without affecting the other parts of the software?

On the other hand, if we divide the program into several components and each component is responsible for one function, the advantages are obvious. Moreover, these modules are available in the MMS system.

The software can be structured in three modules.

- Module of motion planning and task management

This module is responsible for the motion planning and the test management. It should be independent of any specific robot and can also be designed for extending this to other articulated robots with 6 - 8 arms.

- Module for data communication, manual position adjustment

The main function of this module is to establish the communication between the external controller (PC) and the local controller (KUKA robot controller KR C2), the desired settings of motion parameters (velocity, coordinate system, etc) can be sent to the robot local controller and the current settings of the robot can be received. This module is specific to a KUKA Robot, while the technology of the Ethernet communication based on the KUKA Ethernet RSIXML library is employed.

- Module for three-dimensional visualization of measurement results

This module is designed to visualize the test result in three-dimension. It should also be responsible for the documentation, archiving and reviewing of testing results.

4.3.3 KUKA-specific motion module

This module is a specific module designed for the KUKA Robot. It is mainly designed for communication between the external controller PC and the robot local controller KRC2. With this module, communication between the robot controller and the external system

can be established and desired motion commands and settings can be sent to robot local controller and can be used further for the dynamic generation of a motion program in KRL. The current position of the robot can also be sent back in real-time. A send and receive cycle can be finished within 12 ms, that means the robot commands and the current position of the robot can be updated every 12 ms. Other functions necessary for the measuring process are also integrated into this module, such as the function of manual adjustment of the robot position.

4.3.3.1 Communication interfaces

In order to establish the communication between the robot controller and an intelligent external system, a communication interface at both sides of the system had to be built. Due to the KUKA Robot technology packets CREAD/CWRITE and KUKA Ethernet RSI XML which are discussed in section 4.2.3, it is possible to connect the robot controller to an intelligent external system. A communication interface at the robot controller side can be constructed using the technology packet supplied by the KUKA Robot and the communication interface at the external system side can be coded accordingly.

It is possible to realize both serial communication and Ethernet communication between the robot and the external PC. These two communication methods are compared regarding various aspects such as the performance, operability, economical efficiency and availability, in order to choose the more suitable solution for our specific application. Figure 4-19 shows the establishment of the communication interface with CREAD/CWRITE.

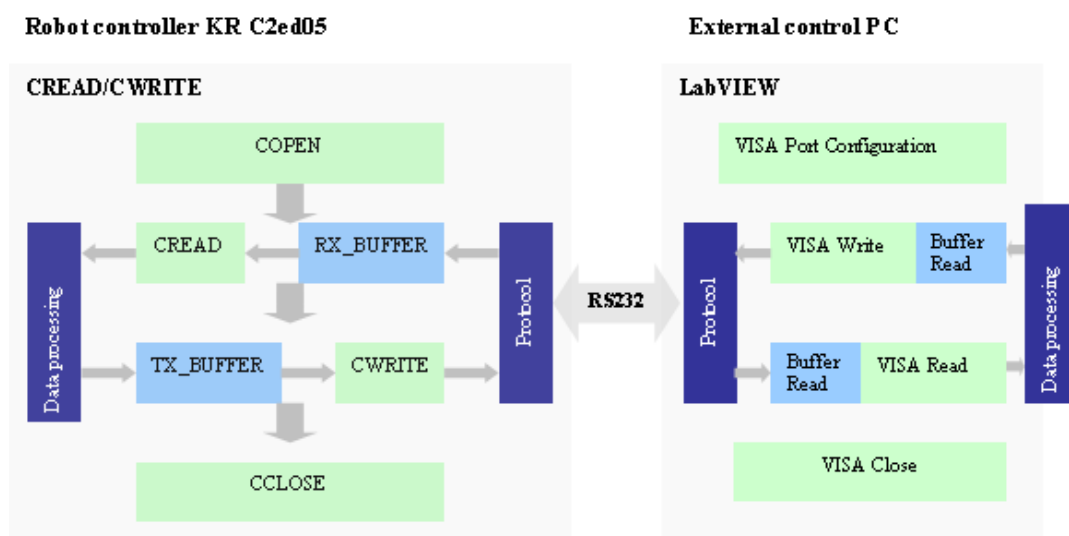


Figure 4-19 Communication based on CREAD/CWRITE

Configuration of serial interface

There are 3 serial interfaces COM1, COM2, COM3 on the robot controller KR C2, but only COM3 labeled as ST5 on the connector panel is available for the data transfer with CREAD/CWRITE. It should be distributed to the KR C operating system VxWorks. The serial interface is configured by setting transfer parameters such as baud rate, character length, stop bits, parity and protocol for data transfer and the selected data transfer protocol is also configured before a connection is established.

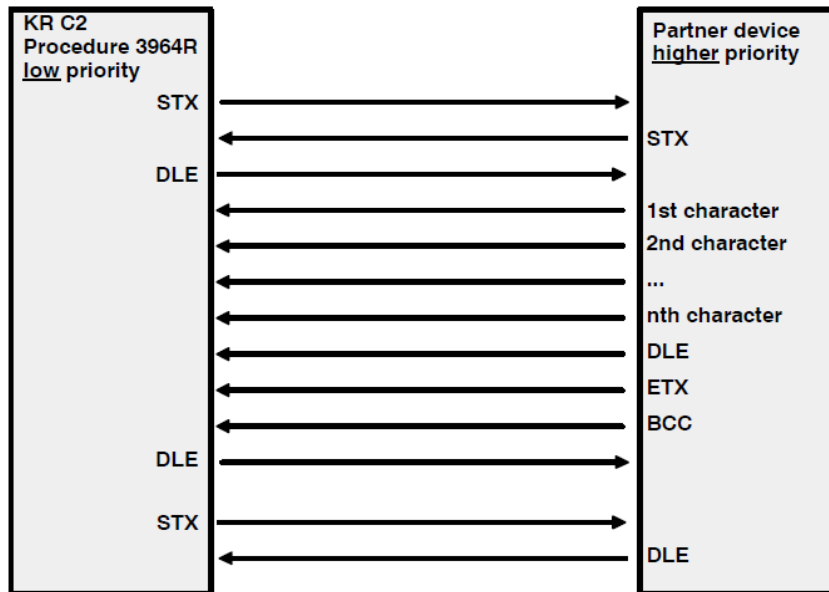


Figure 4-20 Data traffic

Figure 4-20 illustrates the error-free data traffic. With the serial communication established using CREAD/CRWRITE, the robot position and the motion status can be transferred to an external control PC for real-time display in the software window in real-time. The current position of robot can be updated on the at the external PC side every 2 seconds.

The serial communication based on CREAD/CWRITE has advantages in several aspects, for instance the simplicity in transmission principle and easy implementation, good economical efficiency since no extra software module needs to be installed and can be applied directly in programming with KRL (KUKA Robot Language). Serial communication based on CREAD/CWRITE is suitable for such a case in which the speed of data transfer is not a critical factor.

The rate of data transfer is determined by the baud rate (bits per second) and is to be configured the same at both sides of the connection. Therefore, the system with the lower baud rate may impose a limit on the data transfer speed. The transfer rate of the serial communication is relatively low. Attempts to improve the update rate of the robot

real-time position result in the case that the buffer overflows frequently. At least 14 double precision numbers and 6 integer numbers are to be sent and received at each update step. That means an amount of more than 200 bytes of data flows before an update is made. However, the data transfer rate is crucial for our application, since the robot actual position information is very important for the material testing result display. Higher transfer rate means higher spatial resolution during of the measurement. Additionally, the robot motion is dependent on the motion parameter and the coordinates of the set point. Communication with a higher data transfer rate and higher efficiency needs to be established.

KUKA.Ethernet RSXML is an add-on technology package with which the Ethernet based communication between the robot controller and the external devices can be established. It enables bidirectional cyclical data transmission between the robot local controller and an external system in a cycle of 12 ms. It means that data such as current position, axis angles and operating status of the robot can be transmitted from the robot controller to an external system, then the external system should answer the robot controller with a data packet containing set point coordinates, commands and parameters. Such a sending and receiving procedure is a cycle which is kept within 12 ms. All the exchanged data are transmitted via the Ethernet TCP/IP or UDP/IP protocol as a XML string.

This software packet is employed in our application for Ethernet communication between the robot local controller and external controller PC. The application is achieved with three main processes such as connection establishment, data exchange and disconnection.

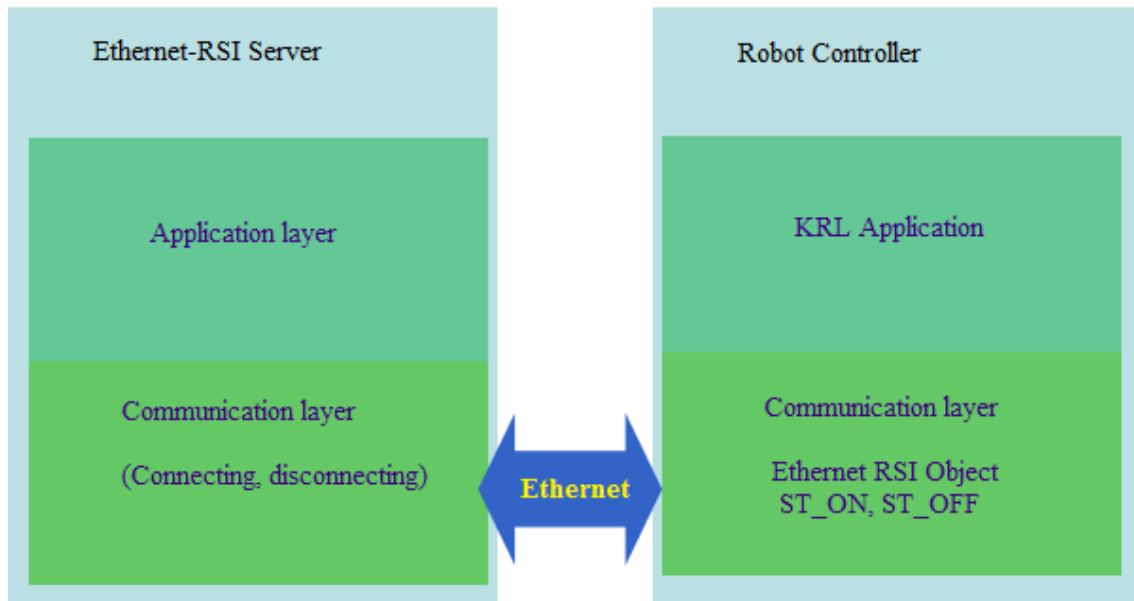
The connections of the robot local controller with the external controller PC is established and maintained with the Ethernet RSI by using a client-server based communication protocol, as the robot controller and the external control PC play a role of client and server respectively. The connection is established by creating an RSI object first in KRL with the information including:

- IP address or host name of the server
- the port number where connection needs to be established
- the type of connection intended (TCP/IP or UDP)
- the number of input and output channels that the object can have

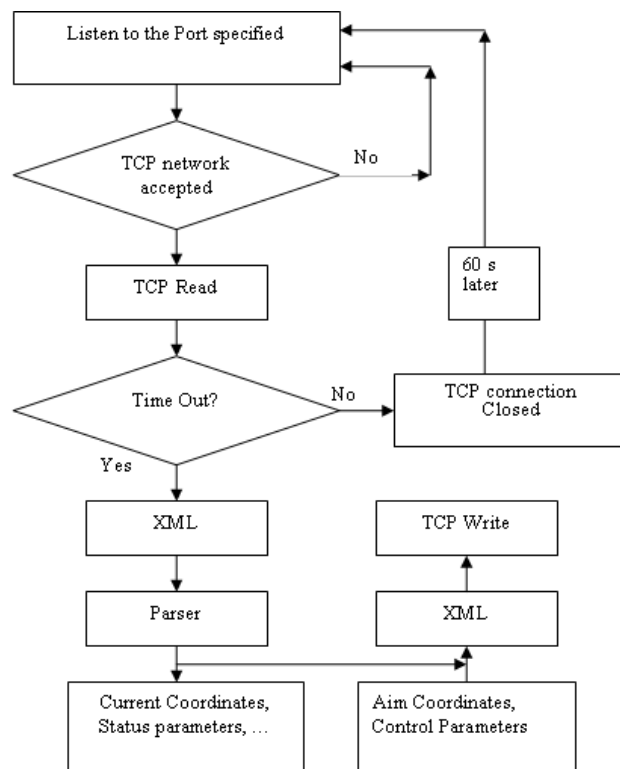
As shown in Figure 4-10, with the object created in KRL, a message is sent to the server application running on the external control PC to request a connection. If the

Ethernet-RSI module does not find the server or detects problems with the connection, it reports an error to the HMI message window of the KUKA robot controller. In the server application running on the external control PC, the listen function of the socket library is called and it waits for the transport layer (TCP) client request for connection. The connection is established once the proper request has been received at the port where the socket is bounded and the accepting function returns successfully for the TCP/IP protocol. After the request message is sent by the Ethernet-RSI client, it enters a ready state to receive messages. In order to enable the data transmission with the server, the output of the Ethernet-RSI object must first be configured to have outputs and the RSI execution should be started in KRL program hosting the RSI applicant. Data message is transmitted at IPO rates (12 ms). However, it cannot be guaranteed that the latest data sent by the server over the connection is available exactly for every IPO cycle.

Hence, if the Ethernet-RSI object is configured to have output channels, and if new data is not available within one IPO cycle, Ethernet-RSI keeps the last received data in the output channels. In order to disconnect the communication with the server, the cancellation will be done in the KRL program hosting the RSI application by executing the close command of the RSI object. A disconnect request can be sent to the server application that the Ethernet – RSI object is disconnecting and releasing all the resources allocated for the connection. The socket is closed by the server application after the disconnect request received. The server application is the program running on the external controller PC. It is realized in the LabVIEW environment and called “KUKA Robot Motion Control” in this work. The functions of the module consist of user operation control, current robot position, status monitoring, and communication. It has two basic layers, as shown in Figure 4-21 a, the communication layer and the application layer. The communication is established, maintained and destroyed within this layer. The application layer is responsible for dealing with the data information received and is preparing for data to be sent according to the user command. The program flow is shown in Figure 4-21 b. After the Ethernet communication is established, data packets are transferred in XML format between robot controller and external PC (see Figure 4-22).



a. Software Structure



b. Program flow

Figure 4-21 Communication establishment

```

concatenated string
<Rob Type="KUKA">
  <Dat TaskType="b">
    <ComStatus>continuous</ComStatus>
    <RIst X="449.7316" Y="-0.0096" Z="687.9707" A="-179.9087" B="84.9888" C="-179.9073"/>
    <RSol X="449.7316" Y="-0.0096" Z="687.9707" A="-179.9087" B="84.9888" C="-179.9073"/>
    <AIPos A1="0.0011" A2="-89.9947" A3="90.0027" A4="0.0077" A5="5.0032" A6="0.0004"/>
    <ASPos A1="0.0011" A2="-89.9974" A3="90.0011" A4="0.0055" A5="5.0026" A6="0.0004"/>
    <EIPos E1="0.0000" E2="0.0000" E3="0.0000" E4="0.0000" E5="0.0000" E6="0.0000"/>
    <ESPos E1="0.0000" E2="0.0000" E3="0.0000" E4="0.0000" E5="0.0000" E6="0.0000"/>
    <MACur A1="0.0000" A2="0.0000" A3="0.0000" A4="0.0000" A5="0.0000" A6="0.0000"/>
    <MECur E1="0.0000" E2="0.0000" E3="0.0000" E4="0.0000" E5="0.0000" E6="0.0000"/>
    <IPOC>155584</IPOC>
    <BMode>3</BMode>
    <IPOStat>4</IPOStat>
    <Tech x="1" p6="0.0000" p7="0.0000" p8="0.0000" p6x1="0.0000" p7x1="0.0000" p8x1="0.0000" p6x2="0.0000" p7x2="0.0000" p8x2="0.0000" p6x3="0.0000" p7x3="0.0000" p8x3="0.0000"/>
    <RGH X="0" Y="0" Z="1" A="0" B="0" C="0" T="00000"/>
    <DiI>1</DiI>
    <Tick>0000000000000000</Tick>
    <RWMode>R</RWMode>
  </Dat>
</Rob>

```

Figure 4-22 Data packet send by robot controller in XML

Figure 4-23 and 4-24 are the software operation windows.

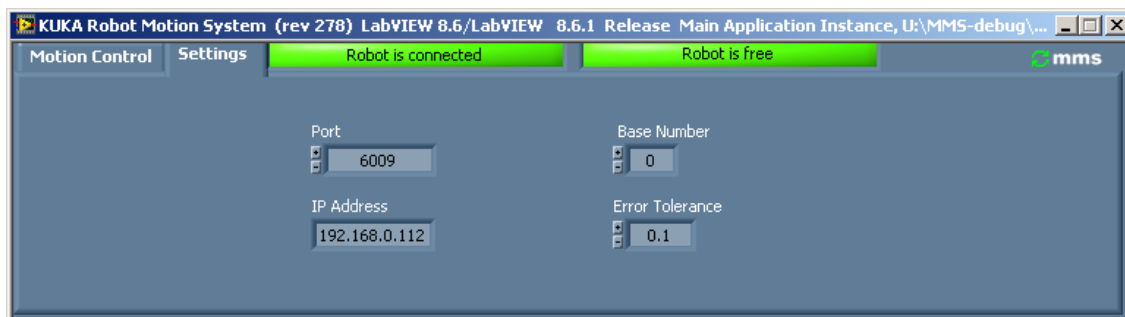


Figure 4-23 KUKA Robot Motion System 1

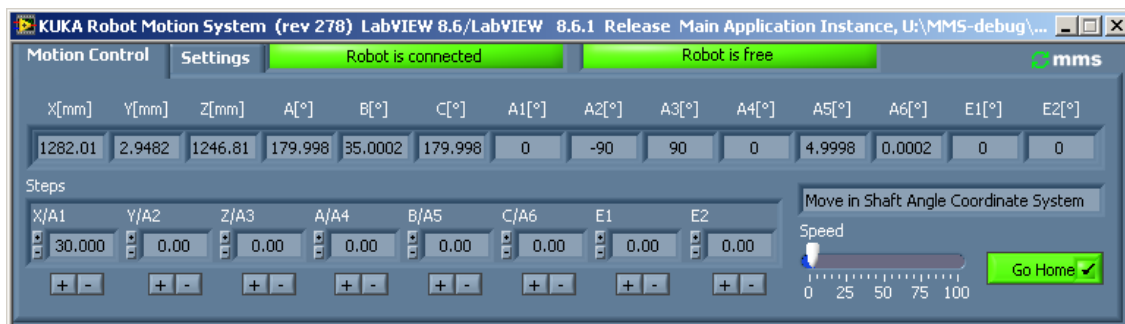


Figure 4-24 KUKA Robot Motion System 2

4.3.3.2 Motion server application in KRL

The KRL program can be divided into three parts in accordance with the tasks to be completed. These are Ethernet communication establishment, data packet preparation, data accessing and exchange of parameters between RSI and KRL, robot movement programming and termination of Ethernet Communication with PC, as shown in Figure 4-25.

In the KRL program, the communication with the external PC is first established with the RSIXML software packet embedded in KRL. Once the communication has been successfully established, a data packet with a fixed data structure is sent and received at the interpolation tact, which means that a cycle of the data packet transfer can be finished within 12 ms. Export data packets are first prepared before sending, which is done by connecting variables from KRL to the input of the RSI object with the communication established with an external PC. The robot status and parameters can be sent together with the current coordinates of the robot end effectors to external PC. A data packet which contains a motion command and parameters is normally received from the external PC within 4ms.

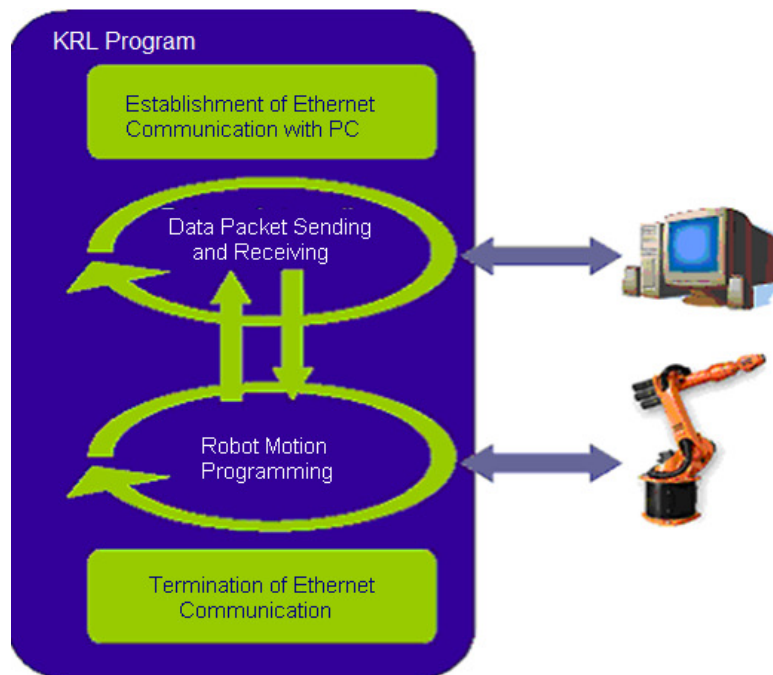


Figure 4- 25 KRL Program

Information included in the data packet can be exchanged with KRL variables by data accessing and data mapping of the RSI object. For example, the coordinates of the set points which are contained in the data packet imported from the external PC can be

mapped in KRL variable, and thus they are available for the robot movement programming. The robot motion status can be accessed by RSI object and be prepared later in the data packet waiting to be exported. After the data exchange with the RSI object, the movement of robot is programmed with the basic move command LIN or PTP, and then it is carried out in a loop.

4.3.3.3 Use of coordinate systems

Different coordinates systems can be used for a robot to carry out a movement task in space. The coordinates systems used by robotics can be divided into two kinds: axis-specific coordinate system and Cartesian coordinates system. The position and the orientation of a point in space can be determined in Cartesian coordinates system by translation X, Y, Z and rotation A, B, C where X, Y, Z values are translation distances in the X-axis, Y-axis, Z-axis, respectively, and A, B, C values are the rotation angles around the Z-axis, Y-axis, X-axis, respectively. By the axis-specific coordinates system, the entire 6 joint angles should be given in order to determine the position and the orientation of the set point for the robot unambiguously.

Since users of the robotic scanning system care more about the scanning track of the end effectors than robot kinematics, it is more applicable to plan the robot movement in the Cartesian coordinates system than to manipulate joint angles of the robot directly.

As shown in Figure 3-15, an aim point in the Cartesian coordinate system is transformed to robot joint angles by carrying out the inverse kinematic mathematical calculations in the KUKA robot controller. Hence, the support points are defined in the Cartesian coordinates system, aim points, which are generated based on the support points of a specimen, are an array of coordinates also defined in the Cartesian coordinate system. As shown in Figure 4-26, there are four coordinate systems predefined for robots, world coordinates system, robot foot coordinates system, tool coordinates system, and base coordinates system.

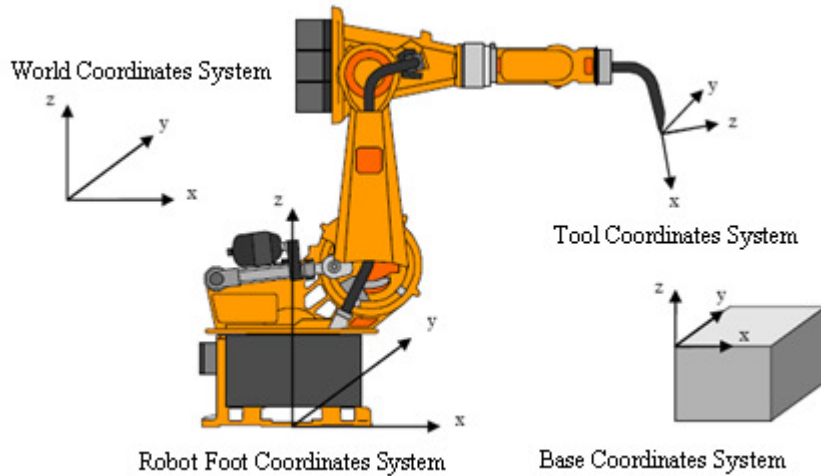


Figure 4-26 Cartesian coordinates for robots

The world coordinates system is fixed and cannot move with the robot. It serves as the original coordinate system for a robot system, reference system for the robot system and also the cell periphery. The robot foot coordinate system located at the robot foot. It works as reference coordinate system for mechanical robot-building and it coincides with the world coordinate system. The tool coordinate system has the origin at tool tip whereas X-axis is the same with the shove direction. The coordinate system moves correspondingly with the movement of the tool. The base coordinate system supplies the reference coordinates to describe the position of the specimen. The origin of this coordinate system is the same as the world coordinate system. For implementation of the scanning system, base coordinates are advantageous for scan movement planning over the other systems. First, the current position of the robot is always calculated with reference to the base coordinate system; Second, through shifting of base coordinates system, only one time of the scan movement planning is necessary to scan several specimens with same size and form at different position; Third, the scan paths of the robot are interpolated with reference to the base coordinates system since sensors are usually mounted on the robot and the specimens waiting to be scanned are usually in a static state, otherwise the tool coordinate system can be used as reference for interpolation.

4.3.3.4 Synchronization

Test results are recorded taking sensor readings and the values of the respective position information. For exact test results, it is crucial that the sensor position matches the corresponding sensor value. Real-time sensor coordinates are received by the external PC every 12 ms from the robot controller through the Ethernet communication

during the scanning. The sensor values are received by the external PC from DAQ hardware through Bluetooth wireless communication.

Due to the fact that sensor positions and sensor values are obtained from two distinct types of communication methods and channels, the sensor values and the sensor positions which are received at the same time by software module running on PC may not be correspond to each other owing to the different data transmissions and the different influence factors on the transmission. Since every element of both the sensor coordinates array and the sensor value array has a time stamp, the sensor positions and the sensor values can be matched to each other by time stamps as long as both time stamps have the same time basis and are compatible.

Hence a key step to solve the problem is to synchronize the data acquisition process with the robot movement. This can be achieved by triggering the data acquisition and the robot movement with the same trigger source. The trigger source can be supplied by a Renishaw sensor, a kind of touch probe, which outputs a digital switch signal with a slight deflection of the probe tip (stylus point).

Figure 4-27 shows the procedure of implementation of the synchronization. A trigger source has been connected at one direction to the DAQ module. It is also connected to the fast measure input located on the robot foot. The input value at the fast measure input of the robot can be accessed by the KRL variable every 125 μ s. Once a trigger event has occurred, the DAQ starts and the interrupt program in KRL is simultaneously triggered. The moment at which the interrupt is triggered can serve as the time base for both DAQ and robot movement.

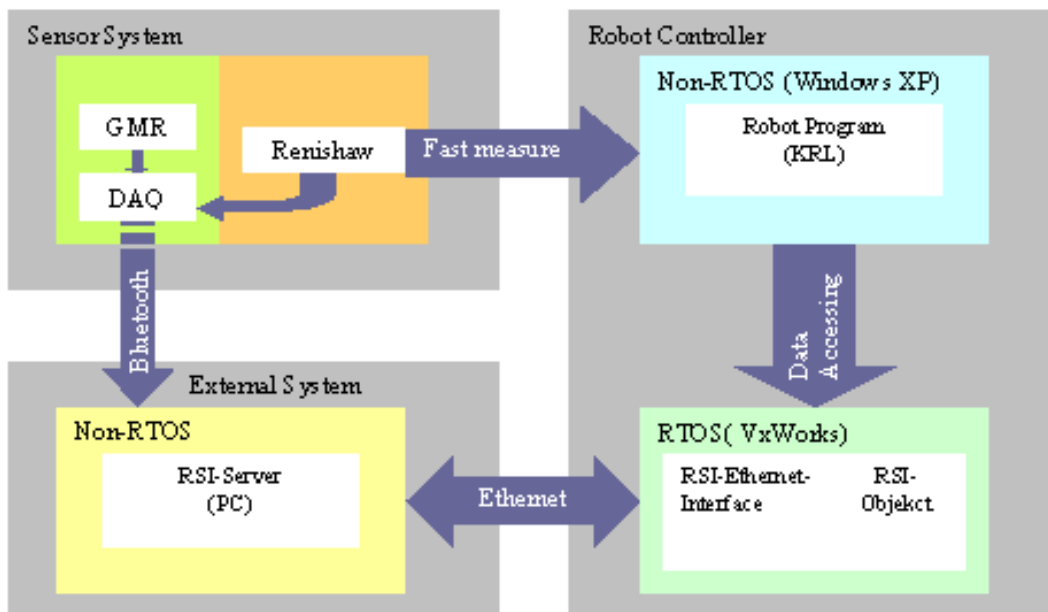


Figure 4-27 Use of Renishaw sensor for synchronization

4.3.4 Robot script controller module (non KUKA-specific)

The general the task of the Robot script controller is to control the measurement process and to perform off-line path planning. Every measurement cycle begins from the controller. For off-line path planning, the position array should be generated based on the geometry of the specimen. In the present work, the geometry of the specimen is described using the support point concept.

4.3.4.1 Support point concept

The geometry form, the space position and the size of a specimen should be described quantitatively first. They are used later to generate the aim points of the robot movements if the specimen has to be scanned automatically by the robot. It is self evident that the geometry, the spatial position and the size of the specimen with basic form can be described by several points, which have been called support points in this work, as shown in Figure 4-28. Array of target positions will be generated based on the description of the geometry of the specimen with several support points. With the support points, the position of the specimen in space and the geometry can be determined accurately. It is obvious that they should be defined first before scanning. The support points can be defined in several ways.

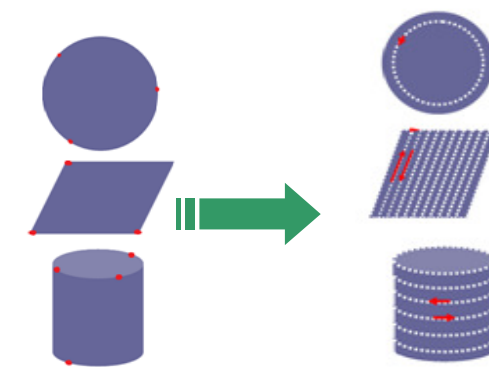


Figure 4-28 Generations of the aim points based on the support points

4.3.4.1.1 Manual support point definition

If the basis and tool are selected in the robot system, then the coordinates of the tool are known. That means if the reference coordinate system is selected and the relative position between the sensor tip and the robot can be obtained, then the current coordinate of the sensor tip can be evaluated and be unambiguously determined with

the help of the “KUKA Motion Module”, which communicates with the robot controller in real time within 12 ms.

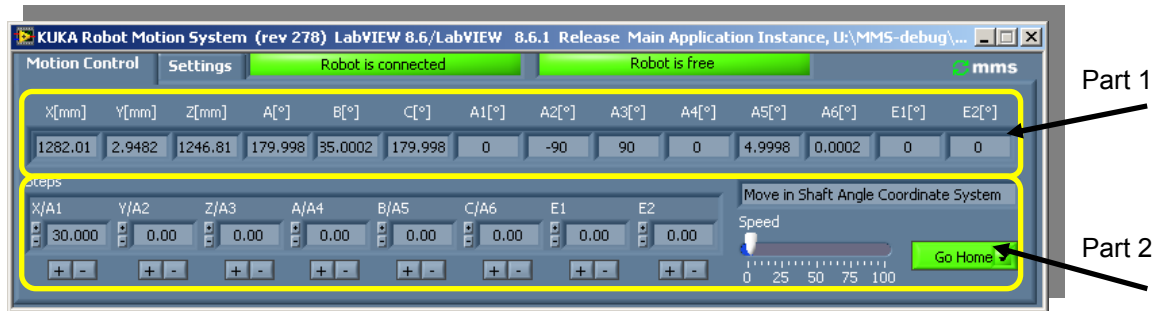


Figure 4-29 Current position of the corresponding tool is shown in part 1; manual movement of the robot is enabled by the part 2

Based on this premise, the supports points can be defined by moving the sensor to the specimen. In automatic mode, the manual movement of the robot can be enabled with part 2 of the “KUKA Motion Module”. After setting the corresponding steps, moving art (robot move in Cartesian coordinates system or with axis angle method) and moving velocity (which should be kept very low in the automatic run mode of the robot system), the robot can move in forward and backward direction with six degrees of freedom (DOF) by pressing “+” or “-”, as shown in Figure 4-29.

When the sensor installed on the robot flange contacts the specimen, the current position of the point is shown in part 1 and can be stored into the support point list shown as Figure 4-30. Thus, one of the support points has been defined. Repeat the process to define enough support points in order to accurately describe the geometry, the spatial position and the size of the specimen.

Since the distance between the sensor and the surface of the specimen during scanning has a great influence on the test result, it should be kept rigidly in a certain range in order to get more accurate results. Although a more precise scanning path can be guaranteed by more accurately defined support points, it is not easy to define the support points by moving the robot manually. Firstly, it is hard to judge the sensor position precisely when the sensor approaches the surface of a specimen. Although instead of observing the position of the sensor from a short distance a monitoring module with camera can be set up to follow the position. It is hard to exclude the influence of subjective factors on the estimated sensor position. Secondly, the surface of the specimen and the sensor can be easily damaged by wrong usage of the control panel (virtual panel in Figure 4-29 part 2) or teach pendant when the sensor is on or near the surface of the specimen. Thirdly, it is time-consuming to move the robot very

slowly with repeated monitoring the sensor-specimen position in order to avoid damage to either to the specimen or to the sensor.

Therefore, a more convenient and safer scheme should be adopted.

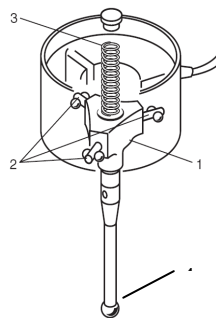
Name	X	Y	Z	A	B	C	A1	A2	A3	A4	A5	A6	E1	E2
p1	648.72	786.85	640.57	-169.00	84.40	-166.31	-69.63	-67.01	124.60	102.11	76.02	-146.9	0.00	0.00
p2	648.72	826.85	640.57	-169.00	84.40	-166.31	-70.53	-65.04	121.02	100.95	76.17	-145.1	0.00	0.00
p3	498.85	786.77	640.54	-169.65	84.40	-166.91	-79.56	-69.10	128.34	93.82	81.38	-147.9	0.00	0.00
p01	598.86	786.74	850.54	-169.45	84.40	-166.71	-72.83	-84.89	121.29	94.19	75.18	-124.9	0.00	0.00
p02	498.85	828.77	850.54	-168.96	84.39	-166.31	-80.07	-83.53	119.75	89.83	80.99	-124.5	0.00	0.00

Figure 4-30 List of support points

4.3.4.1.2 Semi-automatic support point definition

In order to monitor and judge the distance between the sensor and the specimen in a more objective way when the sensor is approaching to the specimen, the result should be obtained through “sensing” or “touching” rather than visualizing. Furthermore, if the movement of the robot can be stopped immediately as soon as the sensor starts to touch the specimen surface, damage to either the specimen or to the sensor can be avoided. This means that a protection mechanism should be employed in a robot scanning system.

Renishaw touch probes are a kind of touch trigger probes which are originally designed to be applied in CMMs (Coordinate Measuring Machines) for precise inspection. Figure 4-31 shows the structure and working principle of the probe.



- 1 pivotal plate 2 bearing points 3 helical compression spring 4 stylus ball

Figure 4-31 Sketch of the Renishaw sensor

The pivotal plate is spring-loaded against three bearing points by a helical compression spring. These bearing points which are formed by a combination of rollers and ball

The event can be handled in KRL as shown in Figure 4-34. Based on the semi-automatic support point definition, the sensor is first brought to the vicinity of the specimen manually, then by turning on the “search” function after setting the search direction and the search range in the “KUKA Robot Motion System”, the robot will search the support points automatically. After the support points have been found, they can be stored in the support point list in the “Robot Script Controller”. Thus, the support point definition process has been simplified and a mechanism to protect the sensor and specimen from damage has been built.

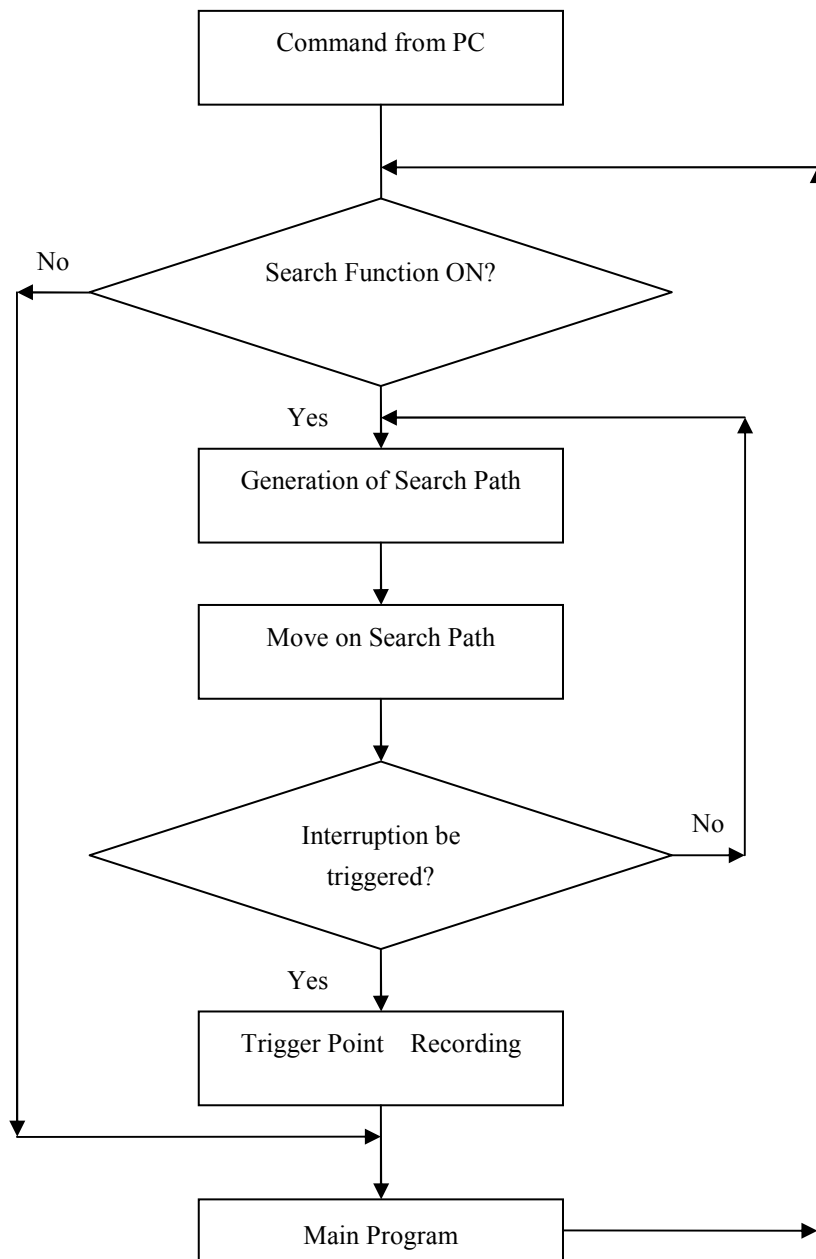


Figure 4-34 Handling of the trigger event in KRL

4.3.4.2 Script-based Geometry programming concept

As stated before, the robot script controller module serves as a manager of the scan task and a generator of the target post to be executed. For scanning a specimen with a specific form and size, the aim points of the scan movement path is generated by the robot script controller depending on the spatial position, the geometry and the size of the specimen, the path arrangement, and the movement type (scan continuously or step by step). For scanning of a specimen with complex geometry which can be decomposed into several parts with simple form, the scanning task should be executed in a series steps.

The key issue here is how the information can be given in such a simple way that it can be quickly grasped by a user who has little knowledge about programming, and describe the scanning serial scanning steps in a defined manner.

Since the script based language can run a sequence of executables automatically and fast, it is the best way to program the scanning task in our case. Figure 4-35 shows the description of the scan task in a script. The script is written conforming to a syntax defined beforehand. Each type of geometry has an individual syntax defined beforehand. Taking the rectangular form of geometry as an example, the scanning task can be described as script conforming to the syntax: **Geometry form, support points, speed, resolutions, priority, mode, scan method, move type, and measurement results.**

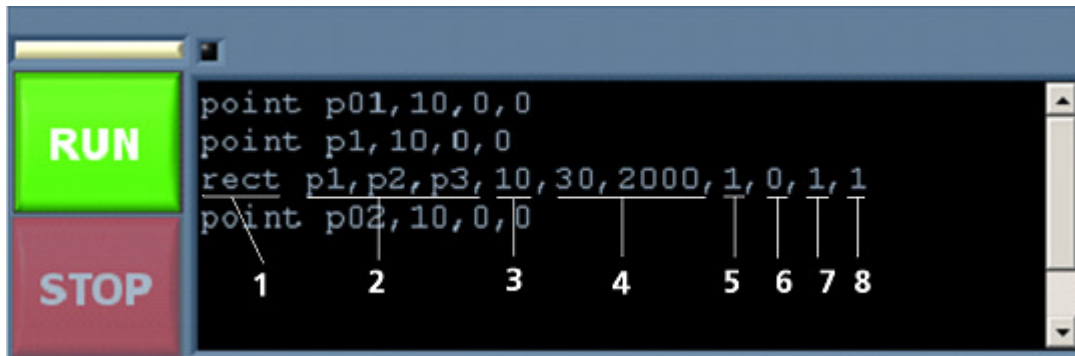


Figure 4-35 Geometry Description as Script

1 indicates the basic form of the specimen, e.g. rect indicates a rectangular form and circ indicates a circular form of the specimen. Basic forms which can be interpreted by the software module include point, line, circ, rect, cylinder, and arc.

2 shows the support points with which the spatial position, geometry and size of the specimen can be decided. They are first defined and stored in the robot script controller before they are used.

3 sets the speed in percent, 10 means that scanning is carried out with 10% of the full speed of the robot.

4 are scan resolutions, which also decide the pixels of the scan result in the “3D visualization module”.

5 gives the priority of the direction by which the scanning begins, 1 means that the scanning begins from the rectangular side that is parallel to the X axis, 0 means that the scanning begins from the rectangular side that is parallel to Y axis.

6 decides the scan mode, whether the scanning is continuous or step by step.

7 indicates the scan method, it decides which coordinated system is chosen, Cartesian coordinate system or axis specific coordinate system.

8 decides if scan with or without sensor DAQ. 1 means that magnetic sensor data acquisition is on during the scanning, 0 means that the scanning process is without magnetic sensor data acquisition.

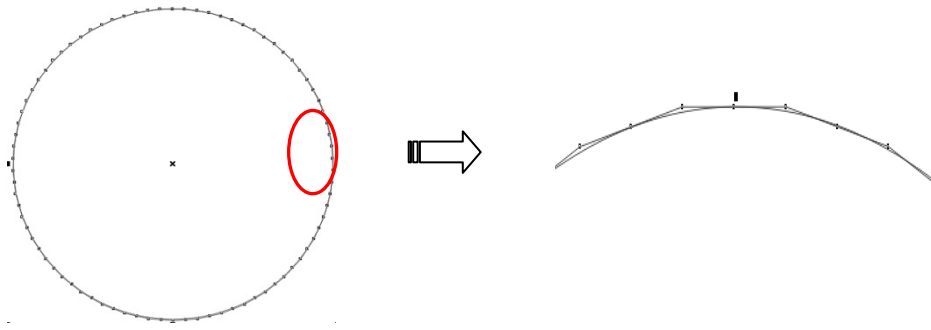
Describing the measurement task in a script has advantages as follows:

- It is easy and fast to describe a scan task with the support point defined beforehand;
- Scan tasks can be randomly mixed and executed in series, if necessary, the executing sequence can also adapt to the task;
- It is possible to scan a specimen with complex form with combination of several commands.

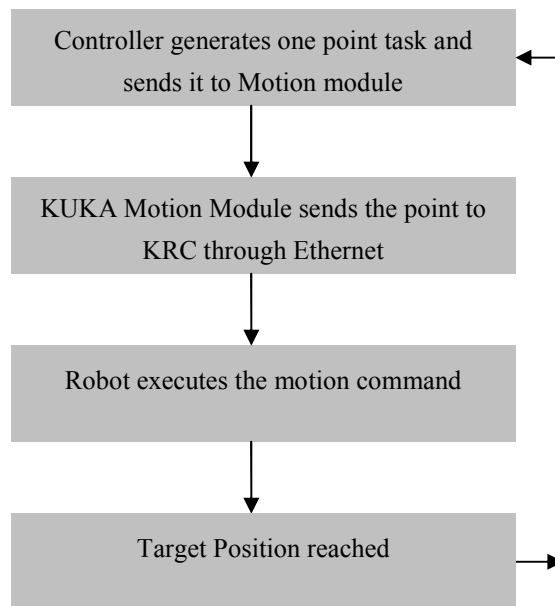
4.3.4.3 Scan of curved surface with basic LIN command

The Robot Script Controller module is designed not only for controlling a specific type of robot but also as a universal controller for various manipulators with up to 8 axes. Although there are specific commands available for curvilinear motion of a KUKA robot, a more common linear movement command is selected, because the specific movement commands may not be available for every type of the manipulator such as an ISEL robot and μ KRoS-316 Robot from BGT.

As mentioned before, each scan movement can be decomposed into several small linear movements and the length of each line segment depends on the required resolution of the test. The procedures of scanning a specimen with curved surface are shown in Figure 4-36 as an example to illustrate the idea behind it.



a. Decomposition for robot scan path



b. Realization

Figure 4-36 Normal process of scan movement

Here the controller doesn't generate the next target position until the previous target position is reached. The scan of a specimen with cylinder form has been carried out, but there is still great potential for improvement of the efficiency and accuracy. Although this process arrangement could be carried out in MMS with no disadvantage, as far as the robot is concerned. However, this process of arrangement is not optimal as a short standstill time of the robot was observed during the test. A schematic profile of robot speed is shown in figure 4-37 and this can explain the situation.

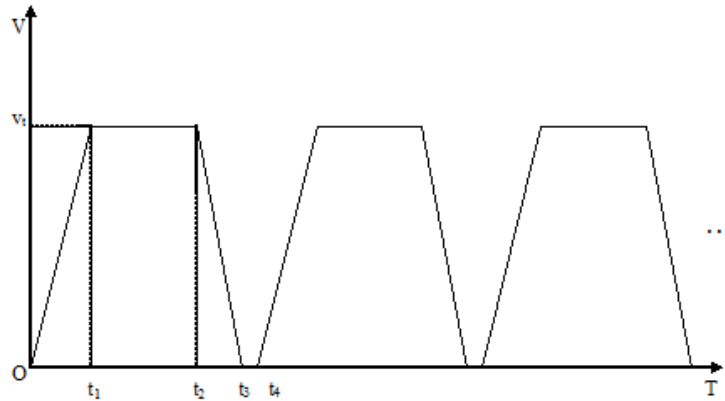


Figure 4-37 Speed profile of the robot during movement

The standstill of the robot during the measurement is due to the work flow of the module on the MMS platform. The modules on the MMS platform are activated in turn for each measurement cycle. Only one module in the whole cycle can be activated at a time, the robot motion module is activated after receiving the command from the robot controller module and is not considered to be finished until the desired position is reached, the robot stands in still after the desired position is reached and before the new command from the external computer arrives. As soon as one cycle is completed, a new cycle starts from the controller which generates a new motion command. During this process, the robot script controller doesn't generate the next position command until the previous one has already been finished, that means the robot will never generate and send an aim point before the previous point task is achieved by the robot.

Thus the robot controller starts to generate the aim point after the robot comes to a standstill. The time duration of standstill is the time needed to generate and send the aim point from the PC to the KUKA robot. Due to the standstill among the movements, frequent acceleration and deceleration are unavoidable which greatly compromises the efficiency of the robot. The performance of the robot has not been considered completely. The problems discussed above can be improved in the following ways:

- 1) Eliminate the standstill of the robot and shorten the duration of the robot movement

Since LIN-LIN regrinding can ensure a continuous smooth movement along complex movement path and uses the acceleration reserves in the most rational way, the MMS program and KRL program running on the robot controller should be improved to make it possible to carry out LIN-LIN regrinding.

- 2) KRL program aspects

For each single regrinding movement, the motion configuration and three points are required. The beginning of each regrinding movement is controlled by the motion

configuration. As shown in Figure 4-38, the three points are the start point (P1), the helps point (P2) and the aim point (P3). A regrinding parabola is calculated by the robot controller automatically before each regrinding movement is carried out. Since in the present work, acceleration and velocity of the movement of the robot during the scan is stable, the regrinding parabola is symmetrical to angle bisector of the two adjacent line movements.

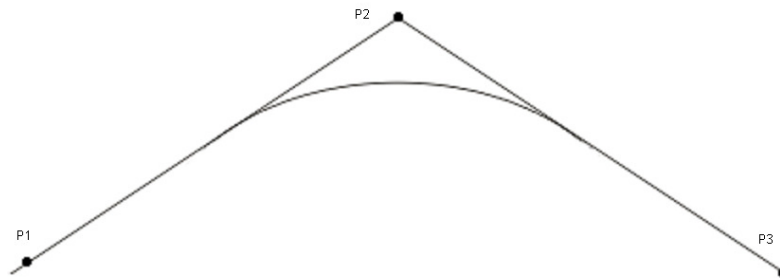


Figure 4-38 Robot movement regrinding

For the scanning of a specimen with a complex form, the regrinding function is performed continuously. Therefore, a data stream of aim points is necessary to ensure a smooth movement path. Aim points will be sent from the PC to the robot controller continuously as a stream unlike the previous discrete sending of the aim points. After the module receives a request from the KRL program, elements of the points from MMS are assigned with an index. Finally, the points assigned with an index will be sent through the Ethernet to KRL (see Figure 4-39).

KRL Program

Points received by KRL are stored in a circular buffer. It can be managed in such a way that it will never overflow. This is suitable for our application as the scan lasts for several hours. The circular buffer works with two pointers as shown in Figure 4-40. At the pointer “Task” the newest received point is stored in the buffer and it will move forward clockwise illustrated with an arrow and then the next received point will be stored at the point “Task” again. The point being operated is at the position of the pointer “Operate”. The two pointers are prevented from overlapping each other in order to guarantee a continuous and undisturbed robot movement.

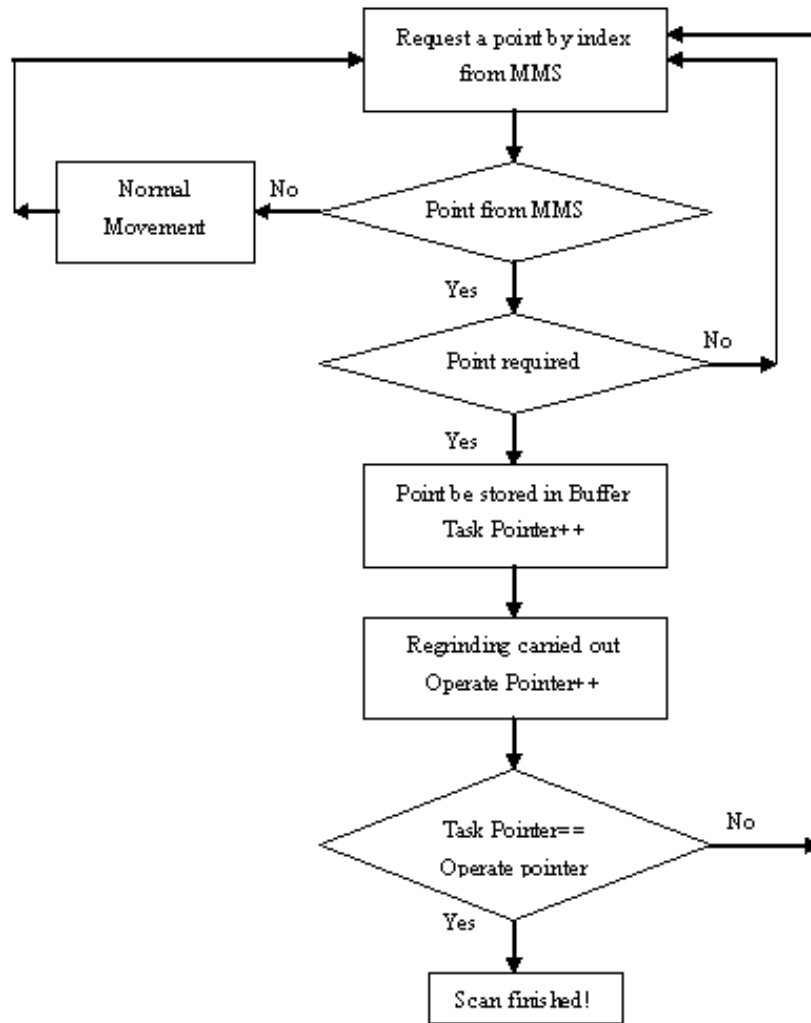


Figure 4-39 Realization of regrinding function in KRL

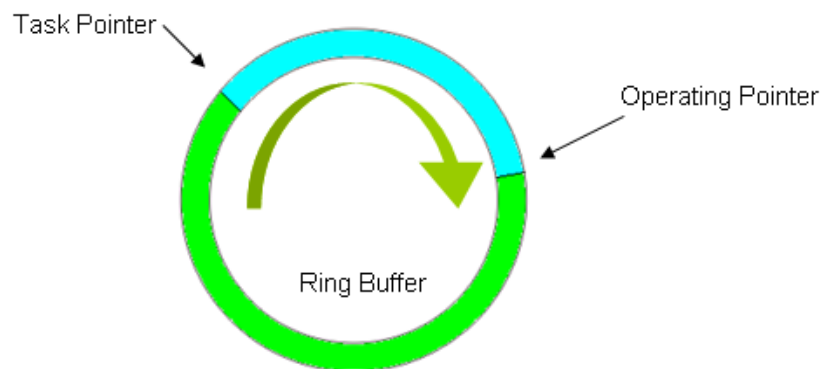


Figure 4-40 Application of ring buffer

4.3.5 3D Result visualization module

Test results should be displayed visually. Given the capability of scanning diversely shaped specimens, the results should also be displayed with this module. Due to the

scanning system's features of 3D scanning, the existing inspector "New inspector Pro" which is meant for 2D scanning is not suitable for displaying a 3D scan result. A corresponding inspector for 3D scan display has been developed, which is shown in Figure 4-41. The OXYZ coordinate system can be shifted or rotated by an arbitrary angle, and the measurement results can also be displayed accordingly.

The testing data array which comes from the former module can be stored by clicking "save" in a binary format. Data which has been stored can also be loaded for future processing. Cursor function has been placed on the specimen.

Scanning of a specimen with complex geometry is done by decomposing the complex geometry into several elements of basic geometry firstly, such as rectangular planes, cylinders, spheres, cones etc. Once an element has been finished, the assignment of the test value to the corresponding coordinates will be done in the module specific to magnetic flux leakage testing. After the assignment, the data array in which the assigned data is stored can be transferred to the 3D visualization module.

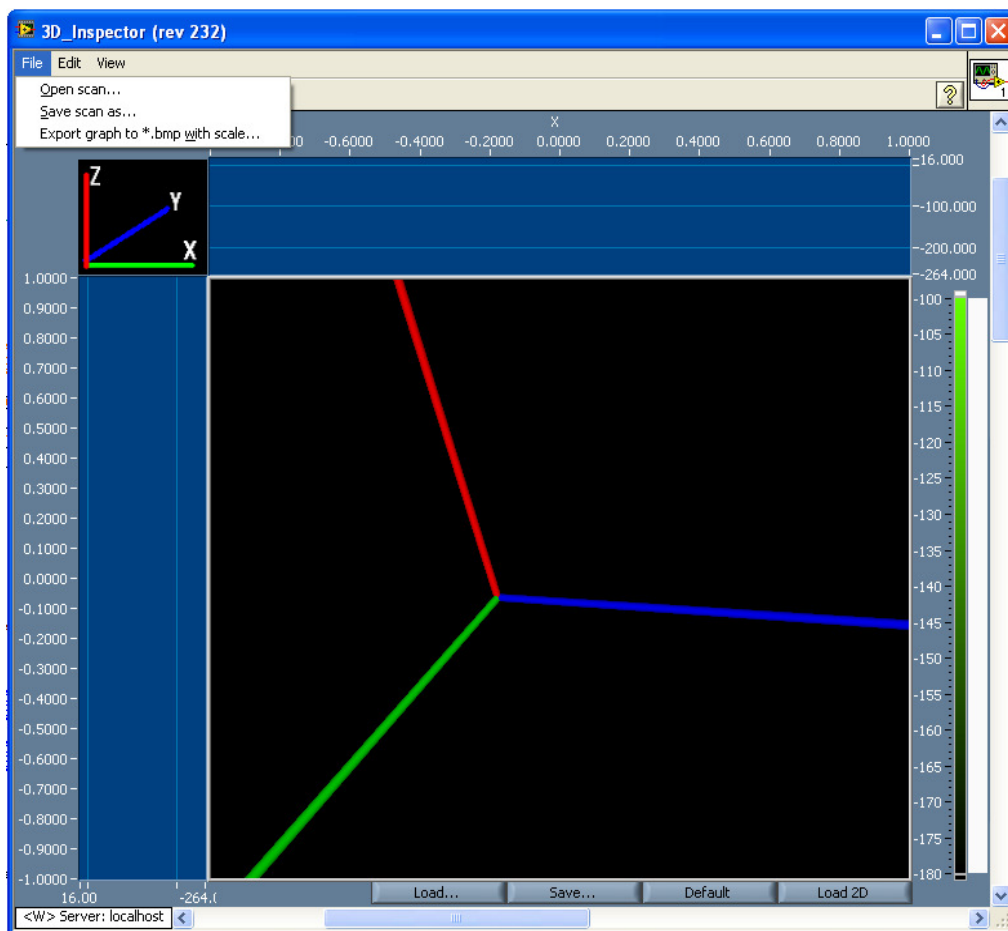


Figure 4-41 3D Scan Inspector

In the 3D visualization module, an intensity graph is constructed from the received data array. At the same time, the geometric model of the current element will be reconstructed using the support points to describe the element. After matching both the function data of the intensity graph and the model, the intensity graph can be mapped on the model.

5 Application examples

5.1 System detectability verification on a test block

A US standard test block P3-10 UTT 1015 is used to determine the effectiveness of the developed system in inspection of surface cracks in ferromagnetic material. The standard test block has the dimension of $200 \times 45 \times 20 \text{ mm}^3$ and has a fatigue crack in the middle of the long side. The crack is parallel to the AD side and has a width of $20 \mu\text{m}$ and a depth of 10 mm (see Figure 5-1).

The objective of the measurement is to test the feasibility and efficiency of the robot supported automated measuring system. The test block is scanned continuously in three-dimension. The scanning parameters such as scanning speed, scanning resolution, scanning mode (step by step or continuously) are adjusted according to the specific requirement of the measurement. The measurement result is displayed automatically after the scanning is finished.

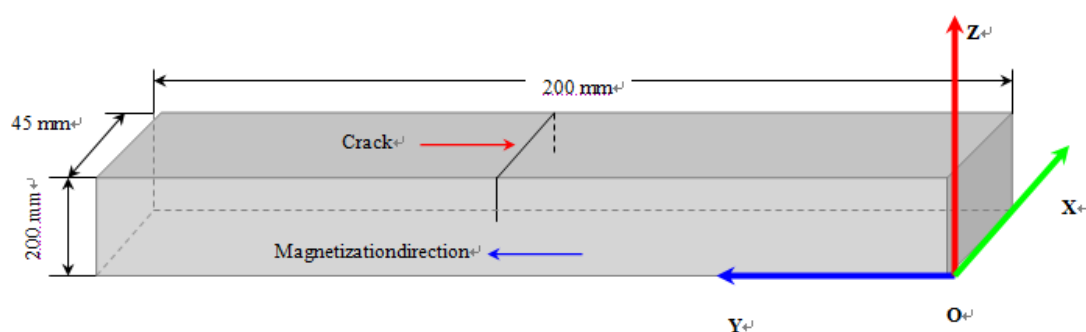


Figure 5-1 Specimen with artificial defect

In order to get a relative uniform distribution of magnetic flux, the specimen is magnetized overall by an electromagnet using the magnetic flow technique. The hysteresis curve of the material is a wide loop and the remanence value of the material is around 0.7 T. It is close to the minimum magnetic flux density that has been specified for the carrying out of magnetic flux leakage testing. Furthermore, there is no sudden cut-off value, below which the MFL leakage testing does not work. There will only be a gradual diminution in flaw sensitivity if lower magnetic fluxes are used. Therefore the residual magnetism is used to carry out magnetic leakage testing. The magnetic field direction is perpendicular to the crack.

Before the measurement starts, support points are collected first, they can be used to determine the scan area on the specimen. The support points are collected by moving the sensor near the specimen manually with the “KUKA Robot Motion System” module, then, with the help of the “Search” function provided by the software module, the robot will automatically approach the surface of the specimen and stop immediately after the sensor contacts with specimen surface lightly, the location of the magnetic sensor becomes the support point and can be stored in the support points list in the “Robot Script Controller” module. After all the necessary support points are collected and stored, the test area on the specimen is determined. The scanning task is then described as a script in the “Robot Script Controller” module and the robot scan path is planned with these support points. The robot scan path is shown in Figure 5-2. Surfaces with crack are scanned continuously with a sequence settled in the script command. Scan task management is shown in Figure 5-3. Each line of the script corresponds to a scanning task. These lines are executed one after another.

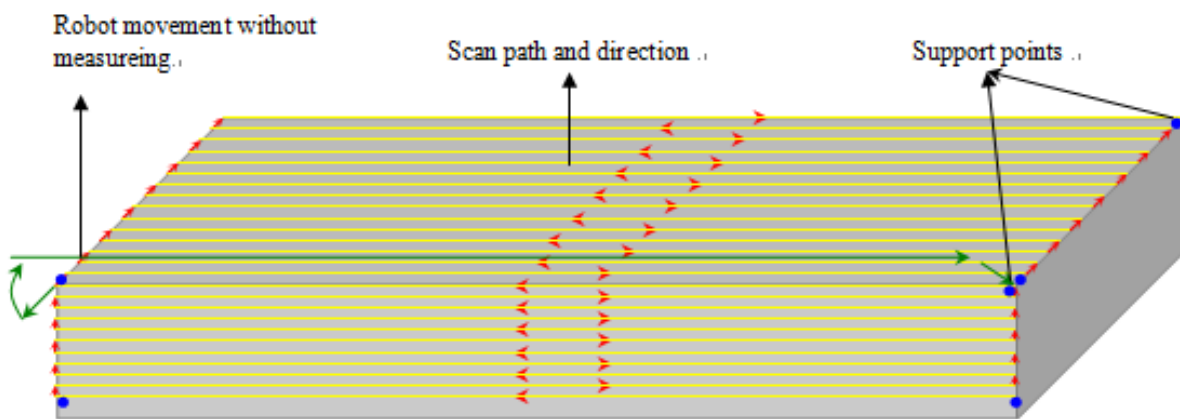


Figure 5-2 Schematic description of scan path

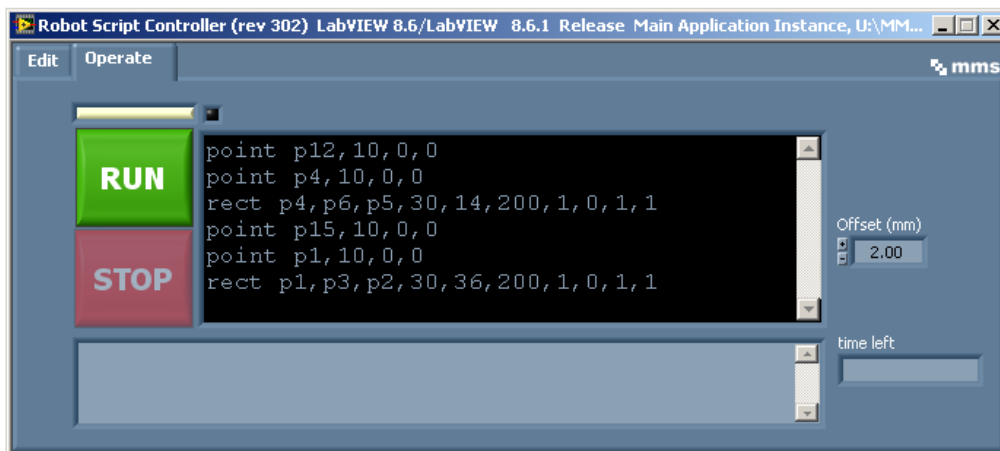


Figure 5-3 Description of the scanning task as script

For a scanning area of the same size, the scanning time depends on the resolution and the scanning velocity which are set at the beginning of the test. The resolution is determined based on considering several factors comprehensively such as estimated dimension of the defect, size of scanning area, the required accuracy and efficiency of each specific test. In the present confirmatory experiment, one of the scanning areas is 14 mm × 200 mm. The resolution is set to be 70×1000 scanning points. The scanning velocity is chosen according to the resolution selected. A proper velocity should ensure that the desired resolution is achieved. The current coordinates of the sensor from the robot controller can be updated every 12 ms, this update rhythm is determined by the communication property and the KUKA robot software packet, and can not be changed. The lower the scanning velocity, the longer the scanning time lasts and the more coordinates need to be recorded. In our testing, the scanning velocity is improved without decreasing the resolution by interpolating the coordinates recorded. For a continuous scan path with length of 200 mm, the resolution is set to be 1000, and the scanning speed is about 17 cm/s. The scan time used for a scan area of size 14 mm × 200 mm with a resolution of 70 × 1000 is about 2 minutes. The whole measuring process includes four steps: support point collection, scan task description, scanning process and result display, it can be finished within 5 minutes. Scanning time can be reduced further if the resolution is set lower, provided the defect can be detected in the reconstructed image.

After the scanning is accomplished, the measurement data from the magnetic sensor and its location obtained during scanning are analyzed and the result of the measurement is displayed in the developed three-dimensional measurement display module “3D Inspector”.

Figure 5-4 displays the measurement result obtained with the “3D Inspector”. The three-dimensional reconstruction of the three surfaces is demonstrated in the module. Cracks on the surface of the specimen can be observed directly and explicitly in the reconstructed image. The tendency of the magnetic leakage field distribution around the crack is also displayed. Location of the crack displayed in the reconstructed coordinate system is consistent with the crack position on the test block.

In order to analyze more explicitly the magnetic field distribution on a specific area of the reconstructed image, a 3D cursor function which is specially designed for the result display module can be used. If one moves the 3D cursor to the point of interest on the reconstructed image, and A-Scan results about this point on the corresponding surface are displayed on the left and top side of the three-dimensional reconstruction image. As shown in Figure 5-4, a cursor is put on the surface in the Y-Z plane of the coordinate

system, an A-Scan that is parallel to Y is displayed on the top side and an A-Scan that is parallel to Z is displayed on the left side. Surface noise due to finishing status of the surface and the non-linearity of the permeability is also seen in the image. Therefore, experimental investigation of the interacting effect of the two adjacent cracks is facilitated. The measurement result can be graphically displayed as a reconstructed image and saved in BMP format or JPEG format. It can also be saved as text format to enable further evaluation. Sensor lift-off can be precisely adjusted with the help of the integrated touch probe system according to the surface status of the specimen. Possible wear of the magnetic sensor and damage of the specimen can be avoided.

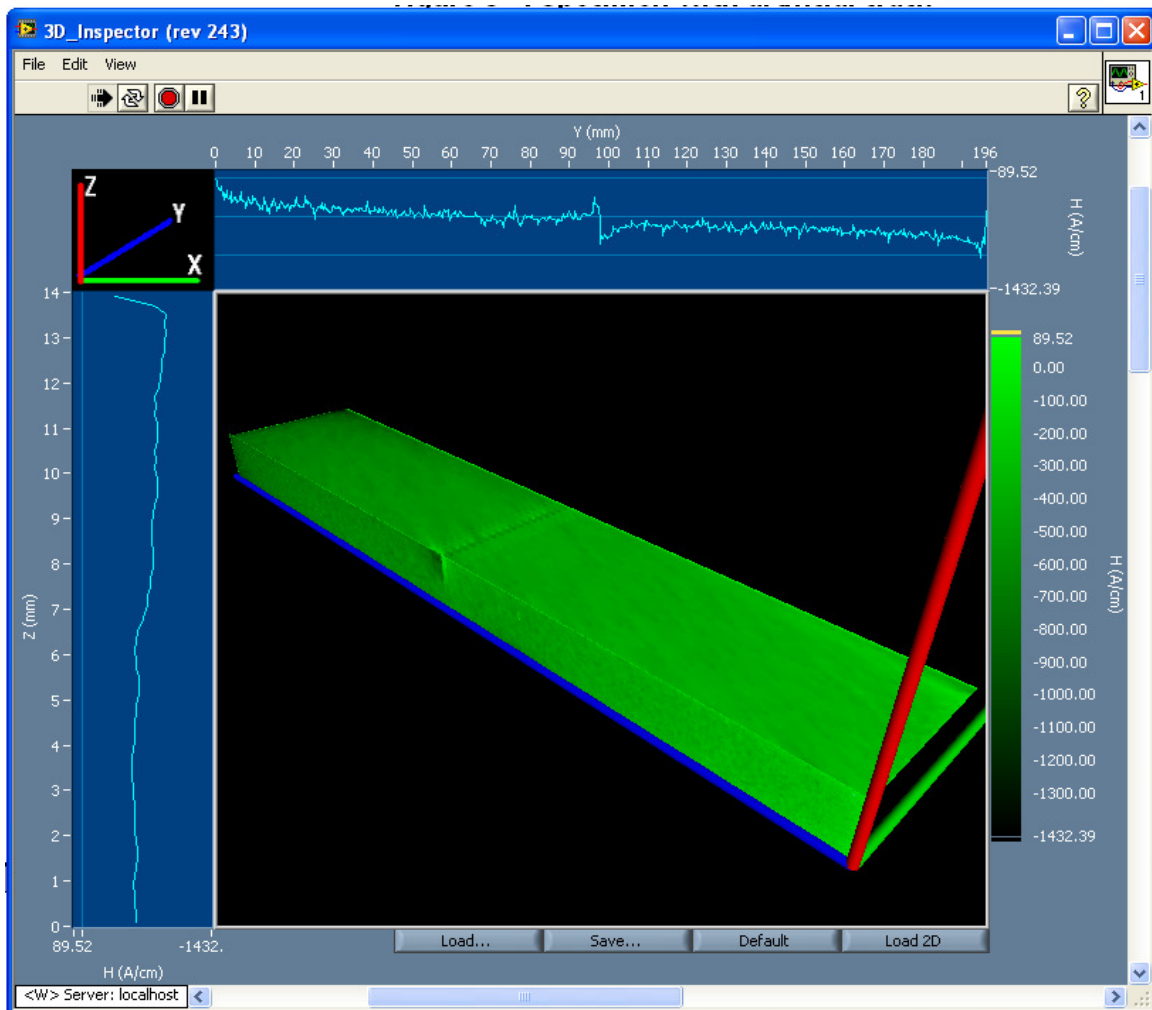


Figure 5-4 3D Display of the measurement result

Since the scanning parameters are programmable during the measurement, hot issues about the magnetic sensor based MFL testing which are mostly studied by simulation method can be effectively verified experimentally with the developed automated measurement system. For example, sensor lift-off, scanning speed and resolution are programmable for each specific measurement. The study of sensor lift-off effect and its

influence on the magnitude of the detected signal, the influence of the magnetic sensor speed during the measurement on the detected signal value, identification of the two cracks can be facilitated. Furthermore, highly accurate measurement results obtained from the precisely controlled measurement process can provide a basis for quantitative study of flaw characteristics based on the fact that peak-peak amplitude of the MFL signals indicates the defect depth and the peak-peak separation distance can be used to characterize the length of the flaw [Lord1978]

5.2 Remanence detection on steel bar

Another application case is the remanence detection on a cylindrical object with relative large dimensions. Circumferential surface of the cylinder is to be scanned. As shown in Figure 5-6, the steel bar has a diameter of about 487 mm and a height of 120 mm.

Due to the fact that sensor lift-off and coupling between the magnetic sensor and the surface to be measured can influence the measurement results strongly, credible measurement result can only be obtained with sensor position and orientation controlled very precisely during the scanning. Although the size of the applied magnetic sensor is relative small compared to the circumferential surface to be measured, the sensor surface still needs to be parallel to the tangent plane of the cylinder during the scan as illustrated in Figure 5-6. Sensor lift-off should also be kept at a constant value. Furthermore, efficiency is also a factor that cannot be ignored for inspection of the surface with a relative large size. The measurement process is to be carried out continuously and automatically.

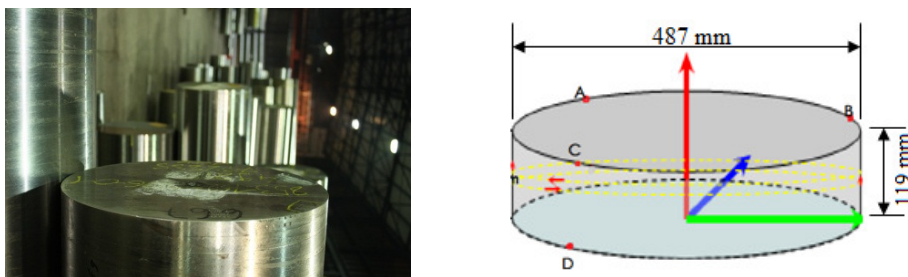


Figure 5-5 Steel bar

For such curved surface scanning tasks with high requirements for accuracy and efficiency, the existing magnetic flux leakage testing system at IZFP can no longer meet the requirement due to the limitation on the size of specimen that can be scanned.

The developed measurement system is applied to the measurement, and the capability of the system to handle such measurement task accurately and efficiently has been tested.

First, support points by which the location and size of the steel bar are determined are collected. The accurate definition of the 3 support points which decide the diameter of the cylinder is important for good contact of the magnetic sensor with the scanning surface. This can only be assured by picking up the support point accurately. Otherwise, the coupling of the magnet sensor and the specimen surface to be tested may not be good. Sensor lift-off can not be kept constant during the test. Therefore for this situation a misleading result may be obtained based on the measurement data received. Some faint remanence may not be detected if there is a too large a lift-off of the magnetic sensor. Furthermore, a large contact force will lead to fast wear of the sensor and the potential damage to the specimen surface.

With the semi-automated support point definition function, support points are defined automatically with efficiency and accuracy. The accuracy is improved due to the integrated high accuracy Renishaw touch probe. A uniform contact force between the magnet sensor and the circumferential surface is ensured, thus a persuasive result is guaranteed. As shown in Figure 5-6, there are 4 support points A, B, C and D. Support point A, B and C on the circumference of the upper surface of the cylinder are used to decide the diameter of the cylinder. Support point D is on the circumference of the lower surface, the straight line between C and D is parallel with the axis of the cylinder. Therefore, C and D can be used to determine the height of area to be test on the cylinder. After all the support points are collected, the testing process is programmed as script in the robot controller module. The measurement starts automatically after the start menu is activated.

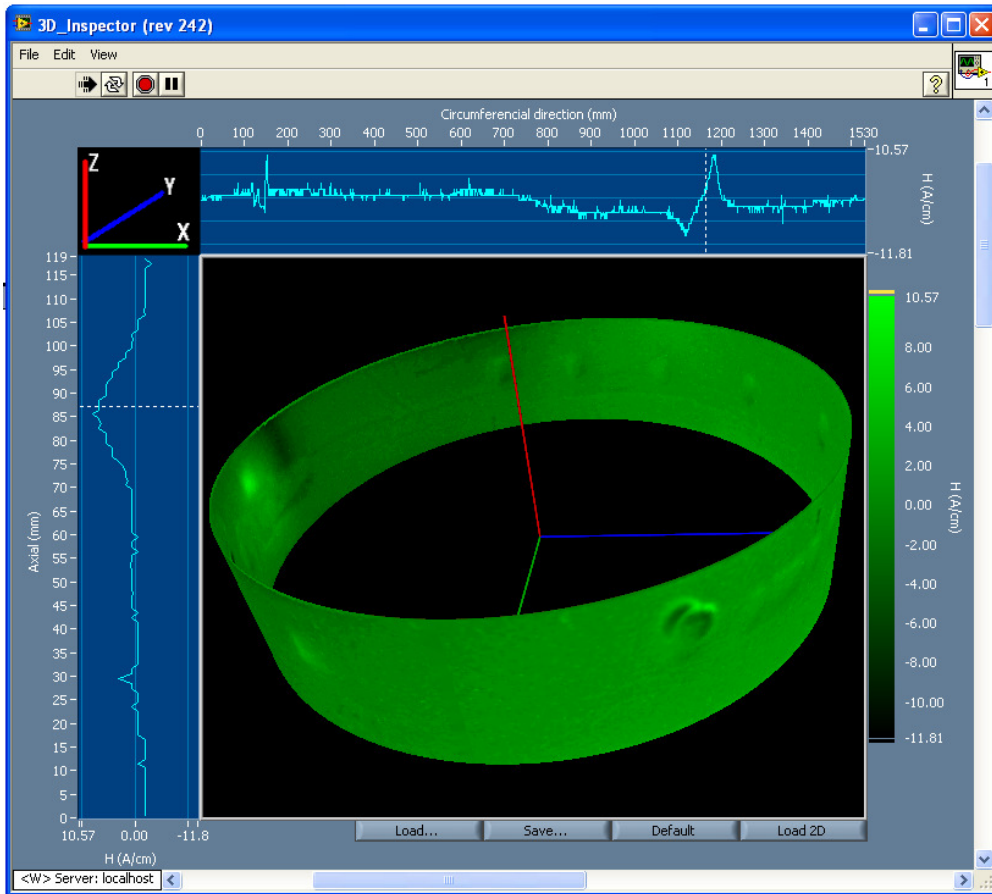


Figure 5-6 3D Demonstration of the measurement result

The reconstruction image of the scanned cylinder is displayed in the “3D Inspector” module automatically after the scan process is finished. Figure 5-7 shows the measurement result. The cylindrical form of specimen is reconstructed in the demonstration module and the remanence can be seen explicitly.

One can move the 3D cursor on the reconstructed image to the desired point. A-scan results around this point are displayed on the left and top side of the three-dimensional reconstructed image. As shown in Figure 5-7, A-scan result that is parallel to the Z-axis is displayed on the left side and circumferential A-scan through the point is displayed on the top.

With the regrinding character of the scanning specially designed for scanning of specimen with curved surfaces, the scanning path transition is smooth and continuous. The robot standstill during the scanning can be avoided and a higher scan speed can be achieved. The cylinder has a diameter of 487 mm, and the scan range in length axis direction is 120 mm. The scan process lasts for 1.5 hours when the scanning speed is

set to be 10% (6 cm/s) of the full speed of robot movement. The efficiency of the measurement is up to about 80% improved.

The example also shows that the developed system can adapt to measurement of a component with different geometry and size conveniently with only little change of script programming and parameter setting. The flexibility of the system is demonstrated.

5.3 Measurement of cheek dimension on crankshaft

The crankshaft is one of the key components of an engine which has the function of translating reciprocating linear piston motion into rotation. The bearing surface of a crankshaft is usually hardened using the induction method or the nitridization method because of higher stresses during operation. In this practical application, the cheek dimension which is a very important reference parameter is to be investigated with the developed system. The cheek dimension is noted in Figure 5-8.

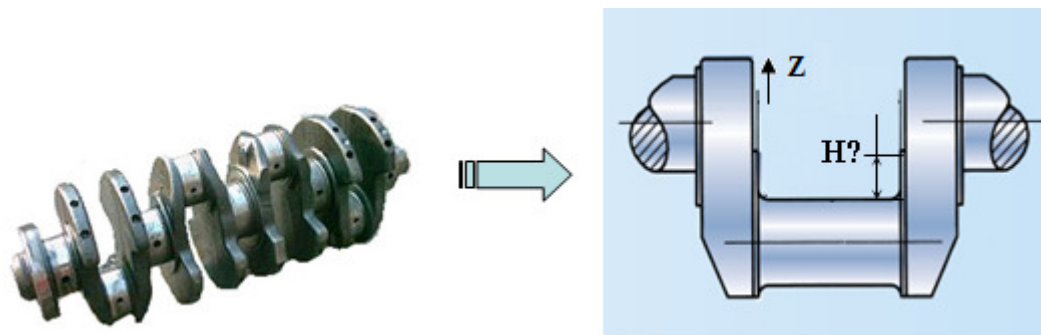


Figure 5-7 Cheek dimension measurement on crankshaft

The measurement concept is shown in Figure 5-9. The cheek dimension can be ascertained from the hardness trend curve that obtained by measuring the hardness difference between hardened layer and base material of the crankshaft. The hardness trend curve is obtained by depicting the hardness of each testing point along the scan path. The hardness of each test point is measured non-destructively by 3MA measurement after the 3MA instrument is calibrated.

This test was previously carried out manually with the 3MA probe held by hand during scanning. Since the cheek dimension to be measured is about 8 mm. A permissible error is 100 μm . A relative big error may be introduced in the manual measurement. Furthermore, as illustrated in Figure 5-9, an offset is to be set because of the influence of fillet on the scanning path. Therefore, a reliable measurement is very difficult to be obtained manually.

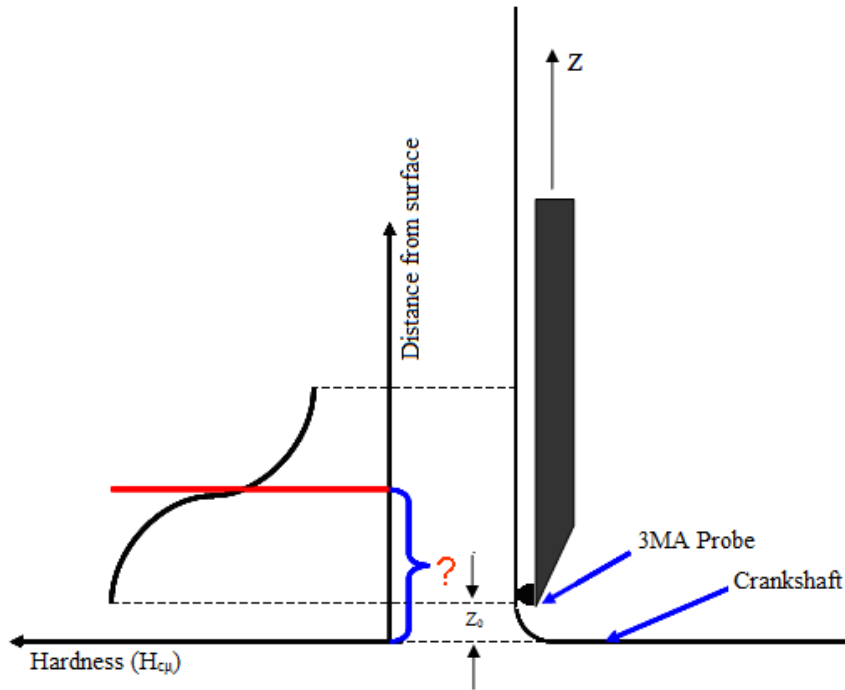


Figure 5-8 Concepts for cheek dimension measurement; $Z_0=2$ mm

As an automated solution for the measurement task described above, the developed system is combined with the 3MA test device by connecting both the robot controller and the 3MA device to the external control PC through the Ethernet. As shown in Figure 5-9, the 3MA Probe with integrated Renishaw touch probe is held by the robot system. A reference point used to set offset is first found by the touch probe system with an accuracy of ± 20 μm . The scan path is then programmed precisely with a step of 100 μm .

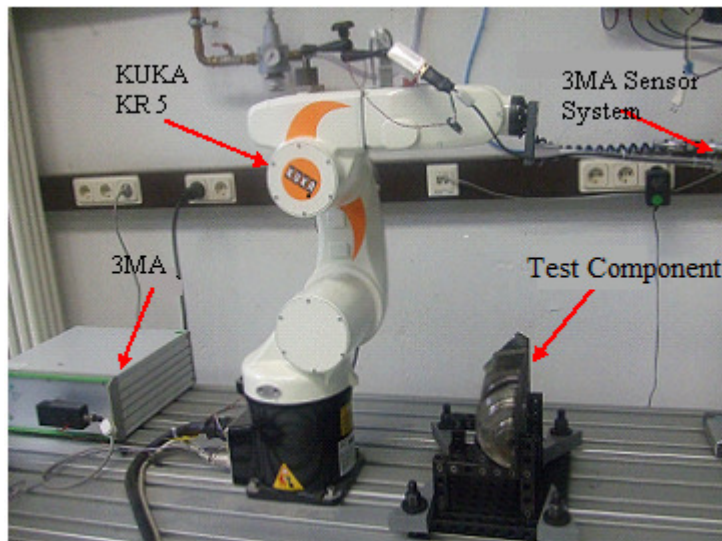


Figure 5-9 Experiment layout

Since the 3MA device is very sensitive to electromagnetic interference, the measurement process can be interrupted by EMI (electromagnetic interference) around very easily. However, as shown in Figure 5-10, much electromagnetic interference can be introduced by robot motors of each axis and the 3MA device can be strongly influenced during the measurement. Furthermore, the 3MA sensor cannot be completely shielded against electromagnetic interferences, the alternating electromagnetic fields in the selected analysis frequency range and/or working frequency range may disturb and alter the inspection results.



Figure 5-10 Source of the EMI

Since EMI only happens if motors of robot are working, the 3MA device can work trouble-free if the robot comes to a standstill and the current for each motor is cut off. Therefore, a key question here is to synchronize the robot movement and the 3MA device measurement process based on the principle that only one process is active at one time, the 3MA works when robot is off and 3MA measurement is on hold when the robot moves. The work principle is illustrated in Figure 5-11.

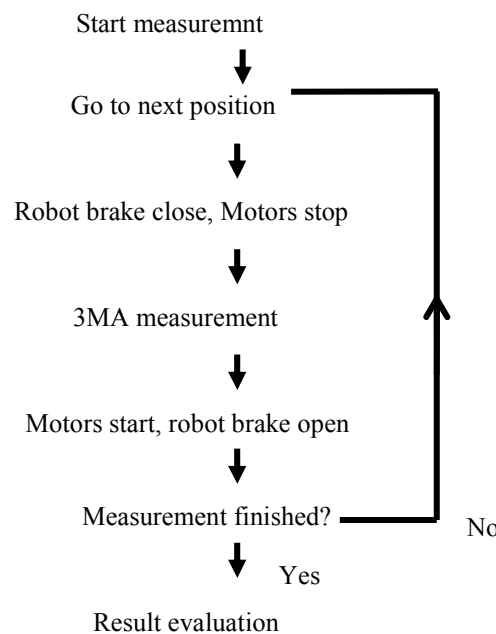


Figure 5-11 Solution for EMI problem

The result of the measurement is shown in Figure 5-12. A hardness trend is depicted and the minimum value indicates the end of the hardened layer. The cheek dimension is

shown automatically after the test data is loaded. A comparative measurement is done manually by which the results are compared to the results obtained automatically. There are 0.1 mm differences which may be caused by the relative poor coupling of 3MA sensor with surface of the specimen at the edge of the hardened layer.

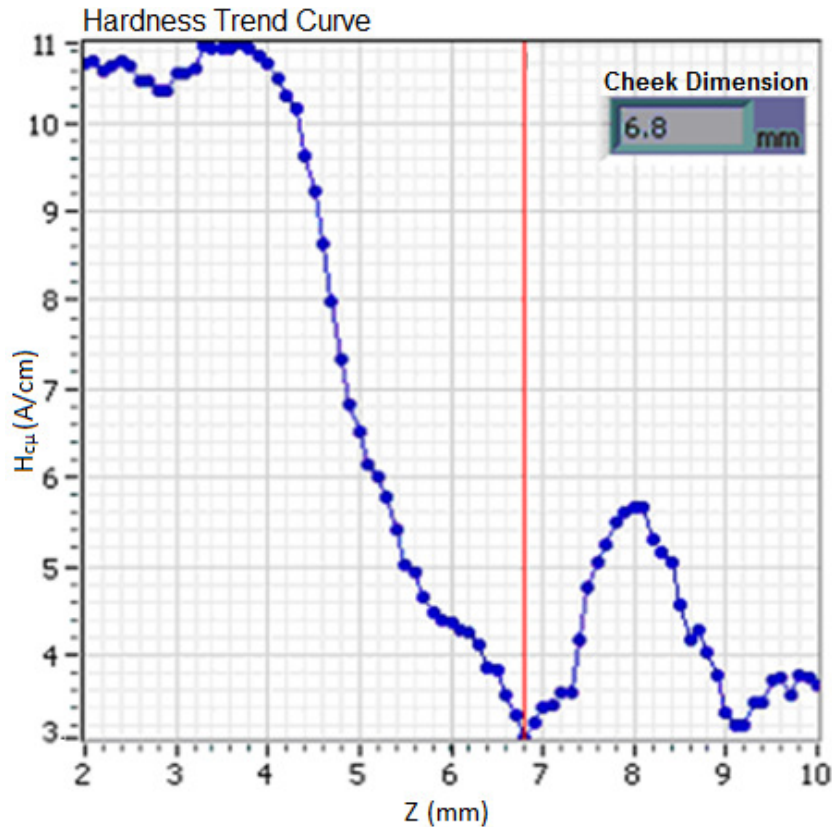


Figure 5-12 measurement result

In this application, EMI problem is eliminated at the cost of efficiency and the wear of the robot. The robot stops at each test point, but current supply for the motors of the robot can not stop immediately after the robot comes to a standstill. The current supply will be cut off in 200 ms if the robot controller received no command within this duration. Thus, with frequent decelerating and accelerating, each measurement cycle take much more time. Furthermore, more noise from the robot is made by the each braking process. The wear of the robot is also unavoidable. A more efficient solution against EMI must be found for the future application of the robot supported measuring system with 3MA testing technology.

This application case shows that the developed system can also be employed for ferromagnetic material characterization by combining with the 3MA test technique. The measurement with the 3MA analyzer can be carried out automatically with efficiency and more accuracy.

6 Conclusion and outlook

In the present work it was the aim to develop a robot based automated measurement system for magnetic flux leakage testing in order to improve the flexibility, efficiency and accuracy of inspection.

An industrial robot is introduced for automated measurement of MFL testing due to the increasing demand for higher flexibility, accuracy and efficiency. The special needs for the application of an industrial robot in MFL testing compared with traditional application are discussed in chapter 3 and 4. Based on this information, a suitable type of industrial robot, meeting the specific requirements of MFL testing, was selected. One of the bottlenecks that have earlier earned much attention and efforts from researchers, was how the robot control and programming can be simplified. In the present work, this issue is solved with a novel robot control and programming concept based on Ethernet communication between the robot controller and an intelligent external system.

With the Ethernet communication established between the robot controller and the intelligent external system, information received by the robot controller from the external system can be used to influence the robot motion in real-time which has been programmed with a robot specific programming language. Thus, the robot can be controlled by a more powerful and flexible external intelligent system. Due to the fact that ordinary users of a automated system may not possess the necessary knowledge and skills for robot control, programming, and operation, the motion program is further simplified which is written in a robot specific programming language. The programming with the robot specific language is done once and for all and real-time robot movement is only decided by the path planned with powerful commercial software running on the external system. All the processes of the measurement e.g. robot programming, measurement task management, result display, etc. can be performed on the external system.

Based on the modular software concept, the application software running on the external system is divided into several modules and each module is responsible for a specific function. These modules are developed in the graphical programming environment LabVIEW. Function modules can be flexibly combined for specific measurements. If required, modifications should only be done on the related module. The "Robot script controller" discussed in section 4.3.4 is the controller module which is mainly responsible for path planning of the robot and process control of the MFL testing. Measurement tasks are settled and managed as a script. It is designed to be

independent from the robot type and manufacturer and it is universally applicable for articulated robots with up to 8 arms. The module “KUKA Robot Specific Motion System” discussed in section 4.3.3 is the robot motion module which is mainly responsible for the establishment of Ethernet communication between robot controller and external control PC, collision detection and manual adjustment of robot position etc. This module is KUKA robot specific. A measurement result display module “3D Inspector” discussed in section 4.3.5 has been developed for collection of sensor data and robot coordinates, data processing and 3 dimensional measurement result display. For inspection of objects with more complex surfaces, the measurement task is decomposed into several simple parts. These parts are arranged in the robot script controller module in a sequence. Measurement results which are 2-dimension intensity graphs are mapped on the geometry, reconstructed with support points. Furthermore, the integration of force/torque sensors into the measurement system makes the robot motion control more intelligent in case of support point searching, collision identification, sensor or object surface protection and other issues.

The robot-based magnetic flux leakage measurement is applied for crack detection on a ferromagnetic test block with rectangular form. The crack has a width of about 1~10 μm . The measurement task is simply decomposed according the surface area to be tested, and the system performance and measurement results are demonstrated in section 5.1. This verifies the detectability and efficiency of the robot-based automatic measurement system for surface crack detection on ferromagnetic material. Another application discussed in section 5.2 is the remanence detection on a steel bar with a diameter of 473 mm. With the same procedure and a slight change in the robot script program, the robot system has been adapted from scanning rectangular objects to scanning cylindrical objects. The basic principle of MFL testing of complex sample shapes remains the same.

Furthermore, sensor lift-off and scanning speeds influence the measurement results strongly. Therefore much attention should be paid to this point in MFL testing in order to obtain accurate results. It is easy to control these two factors to obtain accurate results with the automatic measurement system built in this work as compared to the most often used 3-axis manipulator.

In another application, the automatic measurement system is combined with a 3MA measurement instrument for investigation of cheek dimension on crankshaft. Compared with the common manual testing, reference points are searched automatically with high accuracy and efficiency. The 3MA sensor is positioned precisely to the destination with 0.1 mm accuracy. This shows the capability of the automated system to interact with

other testing technology to improve the measurement performance in terms of accuracy and efficiency. It can serve as an automated platform for other inspection tasks.

Finally, the robot based automatic measurement system for MFL testing that was developed has the potential to be improved further. The following issues should be included to build on the present work:

1. Modern sensor technology can be applied for more intelligent robot programming and a driver program method can also be applied;
2. Other than the support point concept, path planning should also be able to be performed with information from multiple sources, e.g. CAD files, infrared scanning or laser scanning data for surface reconstruction, simulation etc.
3. More advantageous sensor type e.g. TMR, GMI should be applied for magnetic flux leakage testing to obtain enhanced test results.

7 Bibliography

- [Alts1995] Altschuler, E.; Pignotti, E.: *Nonlinear model of flaw detection in steel pipes by magnetic flux leakage*. NDT&E International. 1995, **28**, Pages: 35-40.
- [ASTM2009] ASTM Standard: *E0570-09 Practice for Flux Leakage Examination of Ferromagnetic Steel Tubular Products*. Volume 03.03, 2009.
- [Atzl2010] Atzlesberger, J.; Zagar, B.: *Magnetic flux leakage measurement setup for defect detection*. Procedia Engineering. 2010, **5**, Pages: 1401-1404.
- [Baib1988] Baibich, M. N.; Broto, J. M.; Fert, A.; Nguyen van Dau, F.; Petroff, F.; Etienne, P.; Greuzet, G.; Friedrich, A.; Chazelas, J.: *Giant magnetoresistance of (0 0 1)Fe/(001)Cr magnetic superlattices*. Phys. Rev. Lett. 61 (1988) 2472.
- [Bain1977] Bainton, K. F.: *Characterizing defects by determining magnetic leakage fields*. NDT & E International, 1977, **10**, Pages: 253-257.
- [Blom2005] Blomdell, A.; Bolmsjö, G.; Brogradh, T.; Cederberg, P.; Isaksson, M.; Johansson, R.; Haage, M.; Nilsson, K.; Olsson, M.; Olsson, T.; Robertsson, A.; Wang, J.: *Extending an Industrial Robot Controller*. IEEE Robotics & Automation Magazine. 2005. 1070-9932-05.
- [Boop1995] Boopathy, S.; Radhakrishnan, V.: *An approach to robot off-line programming and simulation for flexible manufacturing systems*. International Conference on Industrial Automation and Control. 1995 (IA&C'95) IEEE/IAS (Cat. No. 95TH8005) Pages: 461-466.
- [Boot1992] Booth, D. E.: *A Robust Multivariate Statistical Procedure for Evaluation and Selection of Industrial Robots*. International Journal of Operations & Production Management, 1992, **12**, Pages: 15-24.
- [Bozo1951] Bozorth, R. M.: *Ferromagnetism*. IEEE Press, New York. 1951.
- [Carb1987] Carbone, C.; Alvarado, S. F.: *Antiparallel coupling between Fe layers separated by a Cr interlayer: Dependence of the magnetization on the film thickness*. Physical Review B, 1987, **36**, Pages: 2433-2435.
- [Cata2003] Catalin, M.; Lynann, C.: *A model for magnetic flux leakage signal predictions*. Journal of Physics. D: Applied Physics, 2003, **36**, Pages: 2427-2431.
- [Chan2003] Chan, S.F.; Kwan, R.: *Post-processing methodologies for off-line robot programming within computer integrated manufacture*. Journal of Materials Processing Technology. 2003, **139**, Pages: 8-14.

- [Ched2003] Chedister, W. C.: *Quantitative Evaluation of Magnetic Particle Inspection Materials*. 2003.
URL: <http://www.aaende.org.ar/sitio/biblioteca/material/T-112.pdf>
- [COMS2005] COMSOL Multiphysics. User's Guide. COMSOL, 2005.
- [Conn2002] O'Connor, S.; Clapham, L.; Wild, P.: *Magnetic flux leakage inspection of tailor-welded blanks*, Meas. Sci. Technol. **13**, 2002, Pages: 157-162.
- [Crai2004] Craig, J. J.: *Introduction to Robotics: Mechanics and Control, 3rd Edition*. Prentice Hall, 2004.
- [Dill2009] Dillhöfer, A.; Rieder, H.; Spies, M.: *Roboterbasierte Detektion von Oberflächenstrukturen in komplexen Freiformflächen mittels Luftultraschall und Methoden der Bildverarbeitung*. DGZfP-Jahrestagung 2009 - Poster 45.
- [DIN2001] Europäisches Komitee für Normung, DIN EN ISO 9934, Magnetpulverprüfung. CEN, 2001
- [Dobm1980] Dobmann, G.; Höller, P.: *Physical Analysis Methods of Magnetic Flux Leakage*. Hrsg.: Sharpe, R. S.: Research techniques in NDT, London, Academic Press. 1980, Pages: 39-69.
- [Dobm1987] Dobmann, G.; Walle, G.; Höller, P.: *Magnetic leakage flux testing with probes: physical principles and restrictions for application*. NDT International. 1987, **20**, Pages: 101-104.
- [Dobm2007] Dobmann, G.; Altpeter, I.; Wolter, B.; Kern, R.: Industrial Applications of 3MA – Micromagnetic, Multiparameter, Microstructure and Stress Analysis. 5th Int. Conference Structural Integrity of Welded Structures, Romania 2007.
URL: www.ndt.net/search/docs.php3?MainSource=56
- [Dutt2009a] Dutta, S. M.; Ghorbel, F. H.; Stanley, R. K.: *Dipole Modeling of Magnetic Flux Leakage*. IEEE Transactions on Magnetics. 2009, **45**, Pages: 1959-1965.
- [Dutt2009b] Dutta, S. M.; Ghorbel, F. H.; Stanley, R. K.: *Simulation and analysis of 3-D Magnetic flux leakage*. IEEE Transactions on Magnetics. 2009, **45**, Pages: 1966-1972.
- [Edwa1986] Edwards, C.; Palmer, S. B.: *The magnetic leakage field of surface-breaking cracks*. Journal of Physics. D: Applied Physics, 1986, **19**, Pages: 657-673.
- [Engl2009] Engl, G.; Kröning, M.; Mohr, M.; Reddy, K.M.; Ribeiro, J.: *Current R&D for Advanced Ultrasonic Inspection Techniques*. Proceedings of: Congresso Internacional sobre Tecnologia de Equipamentos 2009, Salvador, Brazil, May 2009.

- [Ewal2003] Ewald, H.: *3-Dimensional Magnetic Leakage Field Sensor in Nondestructive Testing*. Instrumentation and Measurement Technology Conference, 2003, Proceedings of the 20th IEEE. Pages: 1309-1311.
- [Förs1985] Förster, F.: *On the Way from the Know-How to Know-Why in the Magnetic Leakage Field Method of Nondestructive Testing. Part I and II*. Material Evaluation. 1985, **43**, Page 1398.
- [Förs1986] Förster, F.: *New findings in the field of non-destructive magnetic leakage field inspection*, NDT International. 1986, **19**, Pages: 3-14.
- [Förs2007] Institut Dr. Förster GmbH & Co KG: *CIRCOFLUX®*. Geräteblatt als Datei im PDF-Format.
URL:<http://www.foerstergroup.de/CIRCOFLUX-sensor-system.77+M52087573ab0.0.html> Stand: August 2007.
- [Freu1998] Freund, E.; Rokossa, D.; Rossmann, J.: *Process-oriented approach to an efficient off-line programming of industrial robots*. Industrial Electronics Society. IECON'98. Proceedings of the 24th Annual Conference of the IEEE. 1998, **1**, Pages: 208-213.
- [Grün1986] Grünberg, P. A.; Schreiber, R.: *Layered magnetic structures: evidence for anti-ferromagnetic coupling of Fe layers across Cr inter-layers*. Physical Review Letters, 1986, **57**, Pages: 2442-2445.
- [Grün2001] Grünberg, P. A.: Exchange anisotropy, interlayer exchange coupling and GMR in research and application. Sensors and Actuators A, 2001, **91**, Pages: 153-160.
- [Haas2006] Haase, A.; Schafmeister, A.; Hessert, R.; Satzger, W.: *Charon XRD A New Twin Robot X-ray Diffractometer for Surface Analysis of Complex Aircraft Components*. ECNDT 2006.
URL: <http://www.ndt.net/article/ecndt2006/doc/Fr.2.1.1.pdf>
- [Hart1999] Hartmann, U.: *Magnetic Multilayers and Giant Magnetoresistance: Fundamentals and Industrial Applications*. Berlin/Heidelberg, Springer, 1999.
- [Herz1995] Herzer, R.; Frick O., Keferstein, C.; Arnold W.; Self-tracking ultrasonic inspection, Industrial Robot, 1995, **22**, Pages 25-27
- [Huan2006] Huang, Z.; Que, P.; Chen, L.: *3D FEM analysis in magnetic flux leakage method*, NDT&E International. 2006, **39**, Pages: 61-66.
- [Hwan2007] Hwang, J.; Lee, J.; Jun, J.; Wang, R.; Choi, S.; Hong, S.: *Scan Type Magnetic Camera Images with a High Spatial Resolution for NDT Obtained By Using a Linearly Integrated Hall Sensors Array*. IEEE International Workshop on Imaging Systems and Techniques, 2007, DOI: 10.1109/IST.2007.379591, Pages: 1-6.

- [Hwan2009] Hwang, J.; Jinyi, L.; Kwon, S.: *The application of a differential-type Hall sensors array to the nondestructive testing of express train wheels*. NDT&E International. 2009, **42**, Pages: 34-41.
- [IFR2010] IFR Report 2010: *EXECUTIVE SUMMARY of World Robotics 2010 Industrial Robots*.
- [Inte2011] Kröning, M.: Private information: intelligentNDT System & Services GmbH; Erlangen, Germany, 2011.
- [ISO1994] ISO Standard 8373:1994, Manipulating Industrial Robots.
- [Ivan2006] Ivanov, V. E.; Bashkinova, V. N.: *Visualization and Topography of the Stray Magnetic Field of Crack-Type Discontinuities in Magnetic Materials*. Russian Journal of Nondestructive Testing. 2006, **42**, Pages: 12–18. URL: http://www.worldrobotics.org/downloads/2010_Executive_Summary_rev%281%29.pdf
- [Jile1990] Jiles, D. C.: *Review of magnetic methods for nondestructive evaluation (Part 2)*. NDT International. 1990, **23**, Pages: 83-92.
- [Karl2011] Karl Deutsch Prüf- und Messgerätebau GmbH + Co KG: *DEUTROFLUX Magnetic Particle Crack Detection Bench*. http://www.karldeutsch.de/fm_deutrosu_en.htm Status: 2011.
- [Karn2009] Karnauhov, D.: *Coordinate Interface for Robot-Supported non-Destructive Testing*. Master thesis. Department of Material Science, Saarland University. Saarbrücken, 2009.
- [Kata2002] Kataoka, Y.; Wakiwaka, H.; Shinoura, O.: *Application of GMR line sensor to detect the magnetic flux distribution for non-destructive testing*. Sensors, Proceedings of IEEE, 2002, Pages: 800-803.
- [Kato2000] Katoh, M.; Nishio, K.; Yamaguchi, T.: *FEM study on the influence of air gap and specimen thickness on the detectability of flaw in the yoke method*. NDT&E International, 2000, **33**, Pages: 333-339.
- [Kato2003] Katoh, M.; Masumoto, N.; Yamaguchi, T.: *Modeling of the yoke-magnetization in MFL-testing by finite elements*. NDT & E International, 2003, **36**, Pages: 479-486.
- [Kato2004] Katoh, M.; Nishio, K.; Yamaguchi, T.: *The influence of modeled B-H curve on the density of the magnetic leakage flux due to a flaw using yoke-magnetization*. NDT&E International. 2004, **37**, Pages: 603-609.
- [Kim2004] Kim, J.Y.: *CAD-Based Automated Robot Programming in Adhesive Spray Systems for Shoe Outsoles and Uppers*. Journal of Robotic Systems. 2004, **21**, Pages: 625-634.

- [Klos2005] Kloster, A.: *Grundlagenforschung auf dem Gebiet der Fehlerprüfung mittels elektromagnetischer Prüfverfahren*. IZFP-Bericht Nr. 050139-TW, Saarbrücken, 2005.
- [Klos2008] Kloster, A.: *Aufbau einer Entwicklungsplattform für niederfrequente magnetische Prüfverfahren*. PhD thesis. Faculty 8, Saarland University. Saarbrücken, 2008. URL: scidok.sulb.uni-saarland.de
- [Krön2010] Kröning, M.: Private Communication. 2010.
- [Krön2011] Kröning, M.: Private Communication. 2011.
- [KUKA2009] KUKA Robot User Manual. Status: 2009.
- [LabV2010] Introduction to LabVIEW.
URL: <http://www.df.unibo.it/star/pdf/DOC-LabVIEW.pdf>, Status: January 2010.
- [Li2006] Li, Y.; Tian, G.; Ward, S.: *Numerical simulation on magnetic flux leakage evaluation at high speed*. NDT&E International. 2006, **39**, Pages: 367-373.
- [Liu2008] Liu, F.; Ding, S.; Guo, X.: *Magnetic Flux Leakage and Acoustic Emission Testing Technique for Atmospheric Storage Tanks*, 17th World Conference on Non-destructive Testing, 25-28 Oct 2008, Shanghai, China.
- [Lord1978] Lord, W.; Bridges, J. M.; Yen, W.; Palanisamy, R.: *Residual and active leakage fields around defects in ferromagnetic materials*. Material Evaluation 1978, **36**, Pages: 47-54.
- [Love1993] Lovejoy, D.: *Magnetic Particle Inspection: A practical Guide*. Kluwer Academic Publishers, Netherlands, 1993.
- [Loza1982] Lozanod-Perez, T.: *Robot Programming*. Proceedings of the IEEE. 1983, **71**, Pages: 821-841.
- [Luky2003] Lukyanets, S.; Snarskii, A.; Shamonin, M.; Bakaev, V.: *Calculation of magnetic leakage field from a surface defect in a linear ferromagnetic material: an analytical approach*. NDT&E International. 2003, **36**, Pages: 51-55.
- [Mand1996] Mandal, K.; Dufour, D.; Krause, T.; Atherton, D.: *Investigations of magnetic flux leakage and magnetic Barkhausen noise signals from pipeline steel*. J. Phys. D: Appl. Phys. 1997, **30**, Pages: 962- 973.
- [Mand2003] Mandache, C.; Clapham, L.: *A model for magnetic flux leakage signal Predictions*. J. Phys. D: Appl. Phys. 2003, **36**, Pages: 2427–2431.
- [Muka1998] Mukae, S.; Katoh, M.; Nishio, K.: *Investigation on quantification of defect and effect of factors affecting leakage flux density in magnetic leakage flux testing method*. Nondest Insp. 1988, **37**, Page: 885.

- [Muzs2003] Muzshizkii, V. F.: *A Model of a Surface Defect and Calculation of the Topograohy of its Magnetic Field for Tangential Magnetization with Alternative Magnetic Field. A Quasi Stationary Case*. Defektoskopiya, 2003, **10**, Pages: 3-17.
- [Nemi2010] Nemitz, O.; Schmitte, T.: *Simulation of Flaw Signals in a Magnetic Flux Leakage Inspection Procedure*. COMSOL Conference 2010 Paris.
- [Nest1999] Nestleroth, J. B.; Bubenik, T. A.: *Magnetic Flux Leakage (MFL) Technology*, United States National Technical Information Center, 1999.
- [Neto2010] Neto, P.; Pires, J. N.; Moreira, A.P.: *CAD-based off-line robot programming*. IEEE Robotics & Automation. 2010, DOI: 10.1109/RAMECH.2010.5513141, Pages: 516-521.
- [Nguy2004] Nguyen, B.: Linux Dictionary.
URL: <http://tldp.org/LDP/Linux-Dictionary/Linux-Dictionary.pdf>.
Status: Version 0.16, August 2004.
- [Ni2011] National Instrument™, NI Developer Zone: *Developing a Modular Software Architecture*.
URL: <http://zone.ni.com/devzone/cda/tut/p/id/3252>. Status: January 2011.
- [Norb2004] Norberto Pires, F.; Godinho, T.; Ferreira, P: *CAD interface for automatic robot welding programming*. Industrial Robot: An International Journal. 2004, **31**, Pages: 71-76.
- [Offo1991] Offodile, O. F.; Ugwu, K.: *Evaluating the effect of speed and payload on robot repeatability*. Robotics and Computer-Integrated Manufacturing, 1991, **8**, Pages: 27-33.
- [Park1991] Parkin, S. S. P.: Systematic variation of the strength and oscillation period of indirect magnetic exchange coupling through the 3d, 4d, and 5d transition metals. Physical Review Letters, 1991, **67**, Pages: 3598-3601.
- [Rams2006] Ramsden, E.: Hall-effect sensors: theory and applications. 2006
- [Rubi1988] Rubinovitz, J.; Wysk, R.A.: *Task level off-line programming system for robotic arc welding — an overview*. Journal of Manufacturing Systems. 1988, **7**, Pages: 293-306.
- [Sack2009] Sackenreuther, H.; Maurer, A.; Koch, R.: *Industrieller Einsatz von synchronisierten Standard-Knickarm-Robotern in Verbindung mit neuester Gruppenstrahlertechnik*. DGZfP-Jahrestagung 2009. Mi.4.C.1.

- [Schm1989] Schmidt, J. T.; Skeite, K.; McIntire, P.: *Nondestructive Testing Handbook. Vol 6. Magnetic Particle Testing*. 2.Edition. American Society of Nondestructive Testing, 1989.
- [Shch1972] Shcherbinin, V. E.; Pashagin, A. I.: *Influence of the extension of a defect on the magnitude of its magnetic field*. Defektoskopiya, 1972, **8**, Pages: 74-82.
- [Shur1977] Shur, M. L.; Shcherbinin, V. E.: *Magnetostatic Field Generated by a Flaw in a Plane-Parallel Plate*. Russian Journal of Nondestructive Testing, 1977, **3**, Pages: 92-96
- [Smit1999] Smith, C.; Schneider, R.: *Low-Field Magnetic Sensing with GMR Sensors*. Sensors EXPO. 1999, Baltimore.
- [Star2007] Starman, S.; Matz, V.: *Automated System for Magnetic Particle Inspection of Railway Wheels*.
URL: http://www.ndt.net/article/ecndt2010/reports/1_10_02.pdf
- [Stol1872] Stoletow, A.: *Über die Magnetisierungsfunktion des weichen Eisen, insbesondere bei schwächeren Schädungskräften*. Annalen der Physik. 1872, **222**, Pages: 439-463.
- [Syku1984] Sykulski, J. K.: *Computational Magnetics*. London, Chapman&Hall, 1984.
- [Szie2001] Zielasko, K.: *Aufbau eines modularen Messsystems auf Softwarebasis zur zerstörungsfreien Charakterisierung des Versprödungszustands von kupferhaltigen Stählen*. Master thesis. Department of Electrical Engineering, HTW Saarbrücken, 2001.
- [Tipl1994] Tipler, P. A.: *Physik*. Spektrum Akademischer Verlag Heidelberg, Berlin, Oxford. 1994.
- [Vett2006] Vetterlein, T: *Entwicklung und Aufbau von produktionsintegrierten, vollautomatischen Magnetpulver Rissprüfanlagen mit Machine Vision gestützter Defekterkennung sowie unabhängiger Parameter und Ergebnisdokumentation*. PhD thesis. Faculty 8, Saarland University, Saarbrücken. 2006.
- [Zagi1998] Zagidulin, R. V.: *Calculation of the Remanent Magnetic Field of a Continuity Defect in a Ferromagnetic Article*. Russian Journal of Nondestructive Testing, 1998, **34**, Pages: 727-731.
- [Zats1966] Zatsepin, N. N.; Shcherbinin, V. E.: *Calculation of the magnetostatic field of surface defects. I. Field topography of defect models*. Defektoskopiya, 1966, **5**, Pages: 50-59.
- [Zhan2009] Zhang, Y.; Ye, Z.; Wang, C.: *A fast method for rectangular crack sizes reconstruction in magnetic flux leakage testing*. NDT&E International, 2009, **42**, Pages: 369-375.

Appendix

KUKA KRL Program

```
=====
DEF KRL_Motion_Interrupt( )
Home={A1 0,A2 -90,A3 90,A4 0,A5 5,A6 0,E1 0,E2 0,E3 0,E4 0,E5 0,E6 0}
=====
; Initialisation: BASISTECH INI and USER INI
=====
;FOLD INI
;FOLD BASISTECH INI
GLOBAL INTERRUPT DECL 3 WHEN $STOPMESS==TRUE DO IR_STOPM ( )
INTERRUPT ON 3
BAS (#INITMOV, 0)
    ;ENDFOLD (BASISTECH INI)
    ;FOLD USER INI
        INTERRUPT DECL 21 WHEN $IN[81]==FALSE DO FOUNDP()
        $ANOUT[1]=0
        $ANOUT[2]=0
        $ANOUT[3]=1
        $ANOUT[4]=0
        $ANOUT[5]=0
        $ANOUT[6]=0
; K is INT, the number of coordinate being operated!
; M is INT, the intermediate variable
; N is INT, the index of the coordinates in Buffer
; I is INT, the total number of coordinates received
; S is INT, the number of coordinates having been operated!
K=1
```

```

M=0
N=1
I=1
S=0
    ;ENDFOLD (USER INI)
;ENDFOLD (INI)
;=====
; Simulation function on and Input [1] active
;=====
;FOLD Simulation $IN[1] = TRUE if $IOSIM_OPT = TRUE
; Simulation of inputs
IF $IOSIM_OPT==TRUE THEN
    ; Simulation is switched on
    $INSIM_TBL[1]=#SIM_TRUE ; $in[1]=true
    ;$INSIM_TBL[1]=#SIM_FALSE ; $in[1]=false
ENDIF
;ENDFOLD (Simulation)

;=====
; RSI objects creation, parameterization, linking
;=====
; Insert IP-address of the Ethernet Card on external control PC!
CIPADR[]="192.168.0.112"
;CIPADR1[]="192.0.1.2"
;FOLD Create RSI-Objects
err = ST_COROB(hCoRob, 0, CIPADR[], 6009, eCROn)
IF err<>#RSIOK THEN
    HALT ; Error

```

```

ENDIF

;err = ST_COROB(hCoRob, 1, CIPADR[], 6009, eCROn)

; Object for digital Input $IN[1]

err = ST_DIGIN(hEnable,0,1,0,0)

err = ST_DIGIN(hDiIn,0,81,0,0)

;digital input $IN[81] is used for INTERRUPT operation!

;(ObjectID, container, Offset in Byte from index 8, rang of bit to read in Byte)

; Object to stop the robot

; Object for cartesian and axis correction values

err = ST_PATHCORR(hPath,0)

err = ST_AXISCORR(hAxis,0)

; Outs 1 till 8 directly represented as INTEGER

err = ST_MAP2DIGOUT(hDiOut,0,hCoRob,eCROutDig,2,1)

;Object for modification of the program override

;Send Integer I(Index in Continue Mode) from KRC to PC

err = ST_ANAOUT(hAout1,0,1,0)

;Send Integer P(Interrupt control) from KRC to PC

err = ST_ANAOUT(hAout2,0,2,0)

err = ST_ANAOUT(hAout3,0,3,0)

;indicate the status of robot, in motion or still!

err = ST_ANAOUT(hAout4,0,4,0)

err = ST_ANAOUT(hAout5,0,5,0)

err = ST_ANAOUT(hAout6,0,6,0)

;ENDFOLD

;FOLD  Parameterization of RSI-Objects

; set the parameters

err = ST_SETPARAM(hCoRob, eCRParMaxLate,100)

;err = ST_SETPARAM(hCoRob, eCRParOutputMode, eCRZeroValue)

```

```

err = ST_SETPARAM(hCoRob, eCRParOutputMode, eCRLastValue)
err = ST_SETPARAM(hCoRob, eCRParDebug, eCROn)
;err = ST_SETPARAM(hCoRob, eCRParDebug, eCROff)
;ENDFOLD

;FOLD RSI Objects Linking
; Link up RSI-Objects
; Enable RSI-Ethernet
err = ST_NEWLINK(hEnable,1,hCoRob,eCRInEnable)
err = ST_NEWLINK(hDiIn,1,hCoRob,eCRInDig);8Digital Inputs
err = ST_NEWLINK(hAout1,1,hCoRob,eCRInX); integer 1
err = ST_NEWLINK(hAout2,1,hCoRob,eCRInY); integer 2
err = ST_NEWLINK(hAout3,1,hCoRob,eCRInZ); integer 3
err = ST_NEWLINK(hAout4,1,hCoRob,eCRInA); integer 4
err = ST_NEWLINK(hAout5,1,hCoRob,eCRInB); integer 5
err = ST_NEWLINK(hAout6,1,hCoRob,eCRInC); integer 6
;=====
; Data exchange between KRC system variables and RSI objects
;=====
; Creates a RSI object to map the input signal to the KRL variable
$SEN_PREA[VARIDX]
err=ST_MAP2SEN_PREA(hmap,0,hCoRob,eCROutX,1)
IF (err<>#RSIOK) THEN
    HALT
ENDIF
err=ST_MAP2SEN_PREA(hmap,0,hCoRob,eCROutY,2)
IF (err<>#RSIOK) THEN
    HALT

```

```

ENDIF
err=ST_MAP2SEN_PREA(hmap,0,hCoRob,eCROutZ,3)
IF (err<>#RSIOK) THEN
    HALT
ENDIF
err=ST_MAP2SEN_PREA(hmap,0,hCoRob,eCROutA,4)
IF (err<>#RSIOK) THEN
    HALT
ENDIF
err=ST_MAP2SEN_PREA(hmap,0,hCoRob,eCROutB,5)
IF (err<>#RSIOK) THEN
    HALT
ENDIF
err=ST_MAP2SEN_PREA(hmap,0,hCoRob,eCROutC,6)
IF (err<>#RSIOK) THEN
    HALT
ENDIF
err=ST_MAP2SEN_PREA(hmap,0,hCoRob,eCROutA1,7)
IF (err<>#RSIOK) THEN
    HALT
ENDIF
err=ST_MAP2SEN_PREA(hmap,0,hCoRob,eCROutA2,8)
IF (err<>#RSIOK) THEN
    HALT
ENDIF
err=ST_MAP2SEN_PREA(hmap,0,hCoRob,eCROutA3,9)
IF (err<>#RSIOK) THEN
    HALT

```

```
ENDIF
err=ST_MAP2SEN_PREA(hmap,0,hCoRob,eCROutA4,10)
IF (err<>#RSIOK) THEN
    HALT
ENDIF
err=ST_MAP2SEN_PREA(hmap,0,hCoRob,eCROutA5,11)
IF (err<>#RSIOK) THEN
    HALT
ENDIF
err=ST_MAP2SEN_PREA(hmap,0,hCoRob,eCROutA6,12)
IF (err<>#RSIOK) THEN
    HALT
ENDIF
err=ST_MAP2SEN_PREA(hmap,0,hCoRob,eCROutA7,13)
IF (err<>#RSIOK) THEN
    HALT
ENDIF
err=ST_MAP2SEN_PREA(hmap,0,hCoRob,eCROutA8,14)
IF (err<>#RSIOK) THEN
    HALT
ENDIF
err=ST_MAP2SEN_PREA(hmap,0,hCoRob,eCROutA9,15)
IF (err<>#RSIOK) THEN
    HALT
ENDIF
err=ST_MAP2SEN_PREA(hmap,0,hCoRob,eCROutA10,16)
IF (err<>#RSIOK) THEN
    HALT
```

```

ENDIF
err=ST_MAP2SEN_PREA(hmap,0,hCoRob,eCROutA11,17)
IF (err<>#RSIOK) THEN
    HALT
ENDIF
err=ST_MAP2SEN_PREA(hmap,0,hCoRob,eCROutA12,18)
IF (err<>#RSIOK) THEN
    HALT
ENDIF
err=ST_MAP2SEN_PREA(hmap,0,hCoRob,eCROutDig,19)
IF (err<>#RSIOK) THEN
    HALT
ENDIF
err=ST_MAP2SEN_PREA(hmap,0,hCoRob,eCROutErr,20)
IF (err<>#RSIOK) THEN
    HALT
ENDIF
; $SEN_PREA[1:14] are XYZABCA1A2A3A4A5A6E1E2
; $ SEN_PREA[15] is move type
; $ SEN_PREA[16] is velocity
; $ SEN_PREA[17] is Base Number
; $ SEN_PREA[18] is Interrupt
; $ SEN_PREA[19] is Index of coordinates
; $ SEN_PREA[20] is &&&
;=====
;KRL Motion Programming
;=====
; BASE coordinate system and Absolute integration mode!

```

err = ST_ON1(#base,0)

PTP Home

LOOP

IF \$SEN_PREA[18]>0 THEN

Interrupt on 21

\$ADVANCE=0

\$ANOUT[2]=0

ELSE

Interrupt off 21

\$ADVANCE=3

ENDIF

MOVEP()

Interrupt off 21

\$ADVANCE=3

\$ANOUT[2]=0

; set back to default value!

ENDLOOP

END

;=====

; Unterprogram

; MOVEP()

; +MOVE_Überschleifen()

; +MOVE_Normal()

; ++ COORDINATE_POS (POINT_POS:OUT)

; ++ COORDINATE_AXIS (POINT_AXIS:OUT)

; FOUND()

;=====

```

DEF MOVEP()
;=====
; Dynamical Parameter assignment
;=====
;Base, Tool, Velocity, move type, überschleifen?
BAS_NO=$SEN_PREA[17]*57.29579
BAS ( #BASE,BAS_NO); given indirectly by system variable
BAS(#TOOL,1); given directly
Continue
$OV_PRO=$SEN_PREA[16]*57.29579
$VEL.CP=0.5
IF $SEN_PREA[15]>0 THEN
MOVE_TYPE=1
ELSE
MOVE_TYPE=0
ENDIF
; Überschleifen
IF $SEN_PREA[19]>0 THEN
halt
MOVE_Ueberschleifen()
ELSE
MOVE_NORMAL()
ENDIF
END
DEF MOVE_Ueberschleifen()
; I is INT, the index of the total coordinates received
IF $SEN_PREA[19]==I THEN
IF I>999 THEN

```

```

M=I/999
IF (I-M*999)<=0 THEN
    N=I-M*999+999
ELSE
    N=I-M*999
ENDIF
ELSE
    N=I
ENDIF
P[N].X=$SEN_PREA[1]
P[N].Y=$SEN_PREA[2]
P[N].Z=$SEN_PREA[3]
P[N].A=$SEN_PREA[4]
P[N].B=$SEN_PREA[5]
P[N].C=$SEN_PREA[6]
I=I+1
CONTINUE
$ANOUT[1]=I
ENDIF
IF S<I THEN
    IF K==1 THEN
IF I>999 THEN
LIN P[999] C_DIS; at the turning point in the buffer
    S=S+1
ELSE
    LIN P[1] C_DIS; just at the beginning of the operation!
ENDIF
ELSE

```

```

        LIN P[K-1] C_DIS; normal situation
        S=S+1
    ENDIF
ENDIF
IF $SEN_PREA[19]==I THEN
    IF I>999 THEN
        M=I/999
    IF (I-M*999)<=0 THEN
        N=I-M*999+999
    ELSE
        N=I-M*999
    ENDIF
    ELSE
        N=I
    ENDIF
    P[N].X=$SEN_PREA[1]
    P[N].Y=$SEN_PREA[2]
    P[N].Z=$SEN_PREA[3]
    P[N].A=$SEN_PREA[4]
    P[N].B=$SEN_PREA[5]
    P[N].C=$SEN_PREA[6]
    I=I+1
    CONTINUE
    $ANOUT[1]=I
ENDIF
IF S<I THEN
    LIN P[K] C_DIS
    S=S+1

```

```

IF K<998 THEN
    K=K+2
ELSE
    K=1
ENDIF
ENDIF
END
DEF MOVE_NORMAL()
AIM_PACKET=MOTIONPACKETP()
SWITCH AIM_PACKET.MOVE_TYPE
CASE 0
    B.A1=ABS(AIM_PACKET.AXIS_P.A1-$AXIS_ACT.A1)
    B.A2=ABS(AIM_PACKET.AXIS_P.A2-$AXIS_ACT.A2)
    B.A3=ABS(AIM_PACKET.AXIS_P.A3-$AXIS_ACT.A3)
    B.A4=ABS(AIM_PACKET.AXIS_P.A4-$AXIS_ACT.A4)
    B.A5=ABS(AIM_PACKET.AXIS_P.A5-$AXIS_ACT.A5)
    B.A6=ABS(AIM_PACKET.AXIS_P.A6-$AXIS_ACT.A6)
    B.E1=ABS(AIM_PACKET.AXIS_P.E1-$AXIS_ACT.E1)
    B.E2=ABS(AIM_PACKET.AXIS_P.E2-$AXIS_ACT.E2)
    B.E3=ABS(AIM_PACKET.AXIS_P.E3-$AXIS_ACT.E3)
    B.E4=ABS(AIM_PACKET.AXIS_P.E4-$AXIS_ACT.E4)
    B.E5=ABS(AIM_PACKET.AXIS_P.E5-$AXIS_ACT.E5)
    B.E6=ABS(AIM_PACKET.AXIS_P.E6-$AXIS_ACT.E6)
IF
((B.A1>=0.05)AND(B.A1<=359.95))OR((B.A2>=0.05)AND(B.A2<=359.95))OR((B.A3>=
0.05)AND(B.A3<=359.95))OR((B.A4>=0.05)AND(B.A4<=359.95))OR((B.A5>=0.05)AN
D(B.A5<=359.95))OR((B.A6>=0.05)AND(B.A6<=359.95)) THEN
$ANOUT[3]=1
PTP AIM_PACKET.AXIS_P

```

```

WAIT FOR $BRAKE_SIG==0
$ANOUT[3]=$BRAKE_SIG
ELSE
Z=FALSE
ENDIF
CASE 1
    C.X=ABS(AIM_PACKET.POS_P.X-$POS_ACT.X)
    C.Y=ABS(AIM_PACKET.POS_P.Y-$POS_ACT.Y)
    C.Z=ABS(AIM_PACKET.POS_P.Z-$POS_ACT.Z)
    C.A=ABS(AIM_PACKET.POS_P.A-$POS_ACT.A)
    C.B=ABS(AIM_PACKET.POS_P.B-$POS_ACT.B)
    C.C=ABS(AIM_PACKET.POS_P.C-$POS_ACT.C)
    C.E1=ABS(AIM_PACKET.POS_P.E1-$POS_ACT.E1)
    C.E2=ABS(AIM_PACKET.POS_P.E2-$POS_ACT.E2)
    C.E3=ABS(AIM_PACKET.POS_P.E3-$POS_ACT.E3)
    C.E4=ABS(AIM_PACKET.POS_P.E4-$POS_ACT.E4)
    C.E5=ABS(AIM_PACKET.POS_P.E5-$POS_ACT.E5)
    C.E6=ABS(AIM_PACKET.POS_P.E6-$POS_ACT.E6)
IF
(C.X>=0.05)OR(C.Y>=0.05)OR(C.Z>=0.05)OR((C.A>=0.09)AND(C.A<=359.91))OR((C.
B>=0.09)AND(C.B<=359.91))OR((C.C>=0.09)AND(C.C<=359.91))OR((C.E1>=0.05)AN
D(C.E1<=359.95))OR((C.E2>=0.05)AND(C.E2<=359.92)) THEN
$ANOUT[3]=1
    ST_SKIPLIN(AIM_PACKET.POS_P)
WAIT FOR $BRAKE_SIG==0
$ANOUT[3]=$BRAKE_SIG
ELSE
z=false
ENDIF

```

```
ENDSWITCH
$ANOUT[3]=$BRAKE_SIG
END
DEF FOUND()
END
DEFFCT POXISTYP MOTIONPACKETP()
NMP.POS_P=$POS_ACT
NMP.AXIS_P=$AXIS_ACT
NMP.MOVE_TYPE=1
NMP.VELOCITY=1
NMP.POS_P.X=$SEN_PREA[1]
NMP.POS_P.Y=$SEN_PREA[2]
NMP.POS_P.Z=$SEN_PREA[3]
NMP.POS_P.A=$SEN_PREA[4]
NMP.POS_P.B=$SEN_PREA[5]
NMP.POS_P.C=$SEN_PREA[6]
NMP.POS_P.E1=$SEN_PREA[13]*57.29579
NMP.POS_P.E2=$SEN_PREA[14]*57.29579
NMP.POS_P.E3=0
NMP.POS_P.E4=0
NMP.POS_P.E5=0
NMP.POS_P.E6=0
NMP.AXIS_P.A1=$SEN_PREA[7]*57.29579
NMP.AXIS_P.A2=$SEN_PREA[8]*57.29579
NMP.AXIS_P.A3=$SEN_PREA[9]*57.29579
NMP.AXIS_P.A4=$SEN_PREA[10]*57.29579
NMP.AXIS_P.A5=$SEN_PREA[11]*57.29579
NMP.AXIS_P.A6=$SEN_PREA[12]*57.29579
```

```

NMP.AXIS_P.E1=$SEN_PREA[13]*57.29579
NMP.AXIS_P.E2=$SEN_PREA[14]*57.29579
NMP.AXIS_P.E3=0
NMP.AXIS_P.E4=0
NMP.AXIS_P.E5=0
NMP.AXIS_P.E6=0
IF $SEN_PREA[15]>0 THEN
  NMP.MOVE_TYPE=1
ELSE
  NMP.MOVE_TYPE=0
ENDIF
NMP.VELOCITY=$SEN_PREA[16]*57.29579
RETURN(NMP)
ENDFCT

DEF FOUNDP()
; $ ANOUT[1],
; $ ANOUT[2], responsible for recording of the point found!
; $ ANOUT[3],
; $ ANOUT[4],
; $ ANOUT[5],
; $ ANOUT[6],
  INTERRUPT OFF 21
; $ANOUT[2] is 0 for default
; $ANOUT[2]=1 indicate the point is found
  BRAKE F
$ANOUT[2]=1
SWITCH MOVE_TYPE

```

```
CASE 0
  PTP $AXIS_INT
CASE 1
  LIN $POS_INT
  LIN_REL{Z 10}
  LIN_REL{X 20}
  LIN_REL{Z -8}
  LIN_REL{Y -7}
ENDSWITCH
WAIT FOR $ROB_STOPPED
WAIT FOR $BRAKE_SIG==0
$ANOUT[3]=$BRAKE_SIG
RESUME
END
```